NASA CONTRACTOR REPORT

NASA CR-225

NASA CR-225

AMPTIAC

60223

DISTRIBUTION STATEMENT A
Approved for Public Release
Distribution Unlimited

OPERATION OF A HAYNES ALLOY NO. 25 FORCED CIRCULATION LOOP TO STUDY THE EFFECTS OF HYDROGEN IN A SIMULATED SUNFLOWER SYSTEM

by R. C. Schulze and D. B. Cooper

Prepared under Contract No. NAS 5-462 *by*
THOMPSON RAMO WOOLDRIDGE, INC.
Cleveland, Ohio
for

20011217 167

NATIONAL AERONAUTICS AND SPACE ADMINISTRATION • WASHINGTON, D. C. • MAY 1965

M

NASA CR-225

OPERATION OF A HAYNES ALLOY NO. 25 FORCED CIRCULATION LOOP TO STUDY THE EFFECTS OF HYDROGEN IN A SIMULATED SUNFLOWER SYSTEM

By R. C. Schulze and D. B. Cooper

Prepared under Contract No. NAS 5-462 by
THOMPSON RAMO WOOLDRIDGE INC.
Cleveland, Ohio

for

NATIONAL AERONAUTICS AND SPACE ADMINISTRATION

For sale by the Clearinghouse for Federal Scientific and Technical Information
Springfield, Virginia 22151 – Price $4.00

FOREWORD

This report covers the construction, operation, and evaluation of a forced circulation mercury loop using Haynes alloy No. 25 as the containment material. The work was performed between January, 1962 and December, 1963 in support of the Sunflower program under NASA Contract Number NAS 5-462 with Mr. Jack A. Heller, Space Power Systems Division, NASA Lewis Research Center, as Technical Manager. The report was originally prepared as Thompson Ramo Woolridge Report ER-6005, May 18, 1964.

OPERATION OF A HAYNES ALLOY NO. 25 FORCED CIRCULATION

LOOP TO STUDY THE EFFECTS OF HYDROGEN IN A

SIMULATED SUNFLOWER SYSTEM

by R. C. Schulze and D. B. Cooper

Thompson Ramo Wooldridge Inc.

SUMMARY

As part of an effort to answer some of the questions pertaining to the Sunflower system, a forced circulation mercury loop was designed, constructed, and operated. The primary objectives of this "work-horse" loop were:

1) Evaluate the hydrogen swallowing capability of the Sunflower mercury transfer pump.

2) Evaluate the effectiveness of various separators in removing hydrogen from the system.

3) Evaluate the effectiveness of a getter-type corrosion product separator in removing corrosion products from the system.

4) Determine the corrosion and mass transfer which occurred during operation of the loop.

The centrifugal pump was evaluated separately from the loop for its ability to accept both single bubbles of hydrogen and a constant flow of hydrogen. During these tests, no distinct correlation could be found for either case between the pump performance and the amount of hydrogen entering the pump.

Also, a centrifugal hydrogen separator was evaluated during the operation of the centrifugal pump. Attempts were made to remove hydrogen through a columbium or 1010 steel diffusion window mounted in the separator. However, these attempts met with limited success primarily because of the lack of adequate data on the permeability of columbium to hydrogen at low temperatures and oxidation of the outer surface of the diffusion window.

The centrifugal pump was operated for approximately 1000 hours, during these tests. The only area of the pump that was damaged during test was the volute tongue where an erosive action had occurred.

The loop was designed to simulate the anticipated Sunflower operating conditions, except for the flow rate. The operating conditions were:

Boiler outlet temperature	838-1115°F
Superheater outlet temperature	968-1294°F
Condensing temperature	410-773°F
Flow rate	66-207 lbs/hr

During operation of the loop, erosion specimens fabricated of PH15-7Mo heat treated to conditions RH 950 and TH 1050 and Haynes alloy No. 21 were tested. The specimens were located in a high vapor velocity area just after the orifice at the end of the superheater. In addition, Haynes alloy No. 25 and Croloy 9M hydrogen diffusion windows located in the superheater were evaluated. Similar windows fabricated of Haynes alloy No. 25 and columbium were tested in the condenser. During the last 1459 hours of loop operation, a tantalum corrosion product separator was mounted in the superheater entrance.

Examination of the erosion specimens revealed practically no damage after 5292 hours of exposure to high velocity mercury vapor. However, the PH15-7Mo erosion specimens in both heat treatments (TH 1050 and RH 950) showed significant losses in hardness. The erosion specimen heat treated to TH 1050 changed from Rockwell C of 45 to Rockwell C of 25. In comparison the RH 950 heat treated erosion specimen changed from 44.7 Rc to 32.5 Rc. The Haynes alloy No. 21 erosion specimen increased in hardness from Rockwell C of 31 up to Rockwell C of 60.

The attempts to remove hydrogen from the loop through the various hydrogen diffusion windows met with only limited success. This lack of success was attributed to the following: inadequate permeability data for hydrogen; placement of windows; and oxidation of the outer surface of the windows.

After operation, the loop was dissected and examined for corrosive attack and mass transfer. Examination of the boiler revealed attack in the form of leaching and intergranular penetration to a maximum depth of 0.005 in. Light crevice attack to a maximum depth of 0.001 inch was found in the superheater. The condenser and subcooler regions were relatively unaffected.

In the boiler, the depleted layer was rich in cobalt and tungsten, indicating that chromium, nickel and iron had been leached from this region.

The chromium, nickel and iron removed from the boiler was found deposited throughout the superheater. The greatest amount of the deposit in the superheater was located in the inlet region where it was probably carried over from the boiler. Only a negligible amount of deposition was found in the condenser and subcooler regions.

The tantalum corrosion product separator, which was evaluated during the last 1459 hours of loop operation collected approximately 6.5 w/o of the total corrosion products formed. The efficiency of the separator could not be determined, since it was not in place at the start of the test when the corrosive action was probably the greatest.

TABLE OF CONTENTS

Page

Start

I INTRODUCTION

The materials problems associated with the design and operation of a mercury Rankine cycle power system are fairly well defined. With the exception of refractory metals, no known material is entirely resistant to corrosive attack by mercury at high temperatures. While the loss in strength of the containment material due to the attack by mercury is generally not great enough to reduce the durability of the material significantly, the generation of corrosion products results in a number of secondary problems which seriously threaten the long-term reliability of the system. These problems center around the transfer of the corrosion products from one portion of the system to another. The resultant effect is that the efficiency of the system may be reduced. More serious than this is the fact that regions such as the turbine nozzle and bearing fluid lines may become plugged with corrosion products. One solution to the problem is that of continuous separation of the corrosion products from the working fluid by such techniques as chemical gettering and the use of magnetic fields.

In a solar powered system such as the Sunflower, provision must be made to allow for operation during the shade portion of the orbit. An energy storage device is thus required so that excess energy can be stored during the daylight portion of the orbit. This energy is then released to the working fluid during the shade portion. In the Sunflower system, the storage device is in the form of a hemispherical shell with lithium hydride, the heat storage medium, enclosed within the walls of the cavity-type shell. However, the use of lithium hydride presents a problem because of the transfer of hydrogen into the mercury working fluid by diffusion through the tubing walls. The hydrogen results from the dissociation of the lithium hydride which occurs in the 1200-1600°F temperature range encountered in the Sunflower system. The presence of hydrogen in the mercury could result in serious operational problems, particularly with the centrifugal-type transfer pump which is susceptible to cavitation and possible loss of prime.

In an effort to answer some of the questions pertaining to the Sunflower system, a forced circulation mercury loop was designed, constructed, and operated. The primary objectives of this "work-horse" loop were:

1) Evaluate the hydrogen swallowing capability of the Sunflower mercury transfer pump.

2) Evaluate the effectiveness of various separators in removing hydrogen from the system.

3) Evaluate the effectiveness of a getter-type corrosion product separator in removing corrosion products from the system.

4) Determine the corrosion and mass transfer which occurred during operation of the loop.

In order to meet the above objectives, the work was separated into various tasks. Planned shutdowns between tasks were scheduled so that modifications could be made to the system. These modifications included changing and relocating the various test sections incorporated in the loop.

II SYSTEM DESCRIPTION

A. Loop

Except for the flow rate, the design parameters for the work-horse loop were chosen so as to simulate the anticipated conditions in the final Sunflower system. The flow rate for the loop was about one-tenth of the anticipated flow for the Sunflower system. These conditions included:

Boiler outlet temperature	1100°F
Superheater outlet temperature	1250-1300°F
Condensing temperature	620°F
Subcooler temperature	300°F
Flow rate	82 lbs/hr

Haynes alloy No. 25 (composition given in Appendix I) was the basic material of construction and was chosen because of its relative resistance to mercury corrosion at temperatures up to 1000°F (5)* and its strength at elevated temperatures. Type 316 SS (composition given in Appendix I) was used in low temperature regions of the loop for instrument sensing units and valving. Several other materials were used in small quantities during some of the tests and will be discussed in the detailed description of the system which follows. Figures 1 and 2 show the design of the loop and are referenced during the following description.

In order to minimize the effects of gravity upon the hydrogen injected into the system, the superheater, condenser, and subcooler sections of the loop were located in a horizontal plane. Primarily, this arrangement reduced the possibility of hydrogen collecting above the liquid-vapor interface in the condenser.

1. Boiler and Superheater

The boiler and superheater sections of the loop were fabricated from 1.0 inch O.D. by 0.065 inch wall Haynes alloy No. 25 tubing. Hevi-Duty clam shell heaters were used to supply energy to these sections and were designed to supply maximum overall heat fluxes of 15,000 and 10,000 BTU/hr-ft^2 in the boiler and superheater, respectively. Actual fluxes used during operation were in the order of 10,000 BTU/hr-ft^2 over nine feet of heated boiler tubing and 2600 BTU/hr-ft^2 over eight feet of heated superheater tubing. In order to create turbulence and facilitate the heat transfer, swirl wire was used throughout the boiler and superheater. Haynes alloy No. 25 wire of 0.062 inch diameter was coiled into a helix having an outside diameter of 0.870 inch and a pitch of 3.5 inches.

---

*The numbers in parentheses pertain to references listed at the end of the report.

[The fabrication, assembly, operation [illegible] removal of hydrogen [illegible] are described in detail.] [illegible] page 112

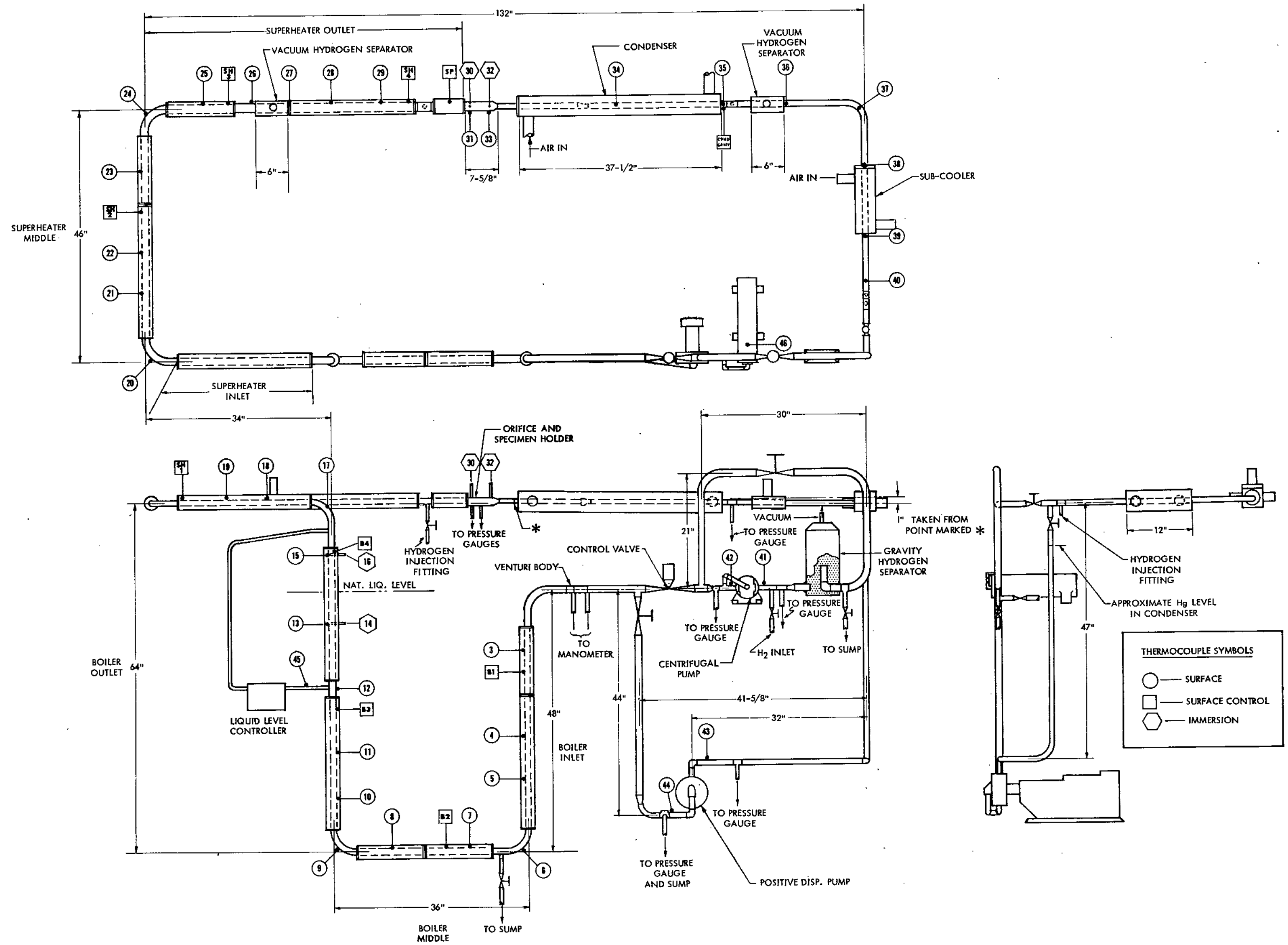

FIGURE 1 SCHEMATIC DRAWING OF THE WORKHORSE LOOP SHOWING THE VARIOUS COMPONENTS ALONG WITH HEATER AND THERMOCOUPLE LOCATIONS

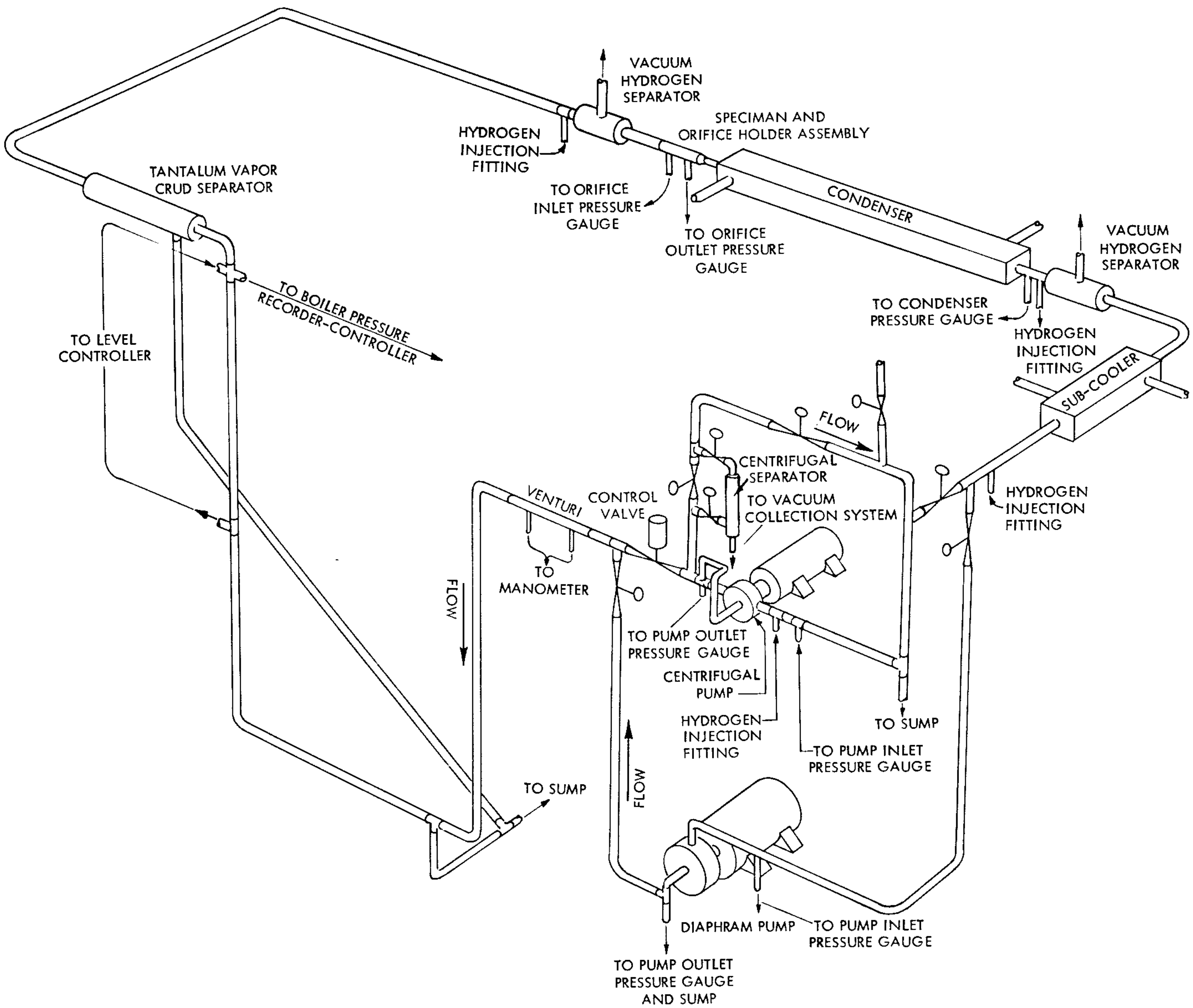

FIGURE 2 ISOMETRIC SKETCH OF THE WORKHORSE LOOP SHOWING THE FINAL CONFIGURATION

2. Condenser and Subcooler

The condenser and subcooler sections of the loop consisted of single Haynes alloy No. 25 tubes having an outside diameter of 0.5 inch and a wall of 0.049 inch. Cooling of these sections was accomplished primarily by air. During initial testing two 195 CFM ventilating blowers were used to cool these sections. The condenser tube was enclosed within a four-inch square by 37-inch long manifold. The subcooler tube was enclosed within a four-inch square by 12-inch long manifold. During initial loop operation, the cooling capacity of the condenser was found to be inadequate. The 195 CFM blower was replaced with one having a capacity of 1000 CFM, and 0.25 inch O.D. copper cooling coils were installed on the condenser manifold. These changes proved to be quite satisfactory and supplied sufficient cooling capacity in the condenser to allow the loop to be operated at a flow rate of 98 pounds per hour.

3. Orifice and Specimen Holder

A sharp-edged orifice was used in the loop to provide the pressure differential between the superheater and condenser. The orifice plate was fabricated from PH15-7Mo heat treated to the RH 950 condition. The 0.050 inch diameter orifice was drilled in a plate 0.032 inch thick. Located immediately following the orifice was a Haynes alloy No. 25 specimen holder which contained three erosion specimens, each having an exposed cross section of 0.25 inch by 0.062 inch. The materials for the erosion specimens were:

Haynes alloy No. 21

PH15-7Mo (RH 950 heat treatment)

PH15-7Mo (TH 1050 heat treatment)

(The compositions of the two materials are given in Appendix I. The heat treatments for the PH15-7Mo are given in Appendix II.) These materials were chosen as being representative of the design materials for the Sunflower turbine. The orifice-specimen holder combination is shown in Figures 3 and 4. The entire orifice-specimen holder was heated with a Hevi-Duty clam shell heater to minimize condensation of the mercury vapor.

B. Controls

1. Heater Controls

Power to the heaters on the boiler, superheater, and orifice-specimen holder sections of the loop was varried by the use of General Radio "Variac" autotransformers. Each heater circuit also contained a Weston ammeter. Alnor type N-14 millivoltmeter-type temperature controllers were used to control the temperature of each heated section of the loop. Temperature measurement for the controllers was made by chromel-alumel thermocouples secured to the surface of the loop tubing near the exit of each heater circuit.

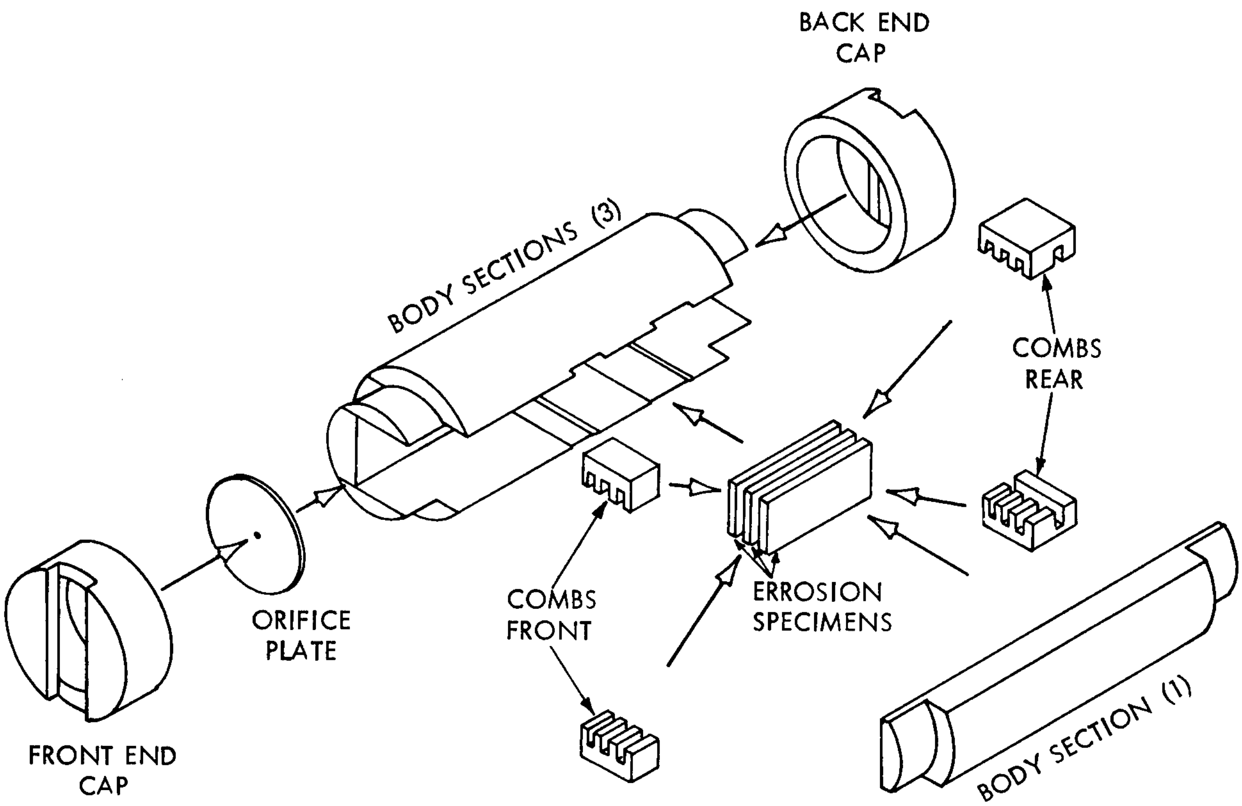

FIGURE 3 ISOMETRIC VIEW OF SPECIMEN AND ORIFICE HOLDER

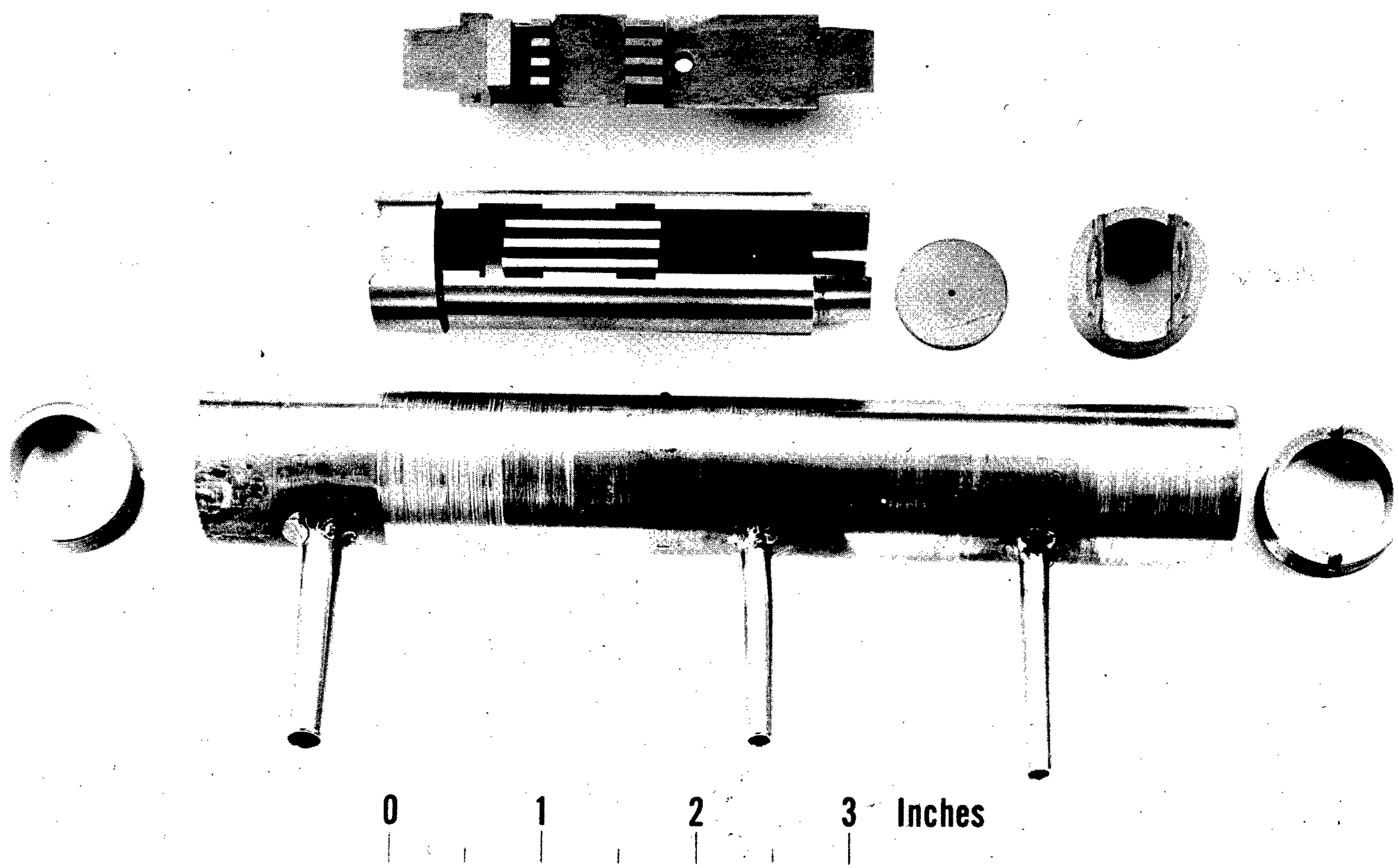

Figure 4. Photograph Showing the Orifice and Specimen Holder Partially Assembled.

2. Condenser and Subcooler Control

The flow of cooling air for the condenser was varied by means of a Minneapolis-Honeywell motor-operated butterfly valve. The input signal to the motor was received from a Weston high-low, millivoltmeter-type temperature controller. This instrument sensed the condenser temperature as indicated by an iron-constantan thermocouple secured to the condenser wall.

The flow of cooling air for the subcooler was manually controlled by means of a butterfly valve.

3. Pressure Measurement

A Minneapolis-Honeywell pressure recorder with an over-pressure control circuit provided a record of the boiler outlet pressure and also served as a safety device in the event of an over-pressure situation. A total of seven Ashcroft pressure gauges were used to measure the pressure at various locations in the system.

1) Orifice inlet pressure (superheater outlet)
2) Orifice outlet pressure
3) Condenser pressure
4) Diaphragm pump inlet pressure
5) Diaphragm pump outlet pressure
6) Centrifugal pump inlet pressure
7) Centrifugal pump outlet pressure

All instruments were actuated by Type 316 SS diaphragm seals connected to the loop by Haynes alloy No. 25 tubing. A constant head of liquid mercury was maintained in the sensing units, and all pressure readings have been corrected for this static head.

4. Temperature Measurement

In addition to the control thermocouples, 48 others were placed at various locations around the loop. Four of these were immersion thermocouples and were located 12 inches before the boiler exit, at the boiler exit, at the orifice inlet, and at the orifice outlet. The remaining 44 were secured to the surface of the tubing. All thermocouples were chromel-alumel. The temperatures were recorded on a 48-point Weston temperature recorder which was equipped with a limit switch to protect the loop against excessive temperature. The panels which contained the various controls are shown in Figure 5.

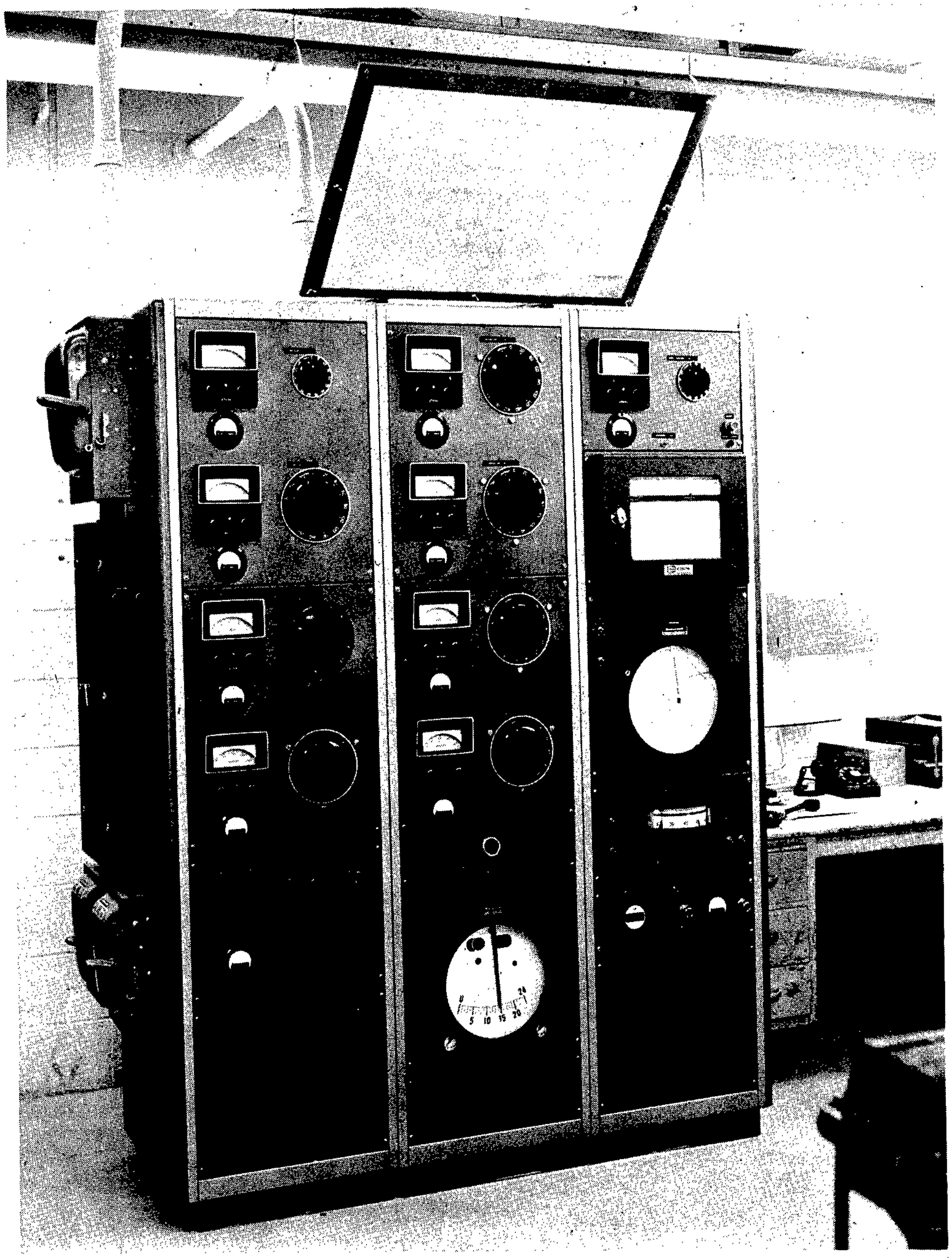

Figure 5. Photograph Showing the Loop Control Panel.

5. Pumps and Liquid Level Control

Two pumps were used in the loop. The primary pump was a Milton Roy positive displacement pump with a pneumatic operated U. S. "Varidrive" variable speed motor. Materials of construction in contact with the mercury included:

Liquid end	Type 316 SS
Diaphragm	Teflon
Ball seats	Type 316 SS
Ball valves	Type 416 SS
Check valve housing	Type 316 SS

The pump had a capacity of 158 pounds per hour of mercury (specific gravity of 13.6) and a maximum discharge pressure of 500 psig.

The secondary pump was of the same design as the Sunflower mercury transfer pump. The design of the pump is shown schematically in Figure 6. The pump was of the centrifugal type and was designed to deliver 25 to 35 pounds of mercury per minute with the pump operating at 35,000 to 40,000 rpm. The pump included a jet by-pass to provide the required flow and discharge pressure of 500 to 550 psi. Since the pump was to be used primarily during testing with hydrogen, a static lip seal was included to limit hydrogen leakage around the shaft. The pump was driven by a Precise Super 60 electrical motor. The motor speed was controlled by varying the input voltage with a General Radio "Variac" autotransformer. Since the capacity of the centrifugal pump was approximately 25 times the design flow in the loop, a by-pass around the centrifugal pump was included to handle the excess flow from the pump. Included in the by-pass line was a gravity hydrogen separator which utilized the force of gravity to separate hydrogen from the mercury so that hydrogen would not accumulate at the pump inlet during hydrogen testing.

A Minneapolis-Honeywell level controller was employed to maintain the proper quantity of mercury in the boiler. Indication of the level was given by a Type 316 SS bellows assembly which sensed the difference in pressure at two points in the boiler section 24 inches apart. A pneumatic signal was transmitted by the level controller to either the variable speed motor on the positive displacement pump or to a Type 316 SS Minneapolis-Honeywell control valve located at the outlet of the centrifugal pump, depending on which pump was in operation.

A Type 316 SS venturi having a 0.035 inch diameter orifice was used to measure the mercury flow at the boiler entrance. The pressure drop across the venturi was indicated by an inverted U-tube manometer of Type 316 SS construction.

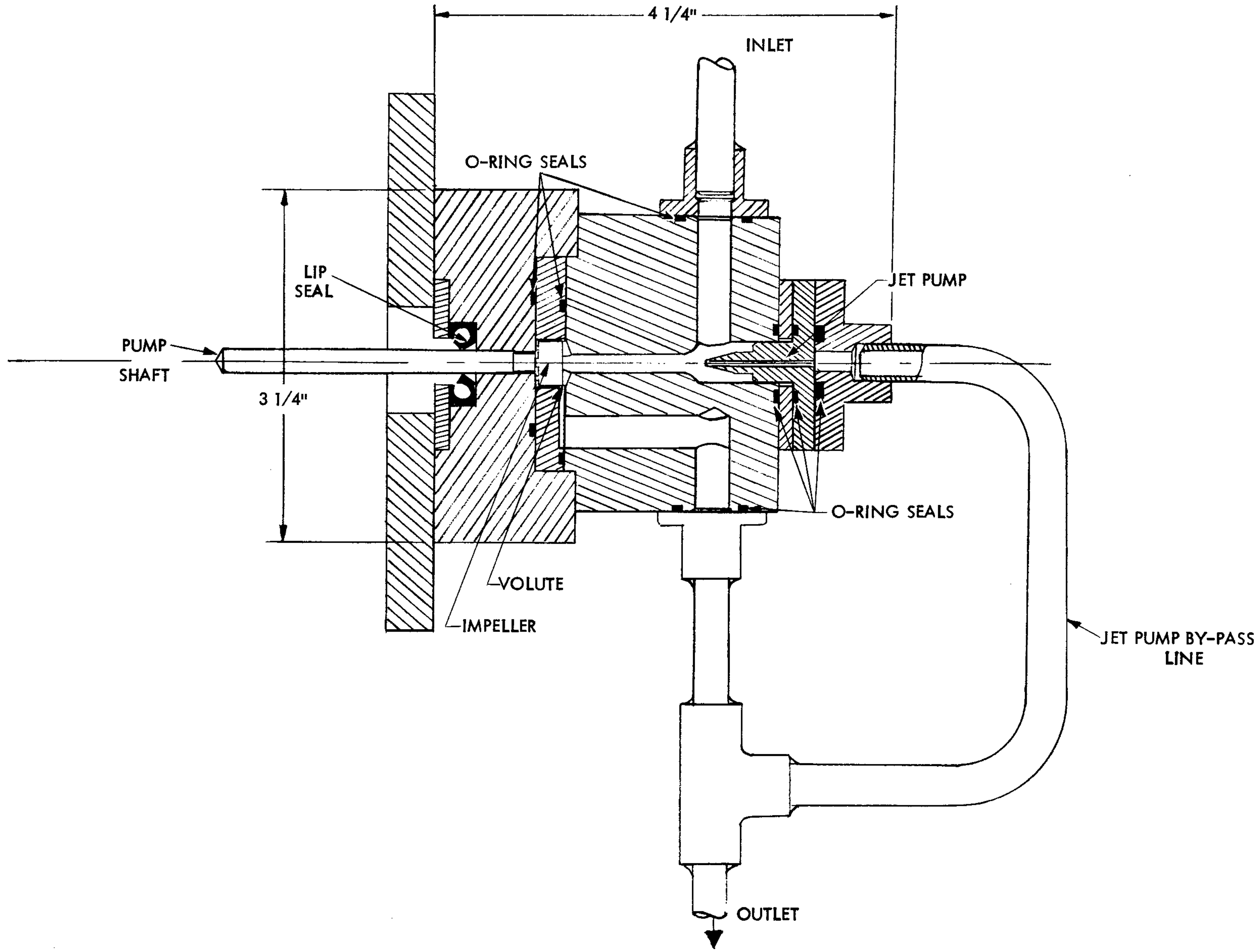

FIGURE 6 SCHEMATIC DRAWING SHOWING THE OVERALL CONFIGURATION OF THE CENTRIFUGAL MERCURY TRANSFER PUMP

C. Centrifugal Hydrogen Separator

A centrifugal separator was included in the centrifugal pump discharge line and was evaluated for hydrogen separation capability. The separator was designed for a total mercury flow of 34 pounds per minute at a pressure of 540 psia and a temperature of 400°F. Design calculations were based on the separation of 0.0001 inch radius hydrogen gas bubbles in a one "g" force field. The final design provided for a 13 "g" force field and, as such, theoretical separation of smaller bubbles should have been possible. The separator was designed to separate hydrogen from mercury at a rate of 0.2 pound per year. The hydrogen separated by centrifugal forces was removed from the separator by allowing the gas to diffuse through the wall of a columbium tube (composition given in Appendix I) which was connected to a calibrated vacuum collection system. The permeability of columbium at 400°F was determined by extrapolation of high temperature data (9). However, the permeability of columbium to hydrogen at 400°F was later determined at TRW to be lower than the value used for the separator design by a factor of approximately 4×10^5 (10). Thus, a considerable error was introduced in the surface area of columbium required for removal of the separated hydrogen. This factor is discussed further in the section concerned with data collected on the separator. Because of the trouble experienced with columbium, a 1010 steel (composition given in Appendix I) diffusion window was also evaluated.

A drawing of the separator is shown in Figure 7, while Figures 2 and 8 show the location of the separator in the system.

D. Corrosion Product Separator

As stated earlier in the report, one of the problems encountered in the Sunflower system is the possible plugging of the turbine by corrosion products. One method to control this problem is to utilize separators to remove the corrosion products. Consequently, after 3833 hours of operation, a corrosion product separator, shown in Figure 9, was installed in the system in the horizontal line at the boiler exit. The location of the separator is shown in Figure 2. The separator utilized tantalum wool (composition given in Appendix I) as a getter for separation of corrosion products carried over in the vapor from the boiler. A drain line was included in the separator so that any separated liquid would be returned to the boiler. The separator was fabricated from Haynes alloy No. 25, with the exception of the tantalum wool getter. A total of 7.5 pounds of tantalum (0.004 inch diameter wire) was used in the separator. The packing factor was 0.073 pound of tantalum per cubic inch of volume occupied by the tantalum. The volume occupied by the tantalum was 12 percent of the total separator volume available.

E. Enclosure

The entire system, with the exception of pumps and instrument sensing units, was installed in a two-foot square enclosure fabricated from sheet metal and Unistrut framing supports. After installation of the loop, the enclosure was filled with vermiculite which served as the insulation. A photograph of the loop installed in the enclosure is shown in Figure 10.

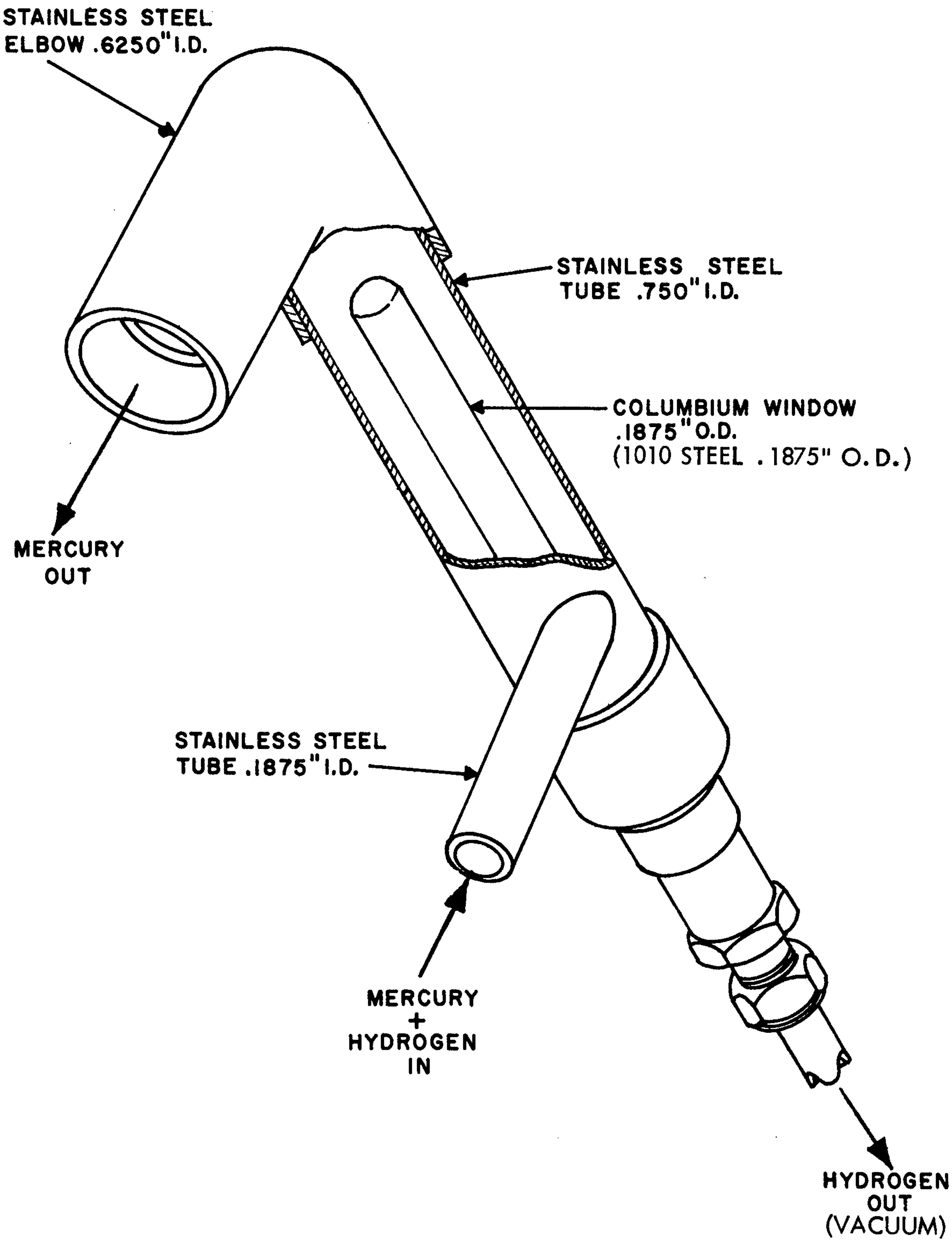

FIGURE 7 ISOMETRIC SKETCH OF THE CENTRIFUGAL HYDROGEN SEPARATOR

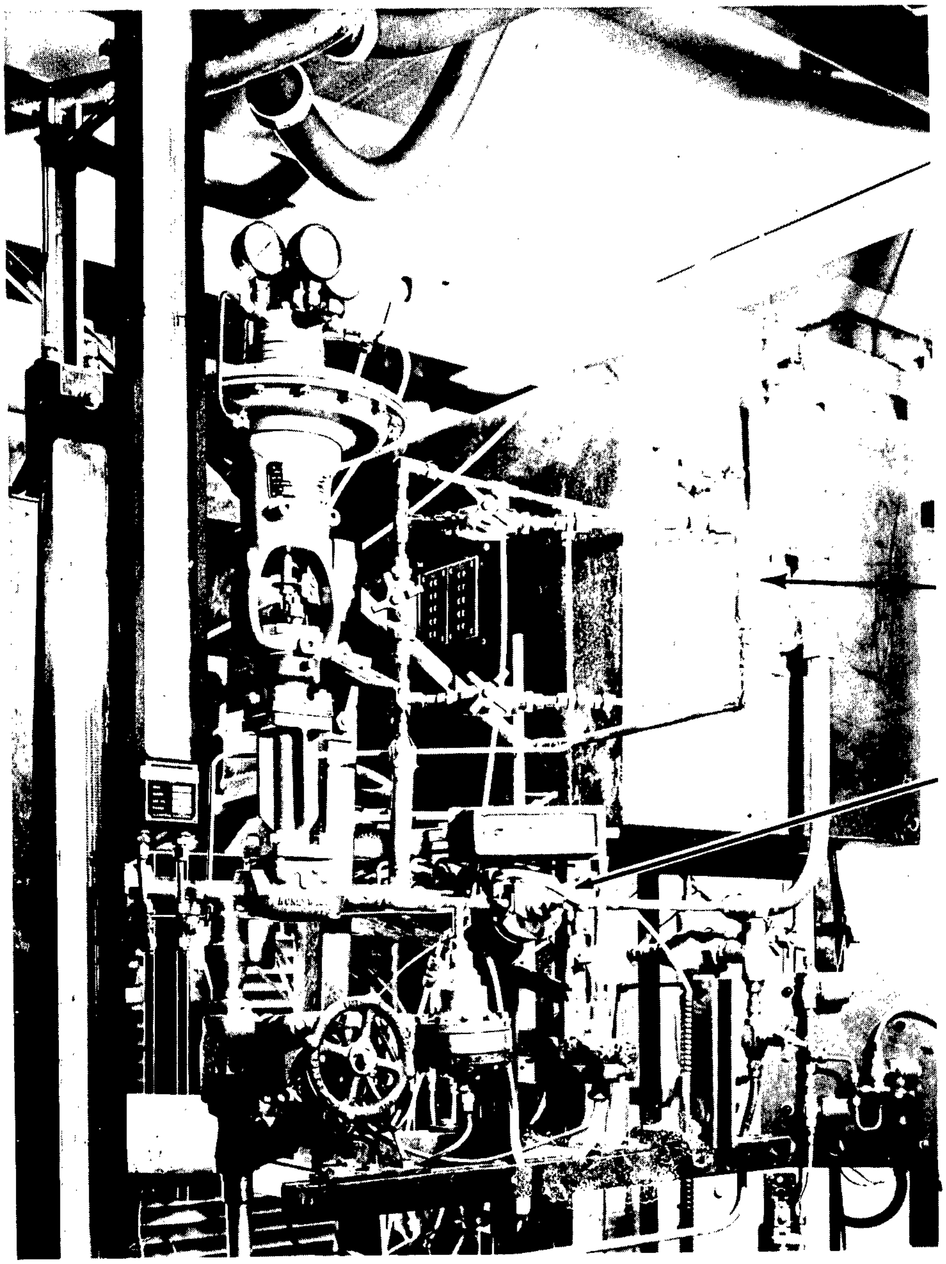

Figure 8. Photograph of the Centrifugal Pump By-Pass Line, Showing the Placement of the Centrifugal Separator.

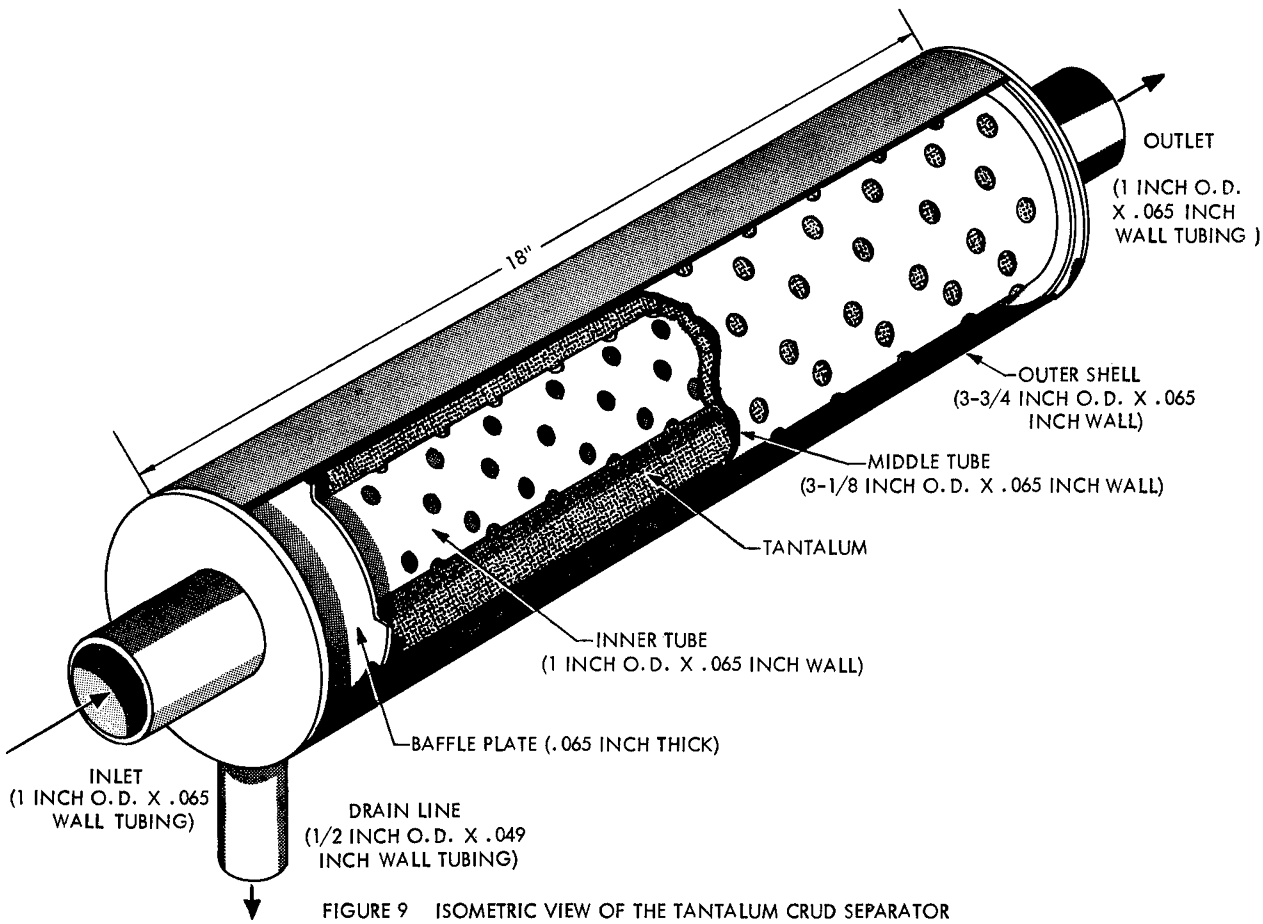

FIGURE 9 ISOMETRIC VIEW OF THE TANTALUM CRUD SEPARATOR

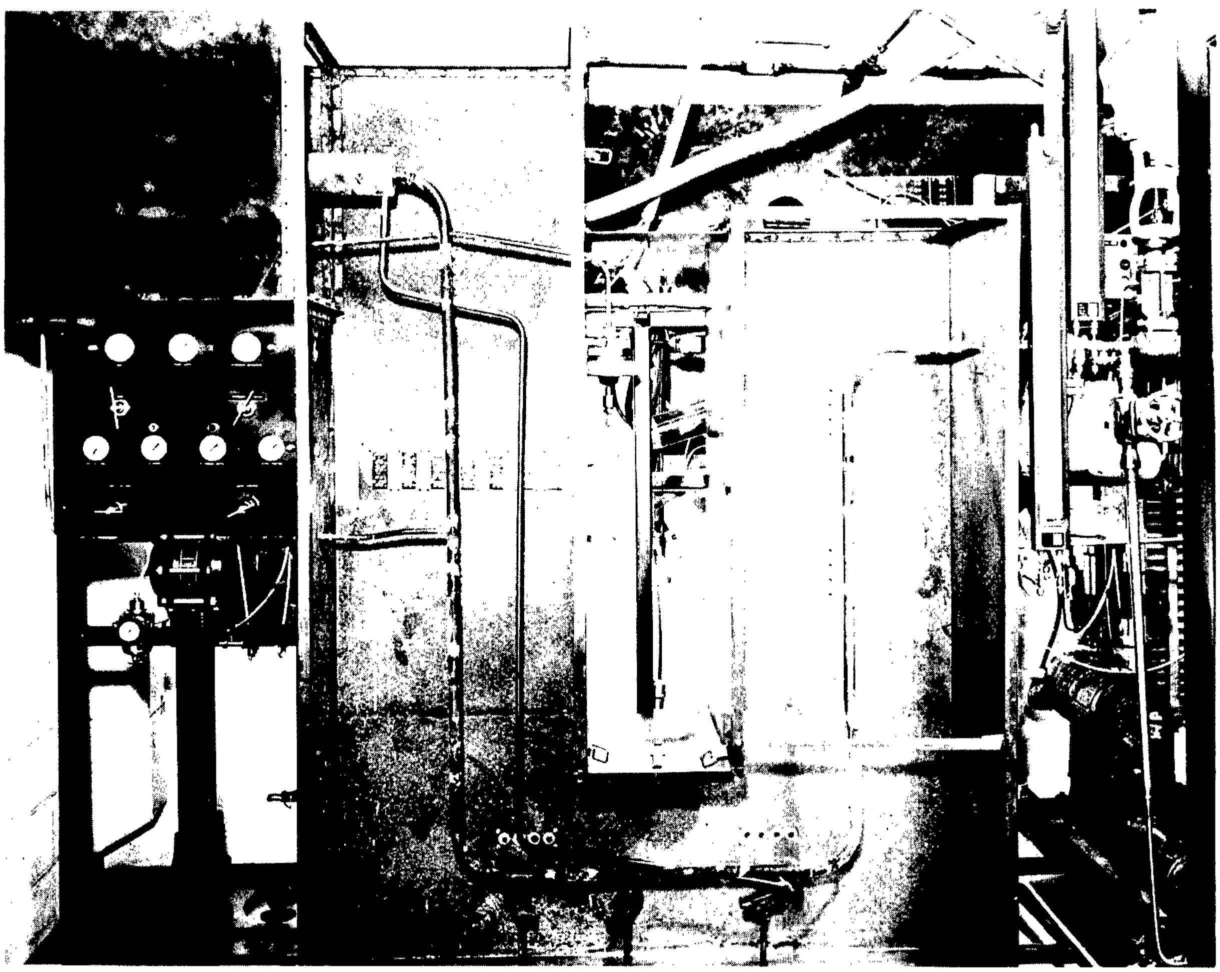

Figure 10. Photograph Showing the Placement of the Loop Within the Insulation Enclosure.

III FABRICATION AND ASSEMBLY

A. Fabrication

The loop tubing was fabricated in sub-sections. Because of the manner in which the sub sections were fabricated, several had one or more bends. The bends in the one-inch tubing were made on a four-inch-center-line radius. A three-inch-center-line radius was used for the one-half inch tubing. Before welding, all the tubing sections were cleaned in a Kolene salt bath followed by an acid pickle.

The fittings required to connect the various components to the loops were made from small pieces of tubing welded together.

The gravity hydrogen separator, located in the centrifugal pump by-pass was made from one-sixteenth inch Haynes alloy No. 25 sheet. The separator was completely welded.

B. Assembly

Sections of the loop, except for the centrifugal pump by-pass and diaphragm pump lines, were pre-assembled on the bench. All welding was done by the tungsten arc-inert gas process. During welding, all the welds were protected by flowing argon through the tubing. At this point the loop skeleton was mounted in the enclosure. The centrifugal pump was then positioned on the enclosure frame and the centrifugal pump by-pass lines were then welded in. The same process was done with the diaphragm pump and associated tubing. The final step was to weld the pressure gauge diaphragms to the loop taps.

C. Leak Testing

After all the components were placed and welded, the loop was thoroughly leaked checked. All leak checking was done with the inlet and outlet lines to the centrifugal pump sealed off. The first check was accomplished by pressurizing the loop to 600 psig and using a soap solution to check for leaks. A few small leaks were found and were immediately repaired. The entire loop was then checked under vacuum. Several other small leaks were found through the use of a mass spectrograph. These leaks were also sealed. A final vacuum leak check conducted over a 15-hour period showed a leak rate of 135 microns per hour. The lowest pressure attained during the leak testing was 50 microns.

D. Pre-Operation

After the 135 micron/hour leak rate was obtained, the entire loop was re-checked using the helium mass spectrograph. During this re-check, no indications of vacuum leaks could be found. Thus it was felt that because of the various valves and external taps located around the loop, this leak rate was the best attainable. At this time, the thermocouples were mounted and the heaters were put into place. The thermocouples were attached by spot welding the individual leads to the tubing with a one-sixteenth inch gap between the two wires. The heaters were mounted on ceramic spacers which centered the heater around the tubing. Stainless steel straps were used to hold the heaters in place. Locations of thermocouples and heaters are shown in Figure 1. The final step before loop start-up was to fill the loop enclosure with insulation. The insulation used was a granular expanded Vermiculite.

Before operation, the loop was pretreated by completely liquid filling the loop with mercury. During the treatment, the loop was operated for 18 hours at 250°F. The loop temperature was then raised to 500°F and the loop operated for an additional 72 hours. During this period, the flow through the loop was approximately 180 pounds of mercury per hour. After the pretreatment, the loop was cooled and the mercury was drained into the sump. All filling and draining operations were done through the sump. During filling, the loop was placed under vacuum and an over-pressure of argon was placed in the sump to force the mercury into the loop. Dumping was accomplished by reverse techniques.

During this pretreatment period, it was found that the diaphragm pump had to be primed before the pump would operate properly. This was done by filling the diaphragm pump inlet line first while the loop was still under vacuum. Filling was made through the hydrogen injection fitting located in the subcooler. After the diaphragm pump inlet line was filled, the rest of the loop was filled through the sump into the boiler.

IV LOOP OPERATION

A. Operating Procedure

The loop was filled in a manner similar to that previously described. The boiler was filled first. Enough mercury was added to fill the boiler exit line up to halfway between the two level controller taps. An additional 10 pounds of mercury were then added through the subcooler hydrogen injection fitting. This additional mercury was used to prime the diaphragm pump. All of the filling operations were done with the loop under vacuum.

During the initial attempts at two-phase operation, the boiler was brought up to operating temperature first. Then attempts were made to bring the superheater up to operating temperature. However, it was found that during the start-ups, the superheater loaded up with liquid mercury. Because of this, the heating of the superheater was erratic. Also pressure surges were experienced because of momentary local boiling in the superheater. In an attempt to rectify this problem, both the boiler and superheater were first heated to 400°F. Then the superheater temperature was raised to 1150 to 1200°F. The boiler was allowed to soak at 400°F while the temperature of the superheater was brought up. Also, the loop was left open to the vacuum pump during this part of the heating. Once the superheater temperatures were achieved, the vacuum pump was disconnected from the loop. The boiler was then brought up to temperature. Once two-phase operation was started, the controls were then adjusted to give the operating conditions. This procedure appeared to be successful and was followed throughout the operating life of the loop. A total of 5292 hours of operation were accumulated before the loop test was terminated.

B. Operation

An overall history of the loop operation is shown in Table 1. Average operating conditions for each run are listed in the table. Also, the length of operation and the cause of shutdown for each run are listed. In all, fifteen different operational runs were made during the lifetime of the loop. Once operating conditions for each run were reached, the controls were able to maintain these conditions. However, because of the temporary shutdowns and other reasons, the actual operating conditions varied from run to run. Because of the variance, the discussion of the loop operation has been divided into several operational periods.

1. Runs 1 through 5

The loop operated at its lowest conditions during these first five runs. As shown in Table 1, the average boiling pressure obtained never exceeded 98 psia in any of these runs. The boiling temperature varied between 838 to 892°F.

TABLE 1

SUMMARY OF WORKHORSE LOOP OPERATING CONDITIONS

Run No.	Start Date and Time	Stop Date and Time	Cause for Shut Down	Avg. Boiling Temp. (°F) TC #14	Theo. Boiling Temp. (°F)	Avg. Boiling Press. (psia)	Avg. S. H. Temp. (°F) TC #31	Avg. S. H. Press. (psia)	Orifice Δ P (psia)	Avg. Cond. Inlet Press. (psia)	Avg. Cond. Temp. (°F) TC #36	Mercury Flow lb/min.	Run Time (hr.)	Total Oper. Time (hr.
1.	1430/11-15-62	1730/11-15-62	Open T.C. (TC #29)	890	892	98	1150	86	48	38	750	3.29	3	3
2.	1330/11-21-62	0730/11-22-62	Open T.C. (TC #18)	797	838	60	968	62	25	37	540	2.10	18	21
3.	1645/11-26-62	0345/11-30-62	Open T.C.	850	856	69	1109	60	38	22	520	2.02	83	104
4.	0930/12-7-62	0930/12-9-62	Open T.C.	850	865	75	1020	72	40	32	700	2.20	48	152
5.	1030/12-13-62	0030/12-18-62	Superheater Leak	837	878	80	1234	101	31	70	462	1.45	110	262
6.	0830/12-27-62	1300/12-29-62	Open T.C.	924	965	148	1244	137	31	106	410	1.79	52.5	314.5
7.	1400/12-31-62	1800/1-10-63	Open T.C.	960	1000	186	1175	157	13	144	773	1.73	244	558.5
8.	1800/1-11-63	0830/2-2-63	Power Failure	1060	1025	215	1294	262	17	245	490	1.69	540	1098.5
9.	0830/2-12-63	1630/2-18-63	Leak in Manometer Line	1067	1070	274	1288	272	34	238	478	3.45	152	1250.5
10.	0830/2-20-63	1800/2-28-63	T.C. Over Shot Temp. Limit	952	960	141	1284	159	147	12	557	3.44	201.5	1452
11.	1500/3-1-63	1800/3-1-63	T.C. Over Shot Temp. Limit	965	972	154	1225	144	135	9	-	1.10	3.0	1455
12.	1500/3-4-63	1500/4-5-63	Loop Maintenance	1045	1050	245	1269	221	210	11	634	1.63	768	2223
13.	1230/4-16-63	1415/6-22-63	Re-Working of Loop	1085	1060	260	1279	265	255	10	609	1.62	1609.75	3832.75
14.	1030/7-22-63	0230/7-23-63	Rupture in Boiler Entrance	1140	1115	346	1285	344	329	15	520	1.20	16	3876*
15.	1515/8-5-63	1600/10-1-63	Loop Test Terminated	1101	1045	240	1272	241	236	5	585	1.62	1416	5292

*Between Run Nos. 13 and 14, 27.25 Hours of Operation were Accumulated. No Data During This Time was Recorded in that the Loop was Shut Down Twice Because of Sporadic Indications of Mercury Leakage.

The superheater outlet temperature varied from 968 to 1234°F. However, considering the low pressure drop across the orifice (25 to 48 psi) plus the temperature and pressure conditions in the condenser, the mercury vapor entering the condenser was apparently low in quality. Although the temperature of the superheater was 170 to 397°F higher than the boiler temperature, the mercury vapor apparently was not drying out in the superheater. In one case, (run no. 5) the superheater pressure exceeded the boiler pressure (80 psia) by 21 psi. Evidently, during this run, additional boiling was occurring in the superheater. The condenser conditions varied as follows: pressure, from 22 to 77 psia; and temperature 462 to 750°F. The flow rate varied from 87 to 197 pounds per hour.

As shown in the table, the first four shutdowns resulted from the spot welded thermocouples opening up. The open junction allowed the temperature recorded to drive upscale beyond the limit point. This would actuate the temperature limit safety circuit and cause shutdown of the loop.

Run No. 5 was stopped when a leak occurred in the superheater. After the heaters were removed, a small crack in the superheater tubing was found. This crack was about one-half inch long and ran at an angle of about 45° to the tube axis. The location of the leak is shown in Figure 11. The ruptured section of tubing was replaced with new tubing. Results of the analysis are discussed in the loop examination section of the report. A total of 262 hours of operation were accumulated during the first five runs.

2. Runs 6 through 9

Operation of the loop during these four runs was similar to that experienced during the first five runs. The only major difference was that the boiling pressure was increased. The average boiling pressure for the runs varied between 147 and 274 psia (965 to 1070°F). Again there was one run (No. 8) where the superheater pressure exceeded the boiling pressure.

As discussed under the first five runs, the same trouble was experienced in obtaining superheat. The outlet temperature of the superheater exceeded the boiling temperature by 218 to 320°F. But, again the pressure drop across the orifice was small (17-34 psi). Also, the temperature and pressure conditions did not correspond with each other. The average condenser conditions were; pressure, 106 to 245 psia; and temperature, 410 to 773°F. The flow rate varied from 101 to 206 pounds per hour.

The first two runs during this series were again stopped because of open thermocouples. After run no. 7, the method of mounting the thermocouples was changed. Instead of spot welding each thermocouple lead to the loop, the ends of the thermocouple were beaded and held against the wall by use of a chromel strap. The strap was spot welded to the tube to hold the bead tightly against the tube wall. The thermocouple bead was protected with Saureisen cement.

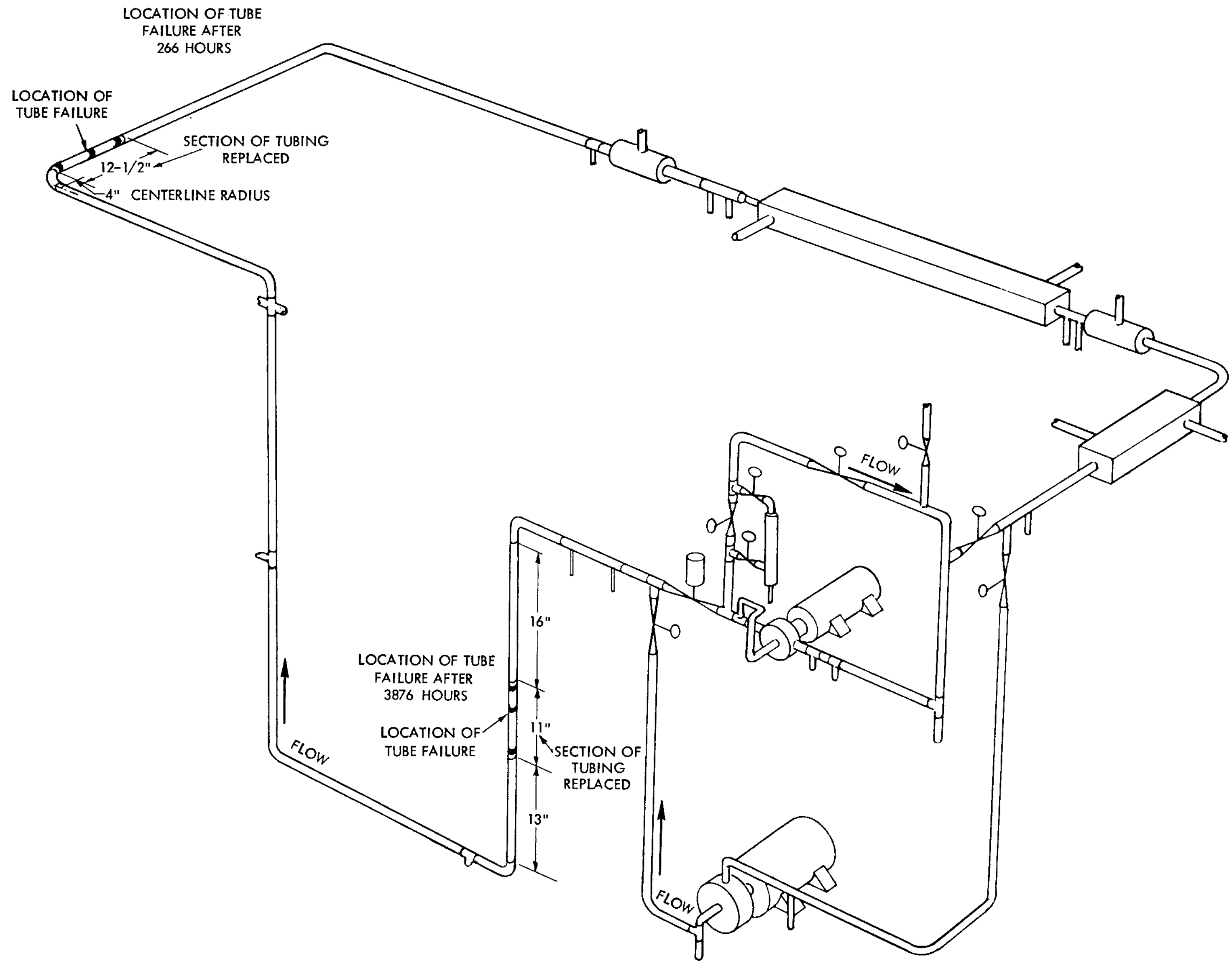

FIGURE 11 ISOMETRIC SKETCH OF THE LOOP SHOWING THE LOCATIONS OF THE TUBE FAILURES WHICH OCCURRED AFTER 266 AND 3876 HOURS

Run No. 8 was stopped as the result of a plant power outage. While attempting to restart the loop, several heaters in the boiler burned out. These were replaced. Run No. 9 was stopped when a leak occurred in the plastic tubing connecting the venturi to the flow measurement manometer. An additional 988 hours of loop testing were accumulated during Runs 6 through 9. The total amount of loop testing time after Run No. 9 was 1250 hours.

While the loop was down following Run No. 9, a new blower was installed in the condenser. Up to this point, the 195 CFM blower was not able to cool the condenser properly. Before the new blower was installed, the condenser tube was wrapped with a 0.125 inch O.D. copper cooling coil. However, plugging of the copper tubing was a continual problem. In order to rectify this difficulty, a new 1000 CFM blower was installed. Also, a 0.25 inch O.D. copper cooling coil was wrapped around the outside of the condenser manifold.

3. Runs 10 through 15

As contrasted to the first nine runs, the last six were quite different. Upon start-up of Run No. 10, a significant pressure drop was obtained across the orifice. The pressure drop was maintained throughout the rest of the loop operation. As shown in Table 1, the average pressure drop varied between 135 and 329 psi. During the last six runs the condenser inlet pressure was maintained between 5 and 15 psia (estimated). The average condenser temperature varied between 557 and 634°F. No correlations between the condenser temperature and pressure were attempted in that the condenser pressure gauge was damaged. In that the condenser pressure could not be measured directly, it was estimated from the pressure measured at the orifice and specimen holder outlet.

As shown in Table 1, the average boiler conditions varied as follows: boiling pressure, 141 to 346 psia; and boiling temperature, 960 to 1115°F. The superheater outlet temperature varied between 1225 and 1285°F. The flow rate varied between 66 and 206 pounds per hour. However, the majority of the time (3838 hours) during the last six runs was accumulated at a flow rate of 98 pounds per hour. Figures 12 and 13 show the average temperature profiles for Runs 13 and 15. As can be seen except for the temperature of the vapor exiting from the superheater, the liquid and vapor temperature varied during each run as much as 166°F. The temperature of the vapor leaving the superheater was fairly constant between 1272 and 1279°F.

Runs 10 and 11 were stopped because of thermocouples located in the boiler exit exceeding the temperature limit. Once the temperature limit was passed, the safety circuit disconnected the power from the loop. Because of the manner in which the safety circuit was connected, the loop had to be manually restarted after the limit control was actuated.

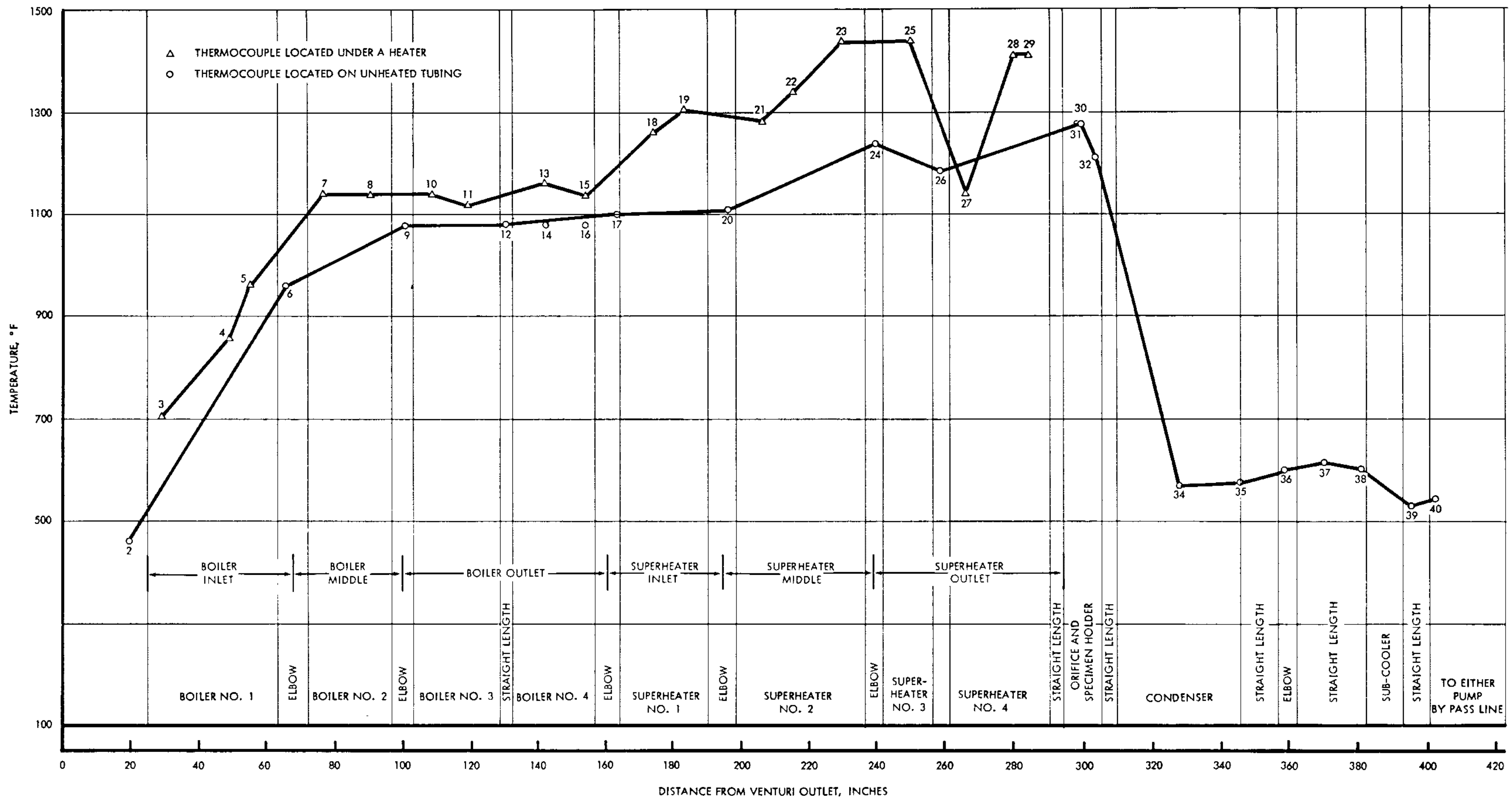

FIGURE 12 AVERAGE TEMPERATURE PROFILE FOR RUN NO. 13, LASTING 1610 HOURS

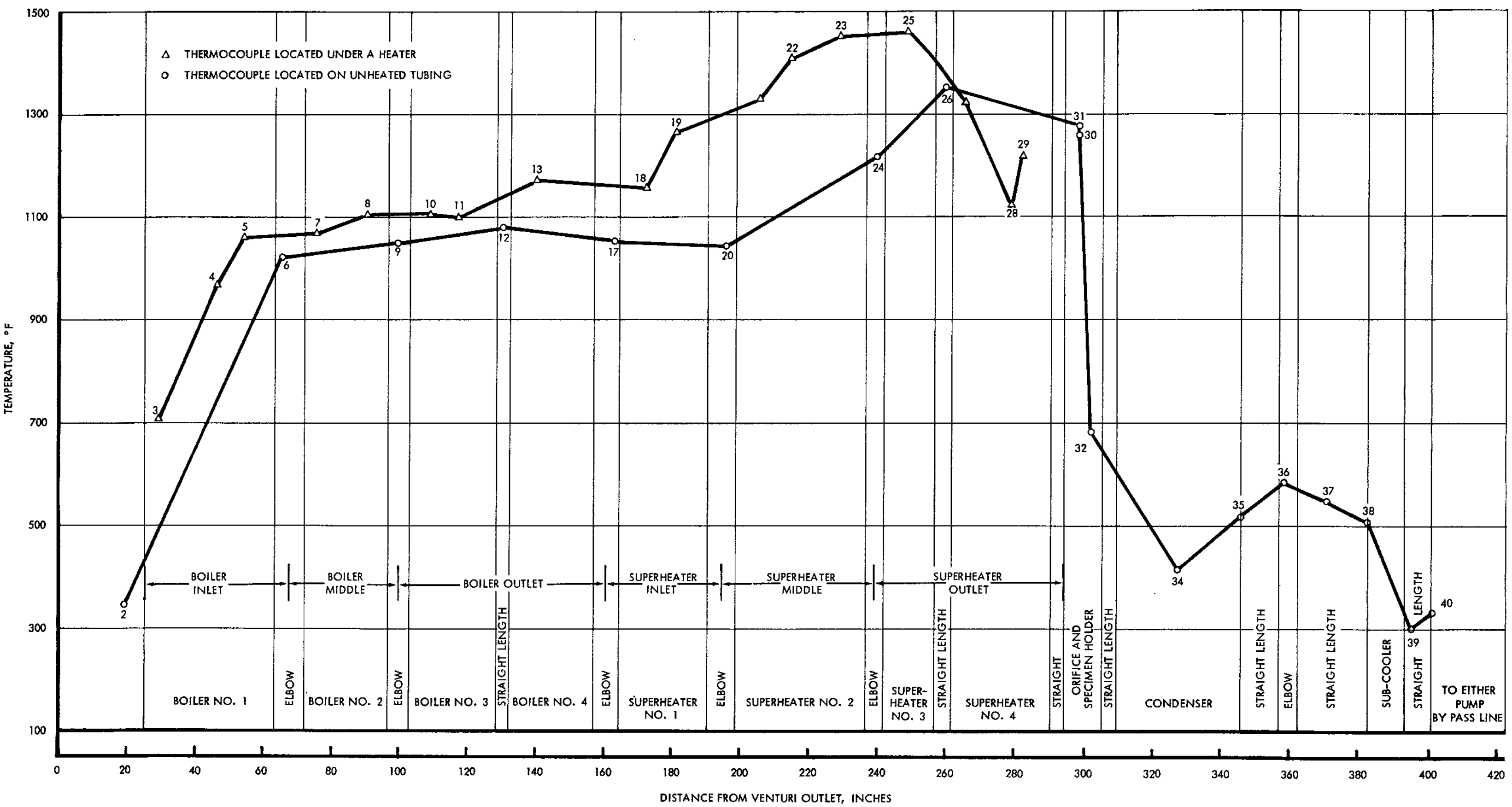

FIGURE 13 AVERAGE TEMPERATURE PROFILE FOR RUN NO. 15, LASTING 1416 HOURS

Run No. 12 was stopped so that planned and scheduled design changes could be made on the loop. The major change was in the condenser. The Haynes alloy No. 25 hydrogen diffusion window was replaced with a columbium tube. Also several other minor changes were made in the centrifugal pump by-pass.

Run No. 13 was also stopped as planned, to allow re-working of the loop. At this time, after 3,833 hours, the vapor crud separator was installed in the entrance to the superheater. The location of the separator is shown in Figure 2. A drain connecting the crud separator to the bottom of the boiler was also added. This drain was used to allow any condensing liquid to drain back to the boiler.

At the same time, a new piece of columbium was placed in the condenser window. Also, a new hydrogen injection fitting was added ahead of the condenser window. The Haynes alloy No. 25 window was removed from the condenser, and a new window, fabricated from Croloy 9M, was installed near the superheater outlet. A new piece of Haynes alloy No. 25 tubing was installed where the old window was removed. These changes are also shown in Figure 2.

Between runs 13 and 14, 27 hours were accumulated. However, no data were taken during this time in that the loop was continually being shut down because of indicated high mercury vapor counts around the loop. Sixteen hours after run No. 14 was started, the loop was shut down because of a loss of flow. Examination of the loop revealed a rupture in the boiler inlet tubing. The failure occurred after 3,876 hours of operation. The ruptured section of tubing was replaced. Results of the examination of the failure are given in the section on loop examination. Run No. 15, which lasted for 1,416 hours, was uneventful. Operation of the loop was normal.

C. Problems

The problems encountered during the operation of the loop were two-fold. The first problem was that of thermocouples breaking and causing shut down of the loop. This was solved by changing the method of attaching the thermocouples to the loop.

The other problem was concerned with obtaining the proper operating conditions. During the first 1250 hours, superheat could not be obtained. Also, trouble was experienced with obtaining proper cooling in the condenser. Upon start-up of Run No. 10, the boiler and superheater finally became conditioned and superheat was obtained. However, the boiling conditions had to be kept below 260 psia and 1060°F to maintain the pressure drop across the orifice at a flow rate of 98 pounds per hour.

V HYDROGEN INJECTION AND REMOVAL

As stated previously, one of the problems associated with using lithium hydride in a heat collector is the transfer of hydrogen into the mercury working fluid by the diffusion through the tubing walls. The hydrogen results from the dissociation of the lithium hydride, which occurs in the 1200 to 1600°F temperature range encountered in the Sunflower system. The presence of hydrogen in the mercury could result in serious operational problems, the most serious of which would be with the centrifugal-type transfer pump which is susceptible to cavitation and resultant loss of prime.

Because of this problem, one of the tasks for the test program was to appraise hydrogen removal techniques. During this task, two different concepts of hydrogen removal were studied. The first involved the diffusion of hydrogen through the tube wall in the vapor regions of the loop. The second method employed centrifugal force to separate the hydrogen in an all-liquid region of the loop. In that a high mass flow rate was required to obtain the centrifugal forces required, this separator was installed in the centrifugal pump by-pass line. Discussion of the centrifugal separator will be made in conjunction with the discussion of the centrifugal pump.

A. Hydrogen Diffusion Windows

As stated, one approach for keeping the influx of hydrogen from becoming a problem would be to provide areas outside of the boiler where hydrogen could diffuse back out of the system. The purpose of this phase was to investigate such areas.

Since the permeability of a metal is a direct function of temperature, any area chosen to act as a window would have to be hot enough so that hydrogen could diffuse through freely. In the Sunflower system, the only area which meets this temperature requirement is the vapor region between the boiler and the turbine. In the work-horse loop, the hydrogen window areas were located in the super-heater and condenser inlet regions of the system.

These windows were segments of the loop tubing which were encased in small vacuum chambers. The chambers served to simulate outer space conditions and to keep the partial pressure of hydrogen on the outer surface of the tube as low as possible. Figure 14 shows the general design of these windows.

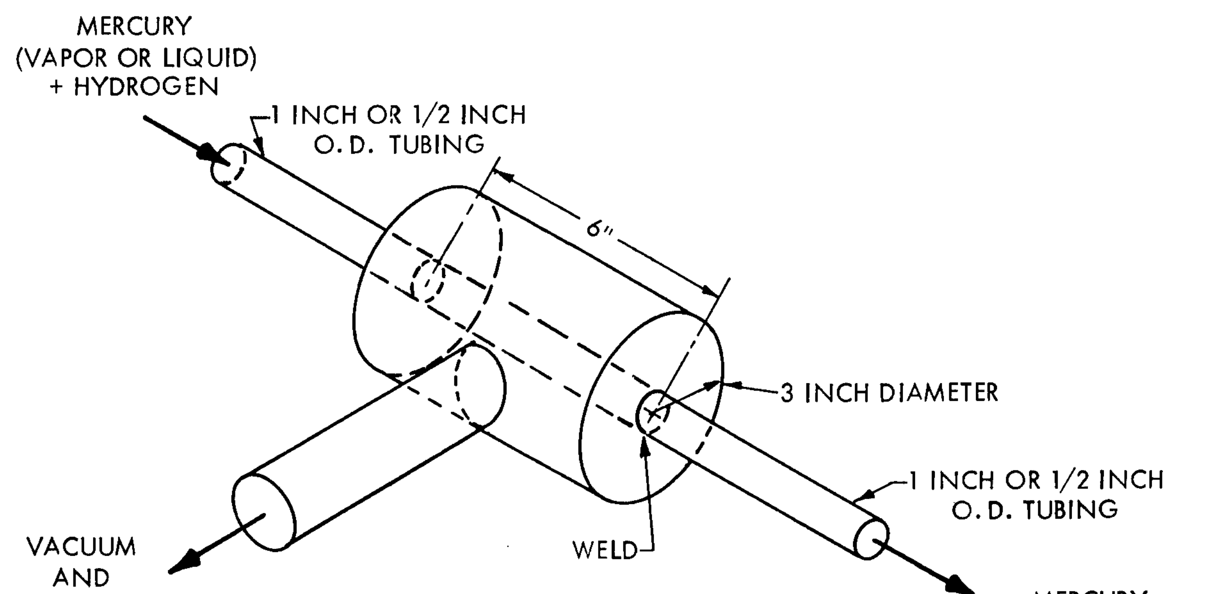

A. ORIGINAL HAYNES ALLOY NO. 25 WINDOWS

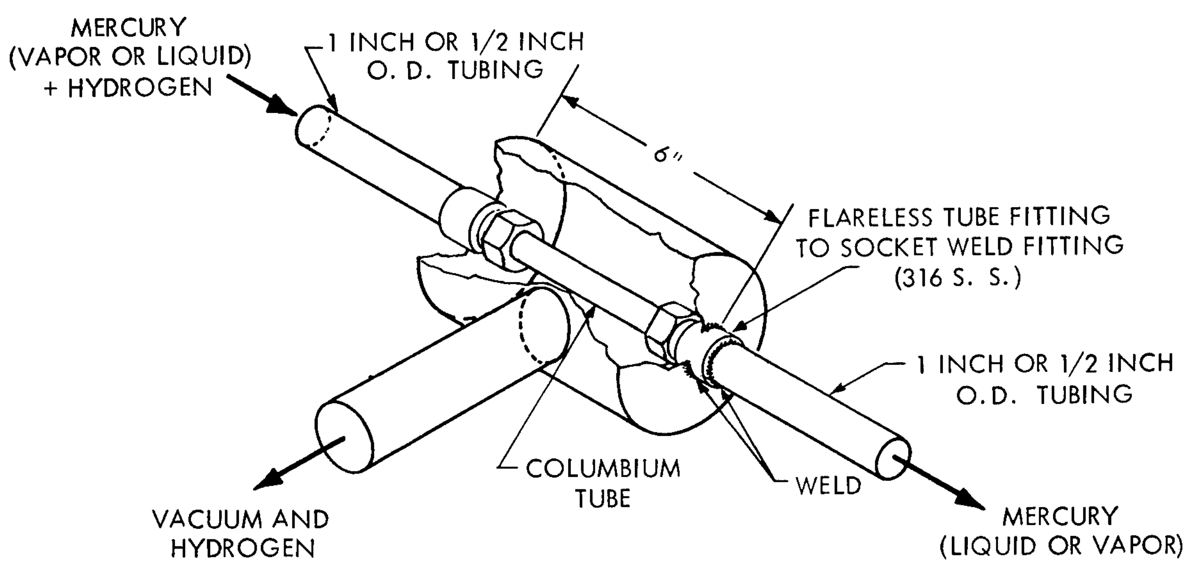

B. COLUMBIUM WINDOWS

FIGURE 14 ISOMETRIC DRAWINGS OF THE HYDROGEN DIFFUSION WINDOWS

1. Materials

The materials tested during the hydrogen removal studies are shown in Table 2. The Haynes alloy No. 25 tubing, which was the first material tested, was part of the original loop. During fabrication of the loop, the vacuum chambers were welded around segments of the tubing to form the windows as illustrated in Figure 14A. The location of these windows is shown in Figures 1 and 2. After 2223 hours of loop operation, the material in the condenser window was changed to columbium. A new chamber was fabricated for this window with a Type 316 SS socket weld-to-flareless tube fitting union welded in each end plate as illustrated in Figure 14B. The flareless tube fittings were used to seal the columbium tubing. The can was mounted in the loop by welding the existing tubing into the socket weld fittings. The location of the window was not changed. Again after 3833 hours of operation, the window materials were changed. The Haynes alloy No. 25 in the superheater was replaced with Croloy 9M tubing and the window was moved closer to the superheater exit. Haynes alloy No. 25 socket weld unions were used to join the Croloy 9M window to the loop tubing. The design of this window was quite similar to that shown in Figure 14B, except that an all-welded construction was used. A new section of columbium tubing was placed in the condenser. Also, a new hydrogen injection port was added to the condenser just ahead of the condenser window. These changes are shown in Figure 2.

2. Vacuum Collection System

The vacuum chambers were connected to a vacuum pumping and collecting system. The pumping part of the system consisted of a mechanical roughing pump, an oil diffusion pump, a Piriani gauge and a McLeod gauge. The measuring part consisted of a collecting chamber and a Toepler pump. The McLeod gauge was used for all pressure readings on both the pumping and collecting system. The complete vacuum system is outlined in Figure 15. Figure 16 shows a photograph of the pumping and collecting portion of the system. The roughing and diffusion pumps were used to pump the system (vacuum and collecting chambers) down to a pressure of approximately 10^{-5}mm Hg. Once the system was pumped down, the vacuum pumps were valved out of the system and the Toepler pump was then used to pump the hydrogen from the vacuum chamber into the collecting chamber. The volume of the collecting chamber was calibrated. Thus, the collecting rate (cc/hr of hydrogen at STP) could be determined directly from the pressure rise in the collecting chamber with time. The pressure was measured manually by means of the McLeod gauge.

Before a collection run was made, a blank leak rate was determined for the entire vacuum system. The leak rate was obtained by valving out the vacuum pumps and measuring the pressure rise in the collecting chamber over a period of time. The Toepler pump was used to insure a positive flow of gas into the collecting chamber.

TABLE 2

HYDROGEN REMOVAL WINDOW MATERIALS

Location	Material	Tube Size O. D. (In.)	Tube Size Wall Thickness (In.)	Joining Method	Hours As Part of Loop
Superheater	Haynes Alloy No. 25	1.00	0.065	Original Tubing	3,629
Superheater	Croloy 9M	0.50	0.083	Welded	1,563
Condenser	Haynes Alloy No. 25	0.50	0.049	Original Tubing	768
Condenser	Columbium	0.62	0.060	Flareless Tube Fittings	2,961
Condenser	Columbium	0.62	0.060	Flareless Tube Fittings	1,563

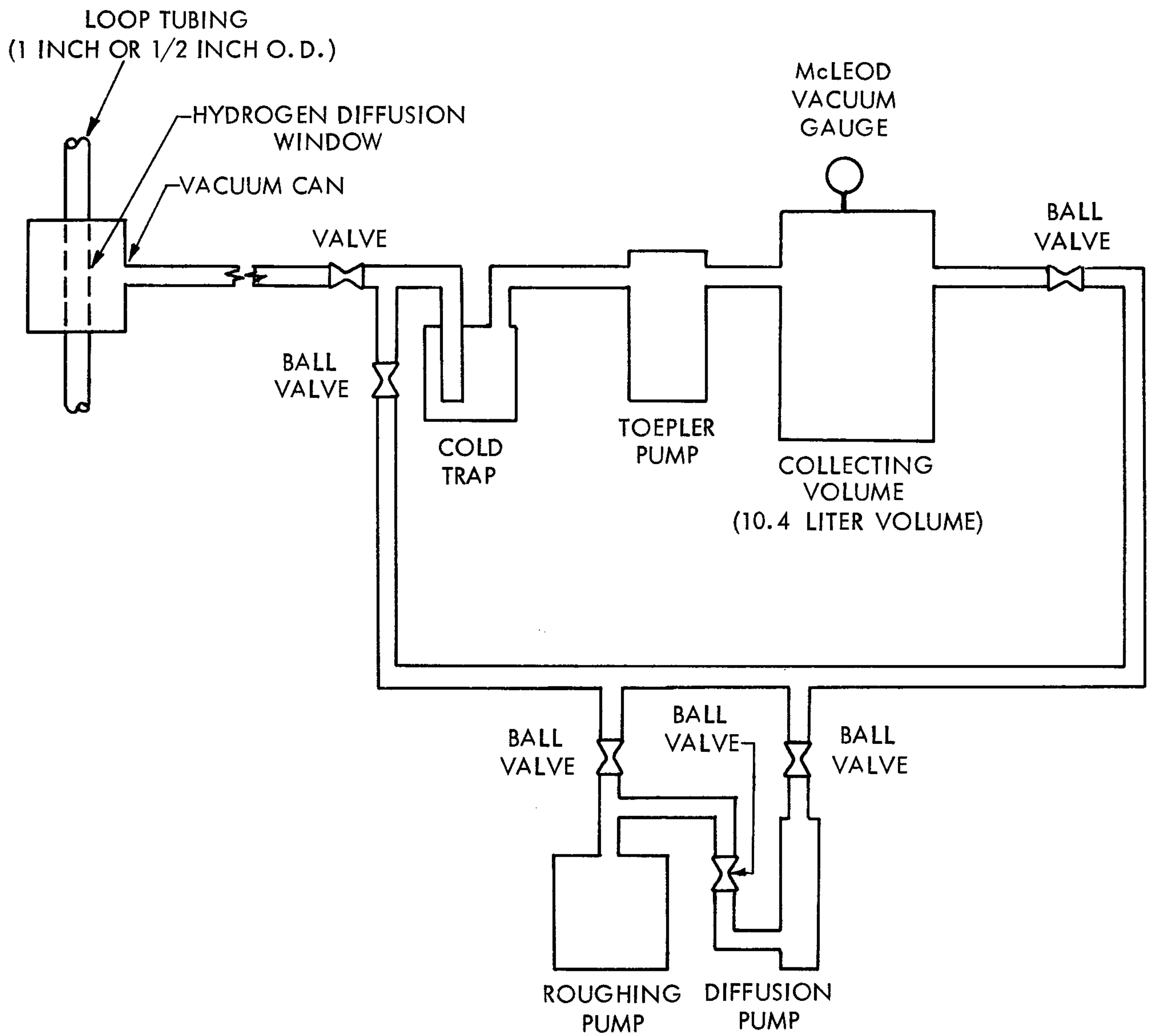

FIGURE 15 SCHEMATIC DIAGRAM OF VACUUM SYSTEM USED FOR COLLECTING AND MEASURING THE AMOUNT OF HYDROGEN COLLECTED

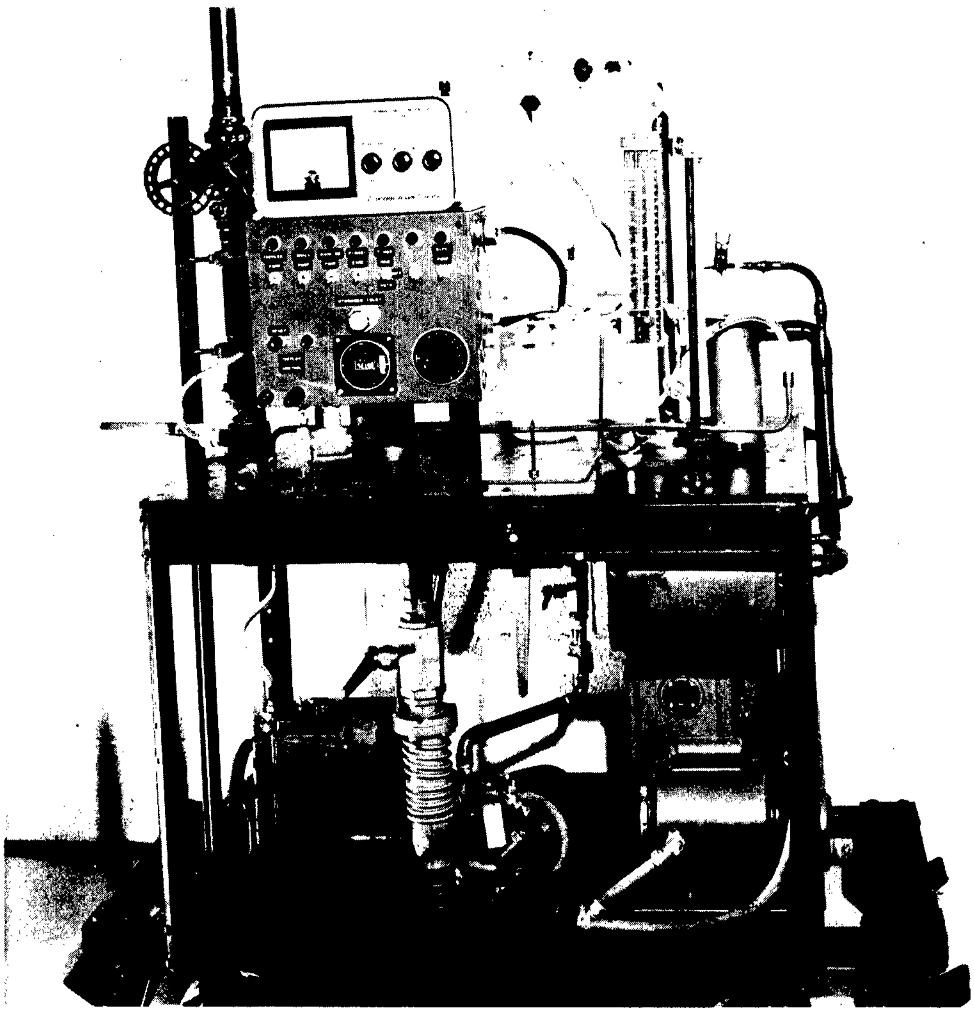

Figure 16. Photograph of Vacuum Hydrogen Collection System.

3. Hydrogen Injection

a. Constant Flow Hydrogen Injection

Two different methods of injecting controlled amounts of hydrogen were used. The first method employed a miniature needle valve to control the rate of hydrogen flow into the loop. This injector consisted of two hydrogen tanks (high and low pressure) and associated pressure regulators, the metering valve and a pressure gauge on either side of the metering valve. Figure 17 shows how the components were arranged. The injector was designed so that the hydrogen flow could be directed into the loop, or diverted to a gas burette for calibration. During an injection run, the rate of flow was regulated by adjusting the metering valve. Throughout the tests in which this injector was used, the pressure drop across the metering valve was held constant at 20 psi. In general, the high pressure tank was used for injecting hydrogen into the loop, whereas the low pressure tank was used for calibration purposes.

With hydrogen gas at conditions between atmospheric pressure and 250 psia, the flow of gas through the metering valve was found to be dependent only on the pressure drop across the valve. Therefore, the calibration of the metering valve was effected by measuring a volume of gas over a given time period for a given set of conditions for the valve. During calibration, the gas pressure inside the gas-burette was held at 1 atm. With a given setting on the valve, the flow was measured while maintaining the pressure upstream of the metering valve at 20 psig. During the injection run, the upstream pressure was adjusted so as to maintain the 20 psi drop across the valve.

Because of the manner in which the work-horse loop was operating at the time, all injection runs were made with an upstream pressure between 200 and 230 psia.

b. Constant Volume Hydrogen Injection

Figures 18 and 19 show the second method used for injecting hydrogen. This method used an automatic pipettor to inject controlled volumes of hydrogen into the loop. As shown in Figure 18, the pipettor was essentially a one cylinder positive displacement pump. Both the pump stroke and pump speed could be varied. Thus, the amount of hydrogen injected per unit time could also be varied. The inlet to the pump was fed from a hydrogen tank equipped with a low pressure (0 to 10 psi) regulator. The outlet of the pump was connected to a manifold containing three solenoid valves. Two of these valves were arranged such that there was an intermediate chamber between the pump and the loop. The purpose of the chamber was to isolate the loop from the pump. This allowed both the loop and the chamber to be

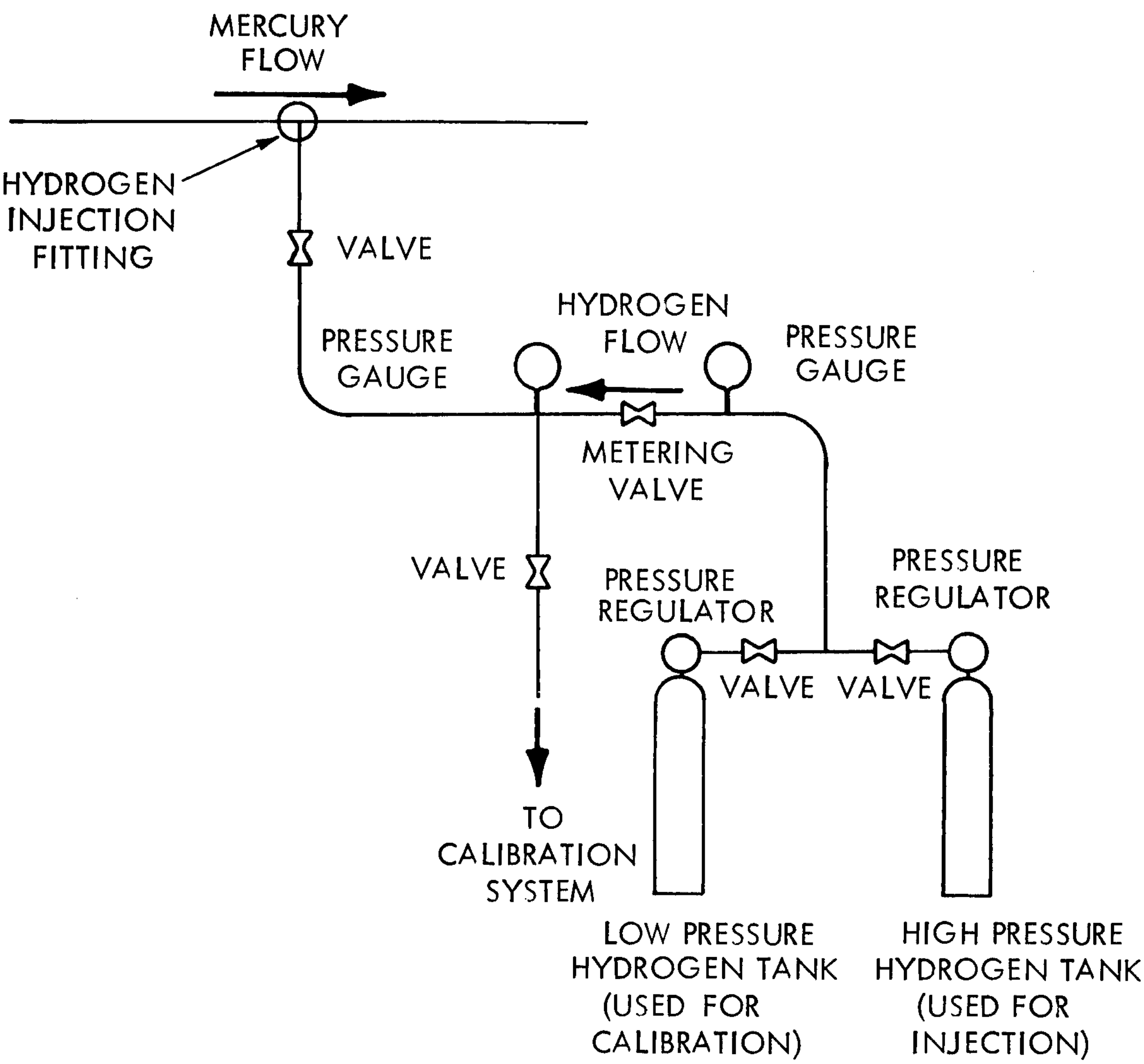

FIGURE 17 SCHEMATIC DIAGRAM OF THE CONSTANT FLOW HYDROGEN INJECTION SYSTEM

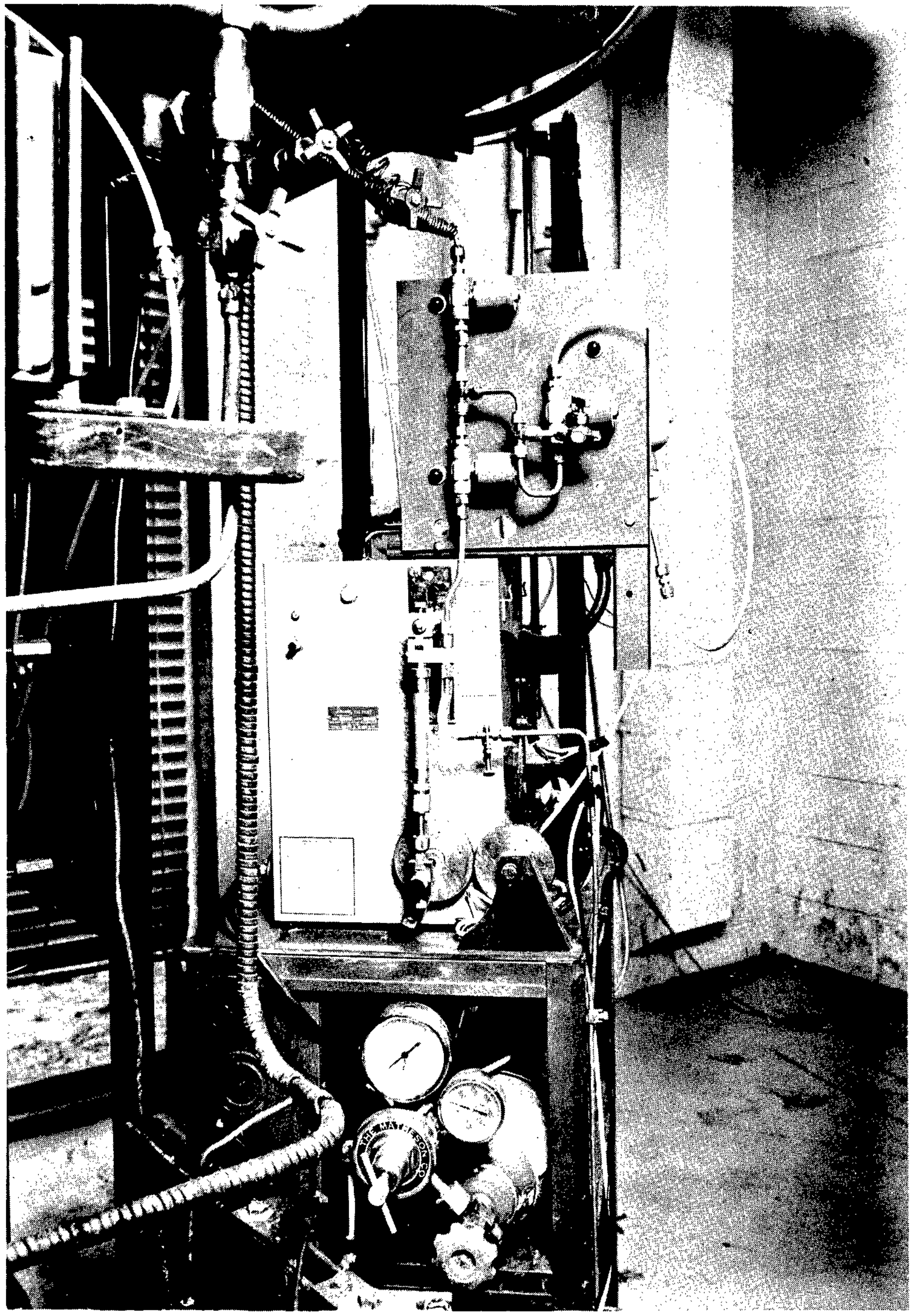

Figure 18. Photograph of Controlled Volume Hydrogen Injection Unit.

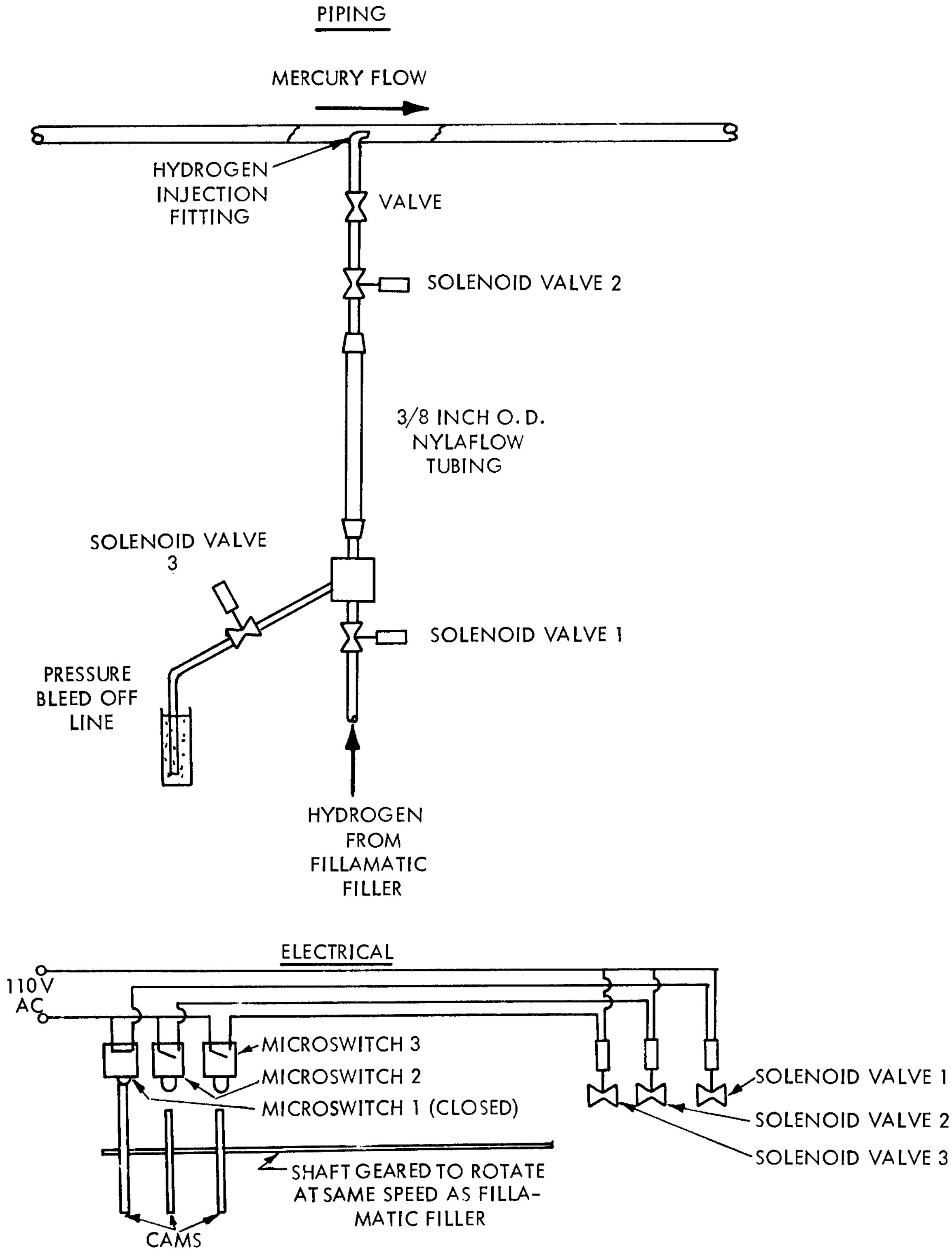

FIGURE 19 SCHEMATIC DIAGRAM OF THE CONTROLLED VOLUME HYDROGEN INJECTION SYSTEM

operated as different pressures. The third valve acted as a bleed off line when going from high pressure back to low pressure. The solenoid valves were opened and closed by micro switches which operated off a cam shaft. The cam shaft was geared to the pump eccentric shaft and rotated at the same speed. The switches were set so that hydrogen would be admitted to the chamber during the compression stroke of the pump. The chamber was closed to the pump and open to the loop during the pump intake cycle. The bleed-off on the chamber was sandwiched between the end of the intake cycle and the beginning of the compression cycle. Operation in this manner allowed a continuous but cyclic injection of hydrogen into the loop.

This system was also calibrated by use of a gas burette. During calibration, the outlet from the chamber was connected to the gas burette which was filled with mercury. The pump was turned on and the hydrogen was allowed to displace the mercury in the burette for a given period of time. Once a volume rate was determined, the injector was connected to the loop and the hydrogen was injected.

4. Injection Fittings

In the original loop configuration, fittings for hydrogen injection were located in the exit of the superheater and subcooler sections (Figure 1). After 3833 hours, the fitting in the superheater was moved upstream of the superheater window as shown in Figure 2. Also, an injection fitting was added in the condenser, just upstream of the condenser window. Figure 20 shows the design of the injection fittings used.

5. Results

A summation of all the work on injection and removal is shown in Table 3. In all, the success was limited. The results can be divided into three categories. In the initial tests, Haynes alloy No. 25 was the window material in both the superheater and condenser. Hydrogen was injected into both the superheater and subcooler and the removal attempts were made on the windows in the superheater and condenser. Except for one run, the amount of hydrogen removed was negligible. In the one run, using the constant flow technique, a removal rate of 5.43 cc/hr. was obtained. However, from observing the operating characteristics of the loop during this run, it appeared as if the loop was overloaded with hydrogen. It did not appear as if there was any relationship between the hydrogen injection and removal locations.

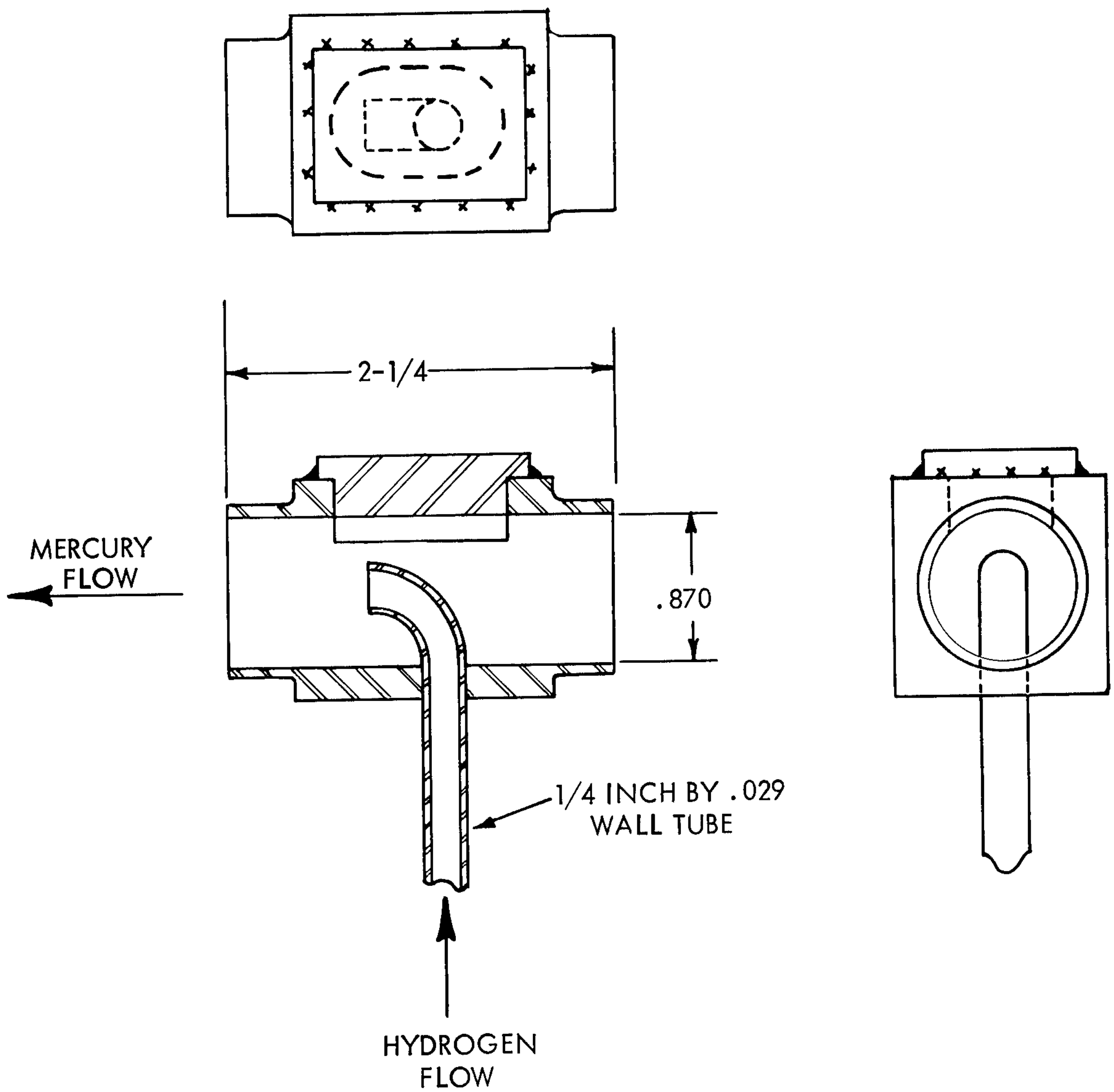

FIGURE 20 SKETCH SHOWING THE OVERALL DESIGN OF THE HYDROGEN INJECTION FITTING USED. THE FITTING USED FOR THE 1/2 INCH TUBING WAS OF THE SAME DESIGN EXCEPT THAT THE I. D. TUBE DIMENSION WAS .402 INCH RATHER THAN .87 INCH

TABLE 3
WORK-HORSE LOOP HYDROGEN INJECTION AND REMOVAL SUMMARY

Run No.	Injection Method	Injection Port Location	Collection Port			Collecting System Check			Injection Data			Hydrogen Collection			
			Location	Material	Temperature °F	Time (Min.)	Volume Collected (cc)	Blank Rate (cc/hr.)	Time (Min.)	Injection Rate (cc/hr.)	Volume Injected (cc)	Time (Min.)	Volume Collected (cc)	Collection Rate (cc/hr.)	Corrected Collection Rate (cc/hr.)
1	Constant Flow	Subcooler	Superheater	Haynes 25	1195	180	0.169	0.056	355	540	a	151	0.176	0.071	0.015
2	Constant Flow	Subcooler	Superheater	Haynes 25	1200	60	0.0615	0.0615	120	414	a	255	0.286	0.067	0.002
3	Constant Flow	Subcooler	Superheater	Haynes 25	1170	60	0.0505	0.0505	180	450	1350 (b)	300	27.4	5.48	5.43
4	Constant Volume	Superheater	Superheater	Haynes 25	1215	60	0.0696	0.0696	120	450	900	180	0.268	0.0953	0.026
5	Constant Volume	Superheater	Condenser	Haynes 25	560	157	0.0533	0.0205	50	13	11	1543	0.425	0.018	0
6	Constant Volume	Subcooler	Condenser	Haynes 25	650	77	0.0725	0.0565	150	9.5	24	2976	1.09	0.0218	0
7	Constant Volume	Subcooler	Condenser	Haynes 25	645	1152	0.137	0.007	180	32	96	2888	0.411	0.009	0.002
8	Constant Volume	Subcooler	Condenser	Columbium	595	72	0.0438	0.0365	310	10	51	360	0.189	0.0315	0.004
9	Constant Volume	Subcooler	Condenser	Columbium	600	6047	1.85	0.0183	160	9	24	420	0.274	0.0391	0.02
10	Constant Volume	Superheater	Condenser	Columbium	580	5880	1.19	0.0122	90	23	35	414	0.100	0.0145	0.002
11	Constant Volume	Condenser	Condenser	Columbium	550	20	0.032	0.096	60	100	100	25	0.13	0.31	0.28
			Superheater	Croloy 9M	1085	6	0.029	0.29				21	0.52	1.49	1.20
			Condenser	Columbium	550							38	0.61	0.96	0.93
			Superheater	Croloy 9M	1085	Blank Rates Same As Shown Above						9	0.21	1.40	1.10
12	Constant Volume	Condenser	Condenser	Columbium	675	35	0.025	0.042	115	100	125	30	0.026	0.052	0.010
			Superheater	Croloy 9M	1165	30	0.186	0.392				30	0.35	0.70	0.31
			Condenser	Columbium	675							40	0.25	0.33	0.29
			Superheater	Croloy 9M	1165	Blank Rates Same As Shown Above						63	1.1	1.05	0.65
13	Constant Volume	Condenser	Condenser	Columbium	675				40	100	67	40	0.111	0.17	0.13
			Superheater	Croloy 9M	1165							48	0.89	1.11	0.71
			Condenser	Columbium	675							66	0.80	0.73	0.69
			Superheater	Croloy 9M	1165							61	1.233	1.21	0.81
			Condenser	Columbium	675							22	0.14	0.38	0.34
			Superheater	Croloy 9M	1165							40	0.69	1.03	0.63

a. A negligible amount of hydrogen entered the loop.

b. Most of the hydrogen injected collected in the condenser-subcooler region and escaped when an attempt was made to bleed off mercury from the sub-cooler.

After 2223 hours of operation, the window material in the condenser was changed to columbium. Three attempts (Runs 8, 9, and 10) were made to remove hydrogen through the columbium window. These attempts were also unsuccessful. However, it was felt that this was partly due to oxidation of the columbium tube. Before installation, the columbium tube could not be protected from surface adsorption of oxygen. Also, the tube was mounted within the vacuum chamber by use of flareless tube fittings because of welding problems. This too caused trouble, in that when the chamber was opened to replace the columbium tube, it was found that the fittings had leaked and allowed mercury to enter the vacuum chamber. Oxidation of the columbium also undoubtedly occurred at this time.

At this time (after 3833 hours of loop operation), the window materials in both the superheater and condenser were changed to Croloy 9M and a new piece of columbium, respectively. Also, a manifold was attached to the vacuum chambers. This was done so that removal could be attempted from either area during the same injection run. Three separate injection runs were made with the removal alternating between the two windows. As shown in Table 3, the absolute amount of hydrogen removed was greater. However, the removal rates were still extremely low.

While testing the columbium window during Run No. 11 (which was not recorded), the leak rate for the separator suddenly increased to 7.5 cc/hr. This occurred after 405 hours of operation had been accumulated on the columbium tube. At this time the vacuum system was disconnected from the columbium window chamber in order to inspect the chamber. The tube fittings apparently leaked, since a pool of mercury about three inches deep was found in the bottom of the chamber.

At the end of loop operation, the columbium tube was removed from the chamber. As with the first tube, the columbium tube was again oxidized on the outer surface.

B. Centrifugal Pump

The capability of the centrifugal pump to accept hydrogen gas without losing prime was evaluated by injecting hydrogen into the inlet side of the pump and observing changes in pump performance as hydrogen was injected. Hydrogen was introduced using two techniques:

1) In the first series of tests, known quantities of hydrogen were injected instantaneously, and the reaction of the pump to these single bubbles of hydrogen was observed.

2) In the second series of tests, hydrogen was injected at a constant rate, and the change in performance of the pump with time was observed.

The test procedure used and results obtained for each series of tests will be discussed separately. First, however, some remarks concerning the performance of the pump in general are in order. Initial check-out of the pump revealed that under certain conditions the seals in the pump leaked mercury excessively to the atmosphere. This situation obviously could not be tolerated during testing with hydrogen since, with leakage, the quantity of hydrogen actually passing through the pump could not be accurately determined. It was also observed that the performance of the pump was far below that of other pumps of the same design (6). For these reasons, the pump was dismantled and examined. Several O-ring seals were found to have been heat affected and were replaced. It was also observed that the impeller had been rubbing against the housing for some reason which could not be explained. These two factors could easily account for the poor performance and excessive leakage experienced.

After re-assembly of the pump, tests were continued to determine the pump's performance. During these tests it was observed that seal leakage was still present and that the leakage increased as dead-head conditions were approached. Consequently, it was decided to determine threshold conditions at which leakage through the seals was detected. These tests indicated that the pump could be operated over a limited range of conditions with essentially zero seal leakage. With these limitations in mind, evaluation of the hydrogen swallowing capabilities of the pump were conducted. At frequent intervals during the testing program, the seal leakage was re-evaluated, and seals were replaced when deterioration first became evident. In all, the pump was operated for a total of approximately 1000 hours.

1. Single Bubble Tests

Hydrogen was injected into the pump inlet using the apparatus shown in Figure 21. The gas was allowed to bubble through the mercury column in the gas burette until the desired quantity of hydrogen had entered the burette. By adjusting the leveling bulb, the quantity of hydrogen was read without the effects of the head of mercury upon the hydrogen. This quantity was then converted to standard conditions. The gas was injected into the centrifugal pump through stopcock A by raising the leveling bulb so as to force the hydrogen bubble into the pump.

During the testing, hydrogen bubbles were injected into the centrifugal pump inlet in increments of 0.17 cc (STP), beginning with 0.17 cc (STP) and continuing until the quantity of hydrogen required to cause the pump to lose prime was determined. The data were obtained as a function of the following variables:

1) Pump inlet pressure

2) Pump outlet pressure

3) Pump speed

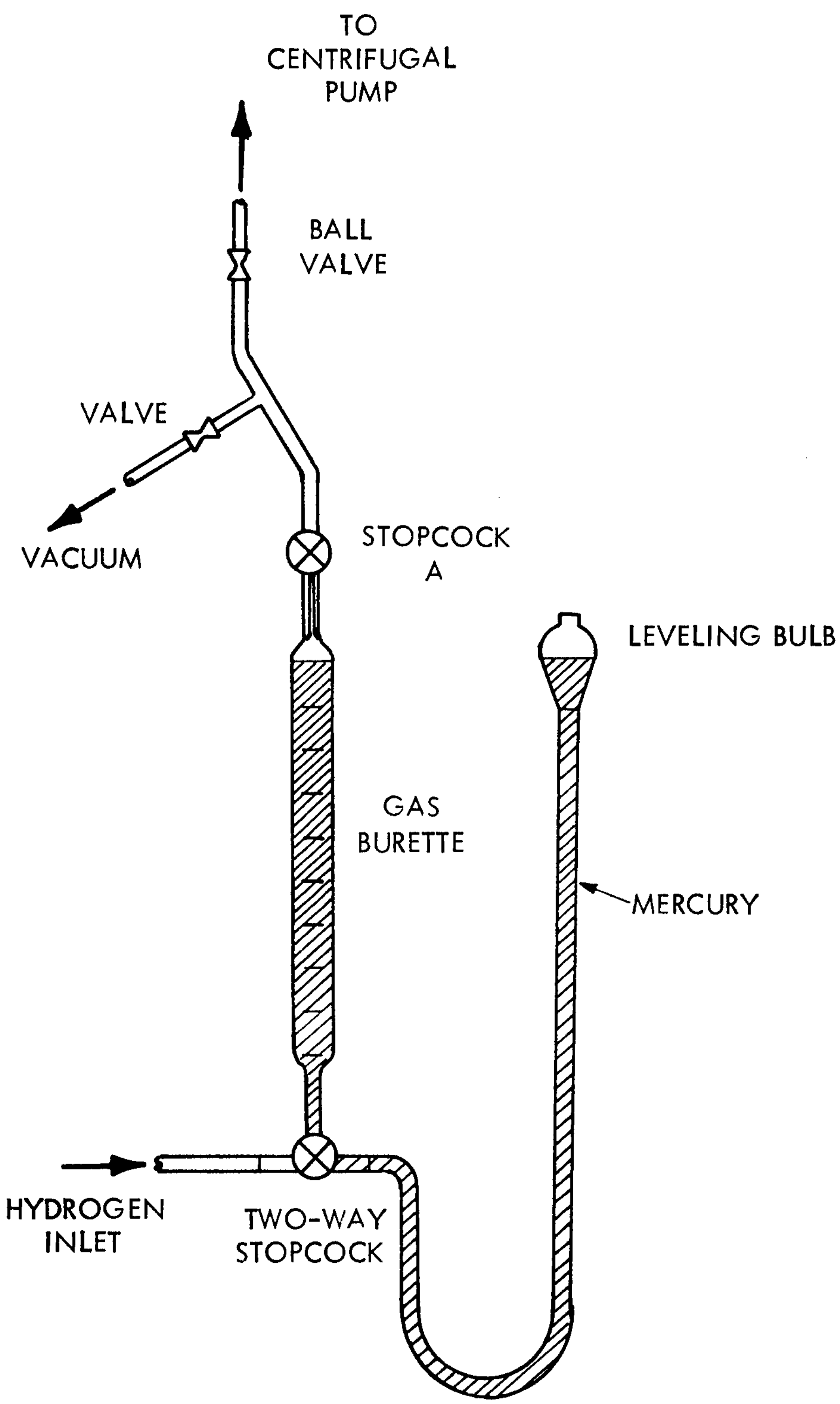

FIGURE 21 SCHEMATIC DRAWING OF THE DEVICE USED TO INJECT SINGLE BUBBLES OF HYDROGEN

When the hydrogen was injected into the pump, these variables were observed closely. It was noted that, as the quantity of hydrogen was increased, the pump performance would drop off but would return to its original level instantaneously. However, there appeared to be a threshold volume at which pump performance would drop and would not be regained, even after two or three minutes. Loss of prime did not always occur with the same quantity of hydrogen for one specific setting of pump conditions. That is, for a given set of conditions, the pump would regain prime one time but would lose it completely when these conditions were repeated.

Table 4 summarizes the data collected with single hydrogen bubbles. This table shows only those data points for which the pump lost prime and failed to regain it. Those cases in which the pump performance decreased but then increased again are ignored here since the most important criterion of pump performance in these tests was complete loss of prime. Figures 22 through 24 show the minimum quantity of hydrogen which caused the pump to lose prime for specific inlet and outlet pressures and pump speeds.

Examination of the data reveals a considerable degree of scatter. Attempts to correlate the quantity of hydrogen required to cause loss of prime with pump speed for specific pump inlet and outlet pressures have shown that no clear-cut relationship is present. It is obvious, however, that as the pump inlet pressure is increased, capability of the pump to accept larger quantities of hydrogen in also increased. In fact, in the case of the tests with an 11.5 psia inlet pressure, the pump showed the capability of accepting extremely large hydrogen volumes. This statement must be made with some reservation since the large hydrogen bubbles tended to break up as they entered the pump. In any event, extreme stability of the pump was demonstrated with an inlet pressure of 11.5 psia.

Further examination of Figurds 22, 23, and 24 shows that, for specific pump conditions, there is a maximum quantity of hydrogen that may be safely intorudced into the pump without experiencing loss of prime. These data were evaluated, keeping in mind the fact that some seal leakage may have gone undetected during testing, and the apparent permissible hydrogen volumes for satisfactory pump operation were determined. This information in summarized in Table 5.

TABLE 4

QUANTITY OF HYDROGEN TO CAUSE CENTRIFUGAL PUMP TO LOSE PRIME

Inlet Pressure psia	Outlet Pressure psia	Pump Speed rpm	Volume of Hydrogen cc (STP)
5.5	201.5	33,000	0.35, 0.35
		34,000	0.35, 0.52, 0.52
		35,000	0.69, 0.69
		36,000	0.35, 0.35, 0.52, 0.52, 0.69
		37,000	1.0
		38,000	0.69, 0.87
		39,000	0.35, 0.35, 0.52, 0.69, 0.69, 0.87
		40,000	0.35, 0.35, 0.52, 0.52
5.5	251.5	33,000	0.52, 0.52, 0.69, 0.87
		34,000	0.69, 0.87, 1.74, 2.60
		35,000	0.69
		36,000	0.35, 0.52, 0.52, 0.52, 0.69
		37,000	0.52, 0.52
		38,000	0.52
		39,000	0.35, 0.52
		40,000	0.35, 0.35, 0.35
5.5	301.5	32,000	0.69
		33,000	0.35, 0.35, 0.52
		34,000	0.35, 0.35, 0.87, 0.87
		35,000	0.35, 0.35, 0.69
		36,000	0.35, 0.35, 0.87, 0.87
		37,000	0.17, 0.17, 0.17, 0.35, 0.35, 0.52
		38,000	0.35, 0.35, 0.35
		39,000	0.17, 0.17, 0.35, 0.35, 0.52, 0.52
		40,000	0.35, 0.35
8.5	201.5	33,000	0.69
		33,500	0.87, 0.87
		34,000	2.08
		35,000	1.56, 1.56
		36,000	1.22, 1.56, 2.08, 2.08
		36,750	0.69, 0.69
		37,000	0.87, 1.39, 1.56
		38,000	1.56, 1.56
		39,000	1.04, 1.04
		40,000	0.69, 0.69

TABLE 4 (Continued)

Inlet Pressure psia	Outlet Pressure psia	Pump Speed rpm	Volume of Hydrogen cc (STP)
8.5	251.5	33,000	> 1.56
		34,000	1.74, 2.08
		35,000	2.61, 2.61
		36,000	1.39, 2.78, 2.78
		37,000	1.56, 1.74
		38,000	1.39, 1.92, 1.92
		39,000	1.22, 1.39, 1.39
		40,000	0.87, 0.87
8.5	301.5	33,000	0.87, 1.04, 1.22, 1.39, 1.74, 2.43
		34,000	1.39
		35,000	2.26, 2.26, 2.61
		36,000	2.08, 2.08
		37,000	1.56, 1.56, 1.74
		38,000	1.22
11.5	201.5	33,000	>6.94
		34,000	>7.81
		35,000	>6.09
		36,000	>13.0
		37,000	>8.69

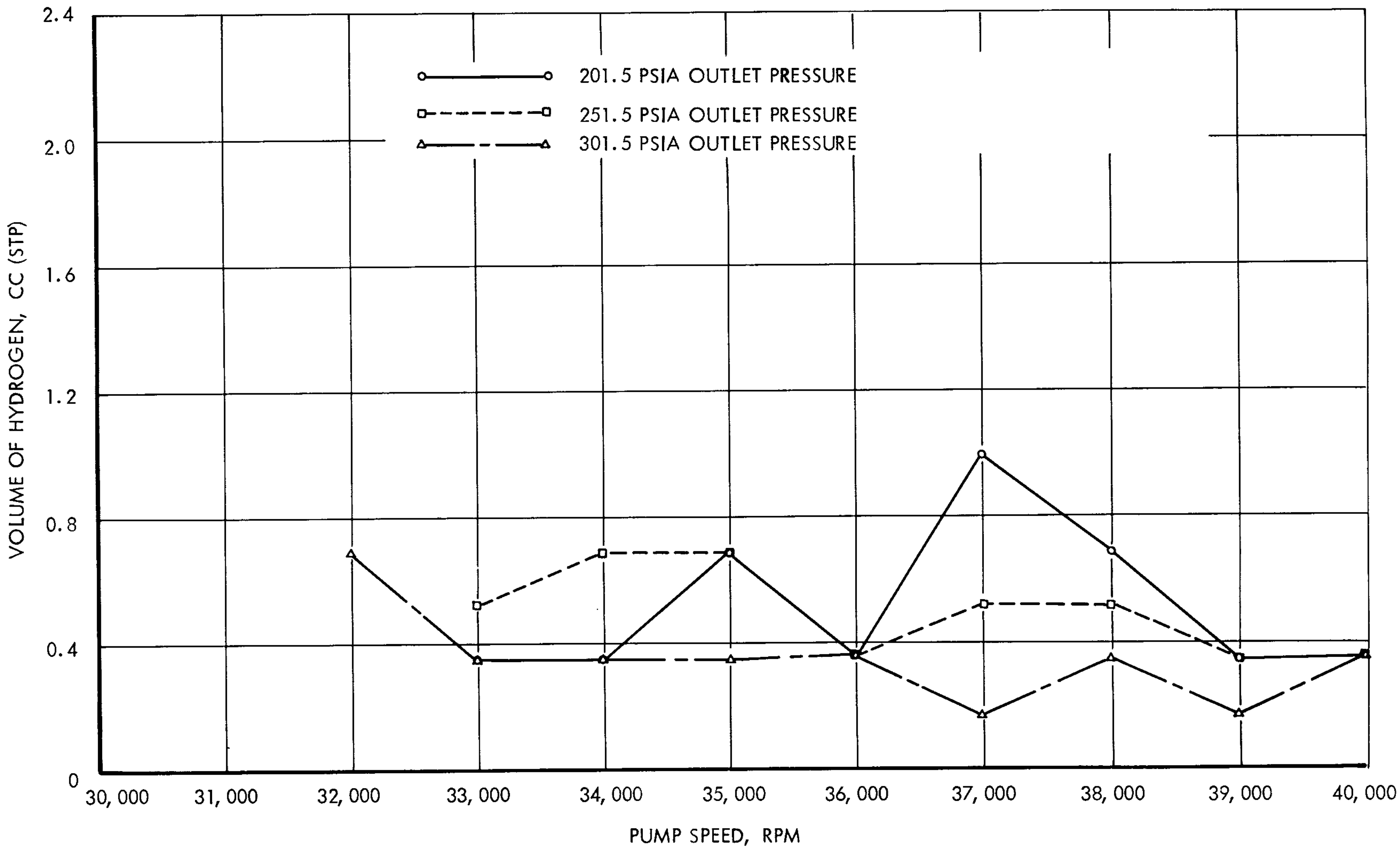

FIGURE 22 MINIMUM QUANTITY OF HYDROGEN TO CAUSE LOSS OF PRIME AT PUMP INLET PRESSURE OF 5.5 PSIA

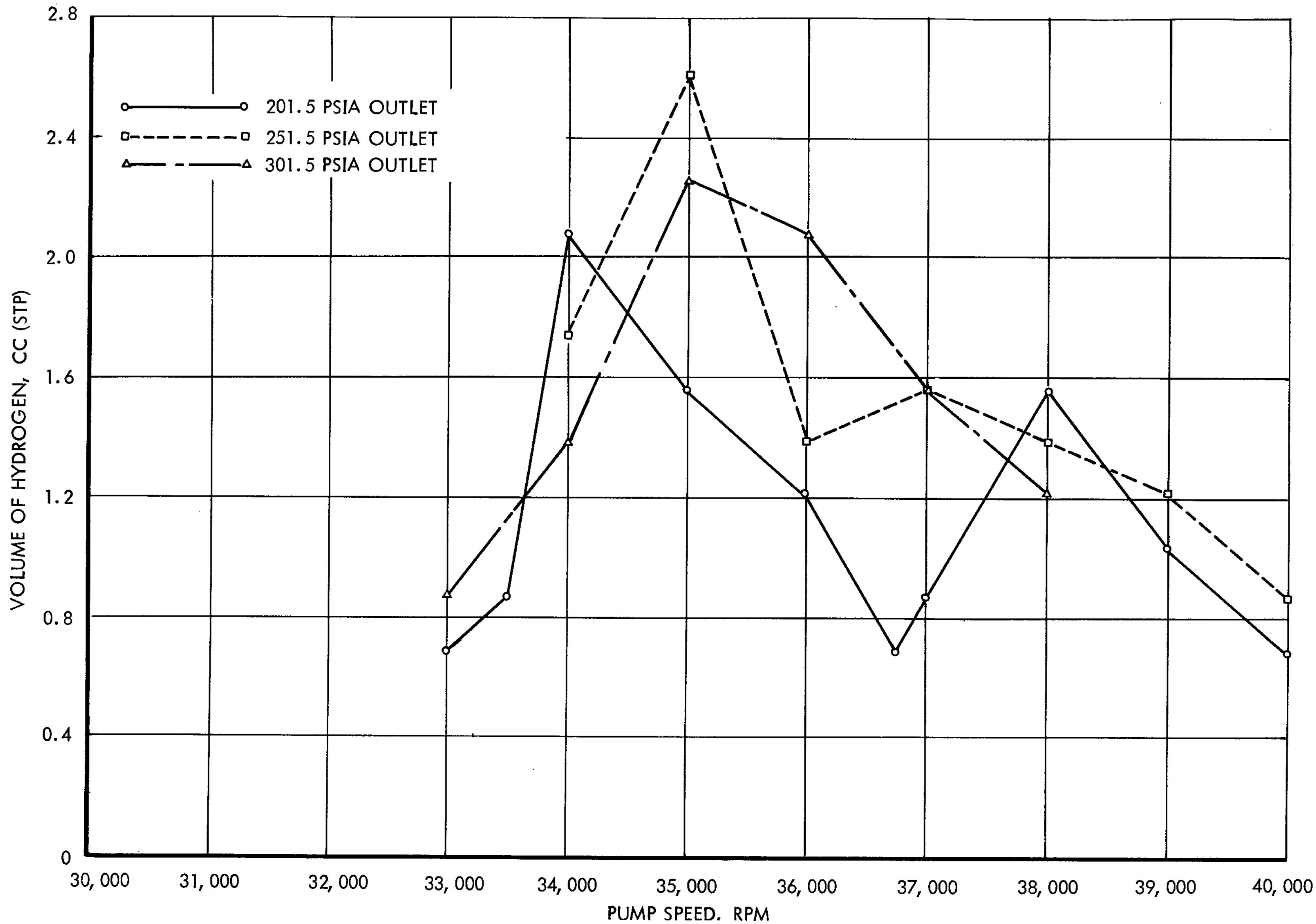

FIGURE 23 MINIMUM QUANTITY OF HYDROGEN TO CAUSE LOSS OF PRIME AT PUMP INLET PRESSURE OF 8.5 PSIA

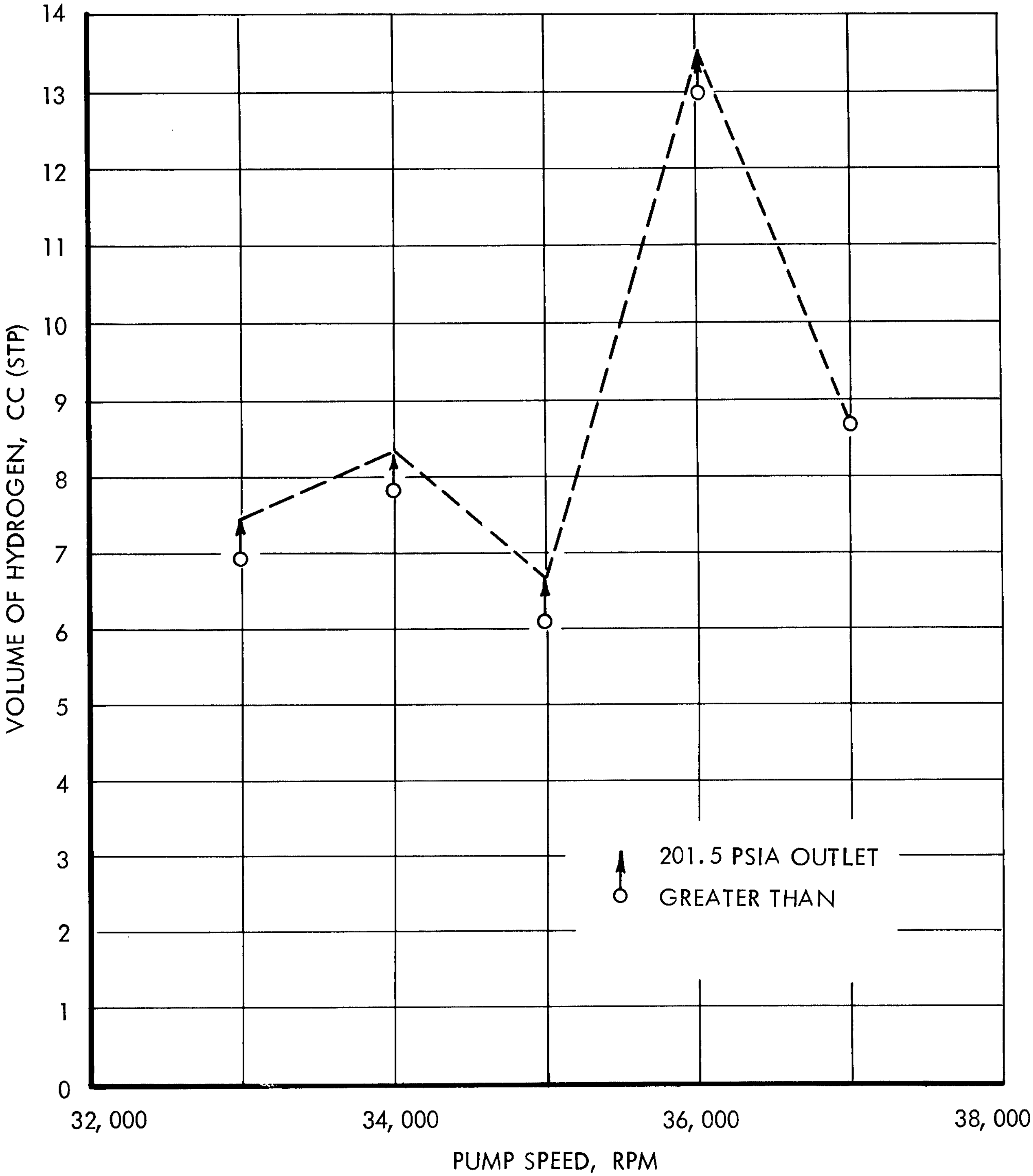

FIGURE 24 MINIMUM QUANTITY OF HYDROGEN TO CAUSE LOSS OF PRIME AT PUMP INLET PRESSURE OF 11.5 PSIA

TABLE 5

MAXIMUM QUANTITY OF HYDROGEN THAT MAY BE INTRODUCED INTO THE CENTRIFUGAL PUMP INLET WITHOUT LOSS OF PRIME

Pump Speed rpm	Pump Inlet Pressure psia	Pump Outlet Pressure psia	Volume of Hydrogen cc (STP)
33,000-40,000	5.5	201.5	0.35
33,000-40,000	5.5	251.5	0.35
32,000-36,000	5.5	301.5	0.35
36,000-40,000	5.5	301.5	0.17
33,000-40,000	8.5	201.5	0.69
33,000-40,000	8.5	251.5	0.87
33,000-40,000	8.5	301.5	0.87
33,000-37,000	11.5	201.5	>6.0

2. Constant Rate Tests

In this series of tests, hydrogen was injected into the centrifugal pump inlet using the apparatus shown schematically in Figure 25. With valves A, C, and E closed, the system was first evacuated through valve B. Valve B was then closed, valves A and E were opened, and hydrogen was introduced into the calibrated volume. After closing valve A, the argon over-pressure was set at 10 psig, valve C was opened, and hydrogen was allowed to bleed into the centrifugal pump inlet at a constant rate through valve F. As hydrogen left the calibrated volume, the level in the mercury reservoir would fall, resulting in a decrease in the level in the mercury pressure switch, breaking the electrical contact. This allowed the solenoid valve E to open, and argon flowed into the mercury reservoir until the original pressure had been re-established, at which time valve E would again close. The hydrogen was thus maintained at a constant pressure (± 2 psig) in the calibrated volume during the course of a test. The quantity of hydrogen introduced into the centrifugal pump was determined by noting the change in level in the calibrated volume with time. These volumes were then converted to standard conditions.

For this series of tests, the gravity hydrogen separator was removed from the by-pass around the centrifugal pump so that the hydrogen injected into the pump inlet could circulate through the by-pass line and re-enter the pump. This type of test thus simulated the condition found in the Sunflower system more closely than if the hydrogen had been removed from the by-pass line after passing through the pump. The performance tests on the pump were also run in conjunction with the centrifugal hydrogen separator. The separator was installed in a by-pass at the pump exit as shown in Figure 2. The entire centrifugal pump by-pass line was wrapped with Briskeat heating tapes, and some tests were conducted at 350°F rather than at ambient temperature in order to improve the efficiency of the centrifugal hydrogen separator. Examination of the data revealed that neither the operation of the centrifugal hydrogen separator nor the increase in temperature to 350°F had any apparent effect on the performance of the pump with continuous injection of hydrogen. Consequently, the data presented on pump operation does not indicate those cases in which the centrifugal separator was operated nor those in which the temperature was increased to 350°F.

All of the pump performance tests were conducted with a pump inlet pressure of 5.5 psia. The pump speed was varied from 35,000 to 40,000 rpm. Tests were conducted with pump outlet pressures of 201.5, 251.5, and 351.5 psia. Hydrogen was injected into the pump outlet at constant rates, and the time required to cause the pump to lose prime was determined. The rate of hydrogen injection was then determined by noting the volume of hydrogen removed from the calibrated volume (Figure 23). The data collected are summarized in Table 6 and Figures 26 through 28.

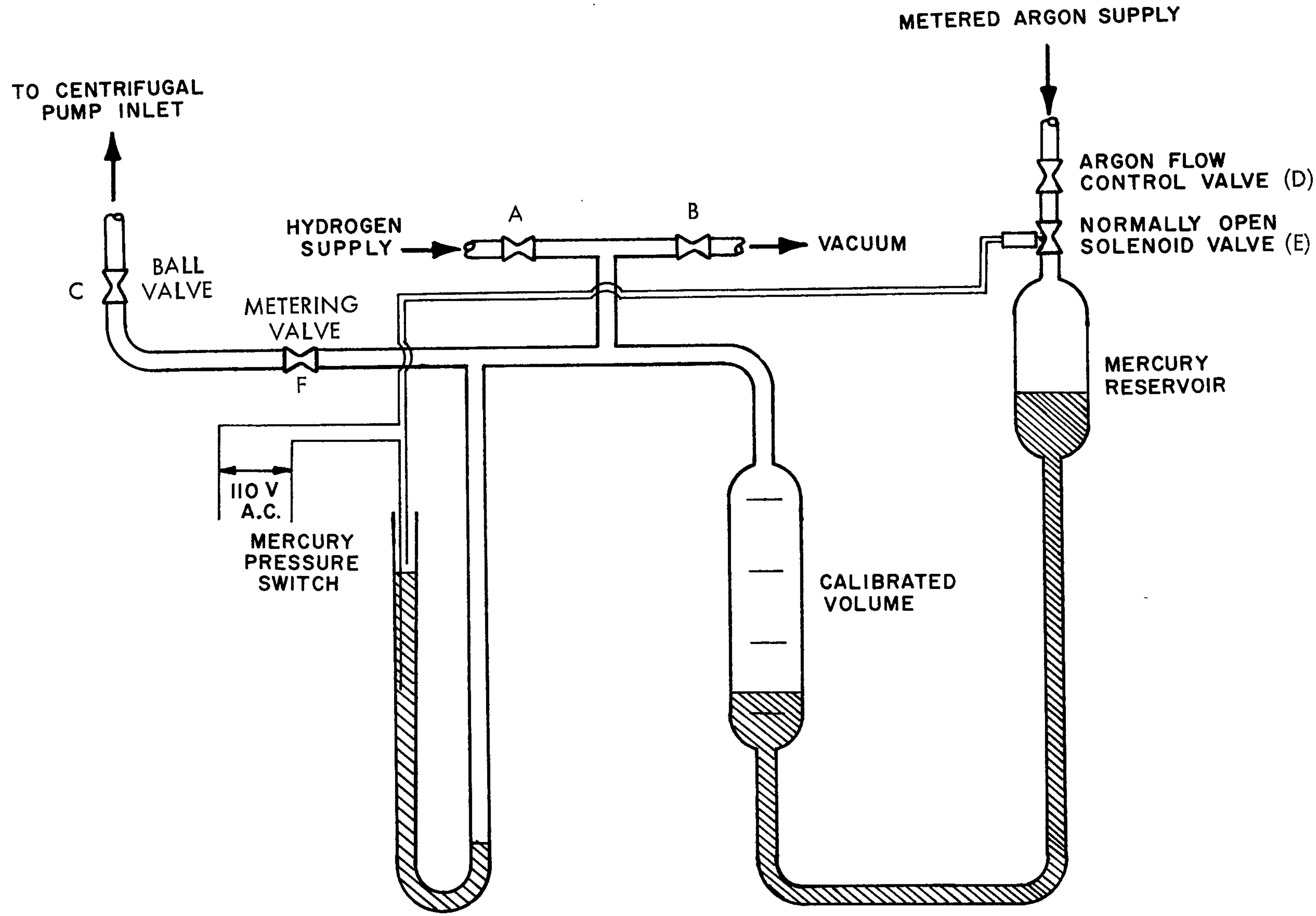

FIGURE 25 SCHEMATIC DRAWING OF THE CONSTANT RATE HYDROGEN INJECTION UNIT

TABLE 6

TIME REQUIRED TO CAUSE LOSS OF PRIME OF THE CENTRIFUGAL PUMP WITH A CONSTANT RATE OF HYDROGEN INJECTION AT A PUMP INLET PRESSURE OF 5.5 PSIA

Pump Outlet Pressure psia	Time For Loss Of Prime At A Given Pump Speed											
	35,000 RPM		36,000 RPM		37,000 RPM		38,000 RPM		39,000 RPM		40,000 RPM	
	Injection Rate cc(STP)/Hr.	Time Min.	Injection Rate cc(STP)/Hr.	Time Min.	Injection Rate cc(STP)/Hr.	Time Min.	Injection Rate cc(STP)/Hr.	Time Min.	Injection Rate cc(STP)/Hr.	Time Min.	Injection Rate cc(STP)/Hr.	Time Min.
201.5	90	25	82	>60	90	30	75	6	75	>30		
	90	20	94	19	98	55	90	20	82	>60	90	>30
	179	5	146	46	170	51	90	>60	90	>30	241	24
	198	27	197	34	197	41	318	14	90	10		
									628	5		
251.5	80	45	122	>55	75	95	168	25	75	>60	119	>15
	90	>60	137	26	117	34	226	>30	208	30	184	>22
	160	14	192	14	223	14	238	15	251	>6		
	241	24										
351.5	90	20	75	60	67	30	72	>50	60	>15		
	96	>80	77	>70	76	70	75	>60	119	15		
	176	>60	179	>60	90	>60	179	10	268	>20		
	248	9	310	13	161	25						
					202	20						

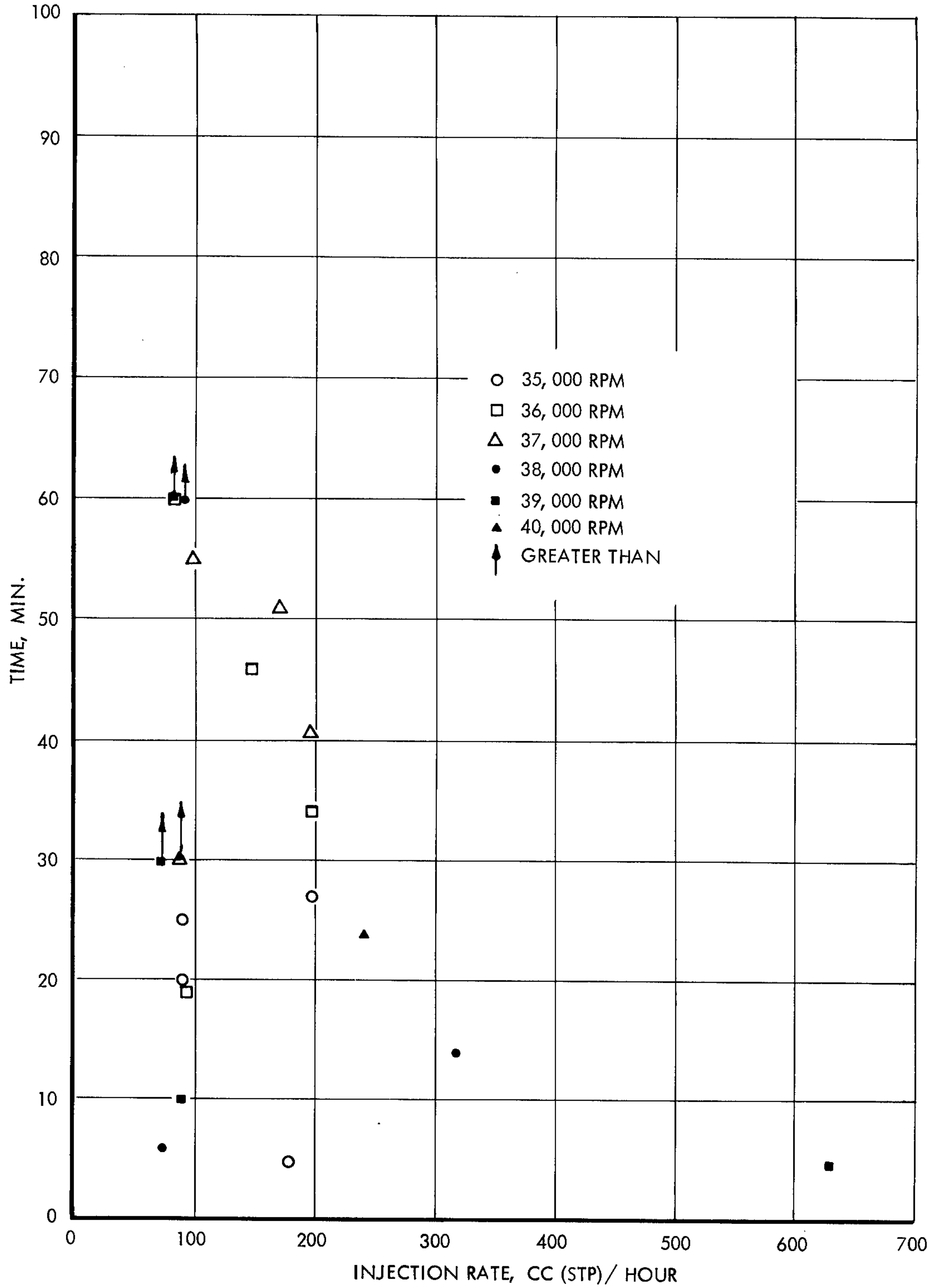

FIGURE 26 TIME REQUIRED TO CAUSE LOSS OF PRIME WITH A CONSTANT RATE OF HYDROGEN INJECTION. 5.5 PSIA PUMP INLET PRESSURE. 201.5 PSIA PUMP OUTLET PRESSURE

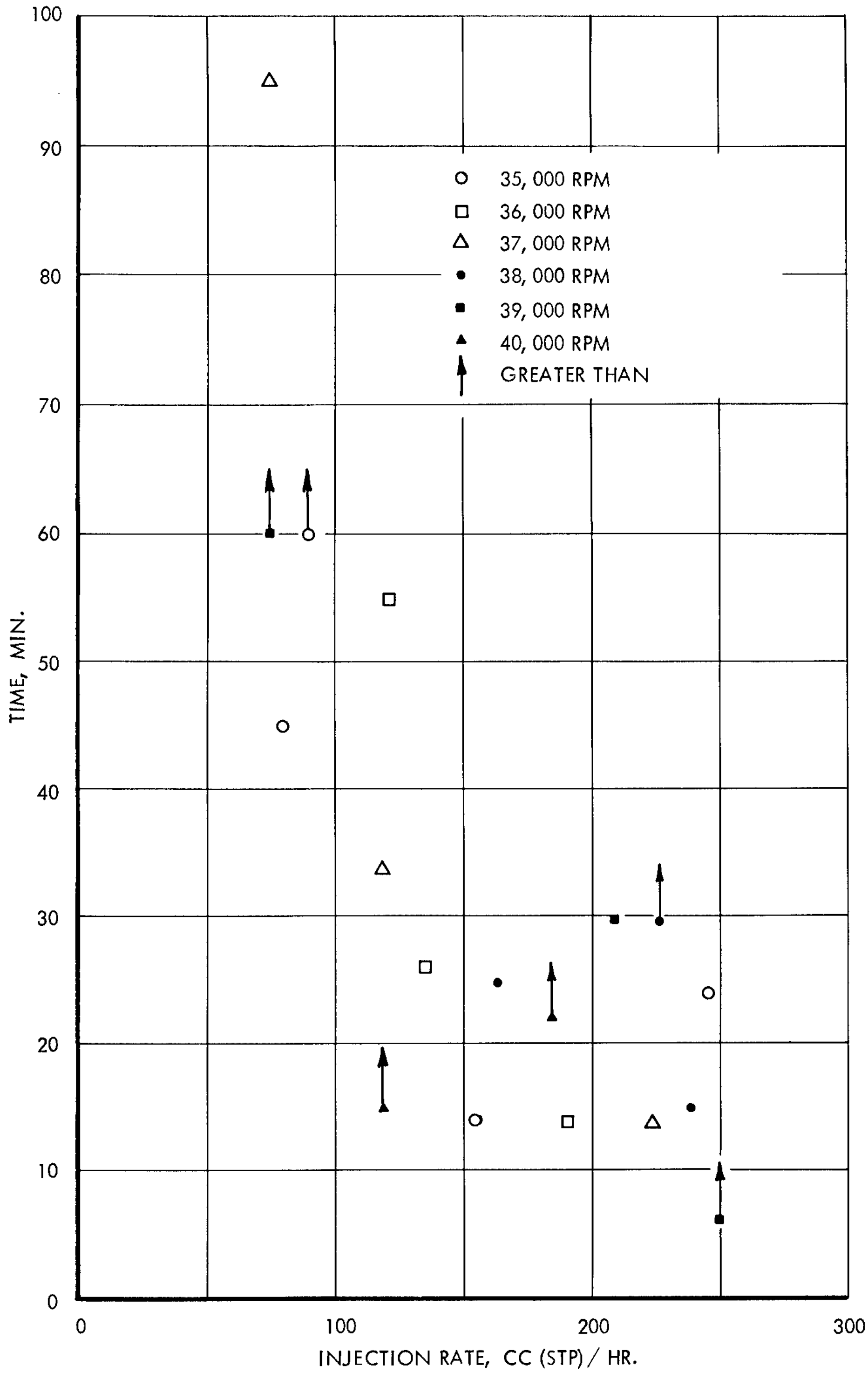

FIGURE 27 TIME REQUIRED TO CAUSE LOSS OF PRIME WITH A CONSTANT RATE OF HYDROGEN INJECTION. 5.5 PSIA PUMP INLET PRESSURE. 251.5 PSIA PUMP OUTLET PRESSURE

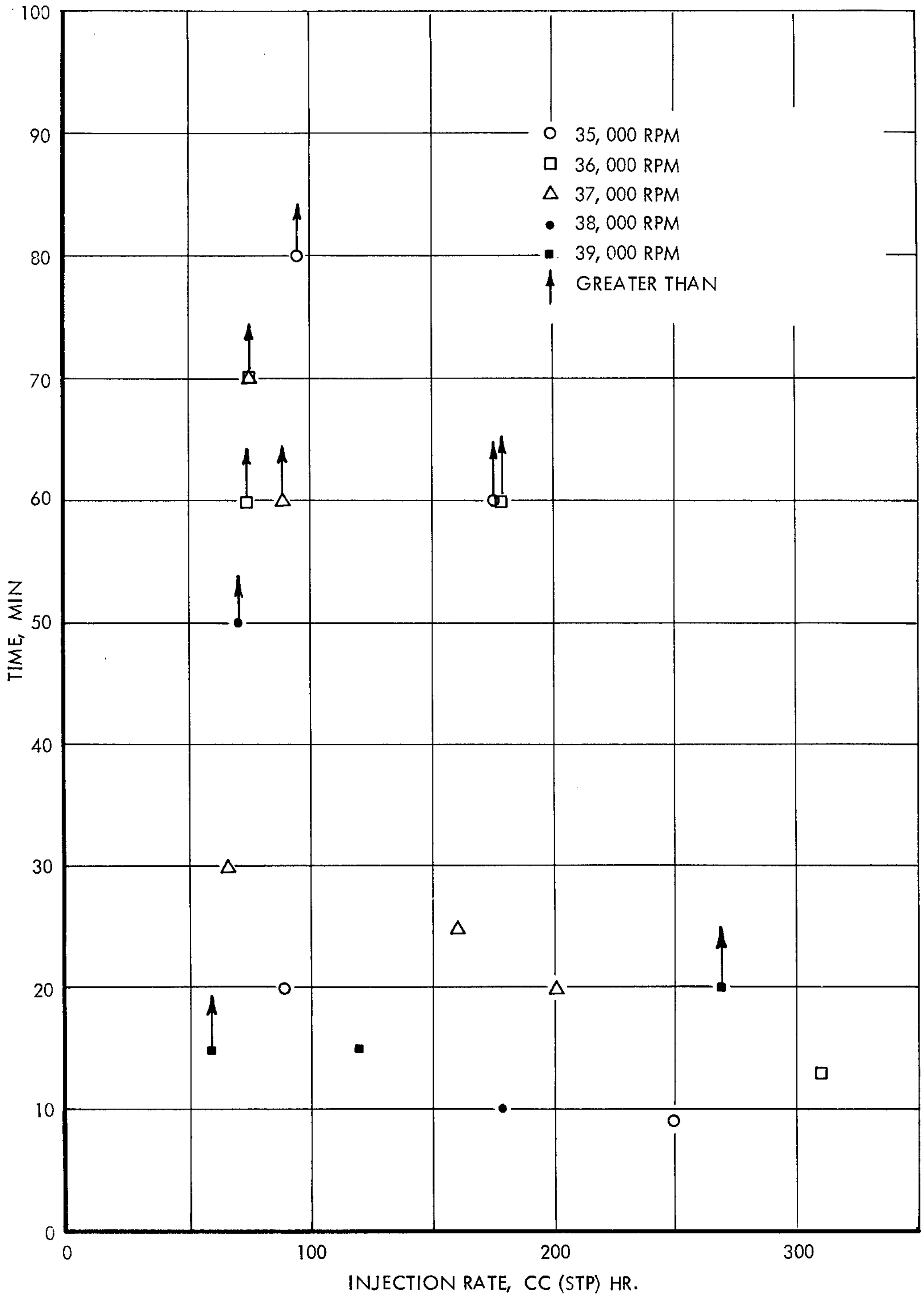

FIGURE 28 TIME REQUIRED TO CAUSE LOSS OF PRIME WITH A CONSTANT RATE OF HYDROGEN INJECTION. 5.5 PSIA PUMP INLET PRESSURE. 351.5 PSIA PUMP OUTLET PRESSURE

It will be noted that in some cases it is indicated that the pump did not lose prime after a specific length of time. Some of the tests were terminated after an extended period of operation, while others were terminated when the pump motor overheated. In the latter case, it was feared that seizure of the bearings in the motor might occur, and for this reason the pump was shut off before loss of prime occurred.

The data indicate no distinct correlation between rate of hydrogen injection and pump performance. Similarly, there appears to be no correlation between pump speed and time required for the pump to lose prime at a given injection rate. In general, it does appear that as the injection rate is increased the time required for loss of prime decreases, as is to be expected. Also, an increase in the pump outlet pressure appears to result in an increase in the time required for loss of prime to occur.

The inconclusiveness of the data may be explained by the fact that leakage of hydrogen through the pump seals was occurring, as was the case with the single bubble tests. It is also believed that hydrogen tended to collect in the by-pass line and that large quantities of hydrogen entered the pump, causing loss of prime. The result of this would be that the data reflect the effects of large, single pockets of hydrogen rather than the effects of a continuous stream of hydrogen gas.

C. Centrifugal Hydrogen Separator

As previously discussed, the centrifugal hydrogen separator was evaluated in conjunction with the centrifugal pump during the constant rate hydrogen injection tests. The separator was tested with both a columbium and an iron (1010 steel) diffusion tube. Both the method of hydrogen injection and the vacuum collection system have been previously described (page 50 and 29, respectively), so no further discussion of either of the two devices will be made.

The pressure and flow conditions in the separator were obtained by varying the centrifugal pump output. Three series of tests were conducted with pump outlet pressures of 201.5, 251.5 and 351.5 psia. The pump speed during each series was varied between 35,000 and 40,000 rpm. All of the tests were conducted with a pump inlet pressure of 5.5 psia and, also, as stated in the constant rate injection tests on the centrifugal pump, the separator was evaluated with the centrifugal pump by-pass line and the separator at both ambient temperature (80°F) and 350°F. Tests were made at each set of centrifugal pump conditions at several different hydrogen injection rates and at both 80°F and 350°F.

The data obtained during these tests are summarized in Tables 7 through 9. As shown, for the most part the attempts to separate hydrogen were unsuccessful. One test (test no. 15), however, was partially successful. During test 15 (Table 8) a hydrogen removal rate of 14.7 cc/hr. (STP) was obtained. Compared to the injection rate of 90 cc/hr., the removal rate was still quite low. However, the rate obtained was considerably higher than the other removal rates obtained.

When the separator was designed, a permeability value of 30 $cc\text{-}mm/hr\text{-}cm^2\text{-}atm^{1/2}$ for the separator was obtained by extrapolating high temperature data back to 350°F (9). However, data obtained by Steigerwald indicated that the permeability of columbium to hydrogen at 400°F was approximately 7×10^{-5} $cc/mm/hr\text{-}cm^2\text{-}atm^{1/2}$ (10). According to this information the design value for the permeability was high by a factor of approximately $4 \times 10^{+5}$. Unfortunately this information was not obtained until the tests had been completed.

In view of this, a final series of tests were conducted with a 1010 steel tube in place of the columbium tube. Information available indicated that the permeability of iron to hydrogen in the temperature range of 350 to 400°F was at least an order of magnitude greater than that for columbium. This series was conducted at pump conditions of 351.5 psia outlet pressure and 8.5 psia inlet pressure and 38,000 rpm. Also, all the tests were made with the separator and by-pass line heated to 350°F.

However, as shown in Table 10, only a negligible amount of hydrogen was removed. After the first and second tests and again after the third test, the tube was removed, cleaned and polished. However, even this did not improve the ability of the separator to remove hydrogen.

TABLE 7

SUMMARY OF CENTRIFUGAL HYDROGEN SEPARATOR TESTING WITH COLUMBIUM WINDOW

PUMP CONDITIONS; INLET PRESSURE, 5.5 PSIA; OUTLET PRESSURE, 200 PSIA

Test No.	Pump Speed (RPM)	Pump Temp. (°F)	Injection Volume (cc)	Injection Time (Min.)	Injection Rate cc/hr.	Vacuum System Check Volume (cc)	Vacuum System Check Time (Min.)	Vacuum System Check Leak Rate cc/hr.	Hydrogen Collection Volume (cc)	Hydrogen Collection Time (Min.)	Hydrogen Collection Rate (cc/hr.)	Hydrogen Collection Corrected Rate (cc/hr.)
8	35,000	80	30	20	90	.026	180	.0087	.027	20	.081	.072
32		80	90	27	200	.089	27	.198	.041	27	.091	-
38		350	15	5	180	.034	76	.027	.007	5	.084	.057
9	36,000	80	82	60	82	.026	180	.0087	.027	70	.023	.014
33		80	112	46	146	.027	101	.016	.137	46	.180	.164
39		350	112	34	198	.034	76	.027	.004	35	.007	-
10	37,000	80	45	30	90	.026	180	.0087	.011	30	.022	.013
34		80	134	41	197	.020	33	.036	.014	41	.020	-
40		350	142	51	167	.034	76	.027	.016	51	.019	-
11	38,000	80	30	20	90	.026	180	.0087	.007	20	.021	.012
35		80	7.5	6	75	.020	33	.036	.007	6	.070	.034
41		350	75	14	320	.034	76	.027	.005	12	.025	-
12	39,000	80	82	60	82	.026	180	.0087	.054	90	.036	.028
13		80	45	30	90	.026	180	.0087	.014	40	.021	.012
42		350	53	5	636	.034	76	.027	.007	10	.042	.017
14	40,000	80	45	30	90	.026	180	.0087	.068	12	.340	.331
37		80	97	24	243	.020	33	.036	.027	23	.070	.043

TABLE 8

SUMMARY OF CENTRIFUGAL HYDROGEN SEPARATOR TESTING WITH COLUMBIUM WINDOW

PUMP CONDITIONS; INLET PRESSURE 5.5 PSIA; OUTLET PRESSURE, 250 PSIA

Test No.	Pump		Injection			Vacuum System Check			Hydrogen Collection			
	Speed (RPM)	Temp. (°F)	Volume (cc)	Time (Min.)	Rate cc/hr.	Volume (cc)	Time (Min.)	Leak Rate (cc/hr.)	Volume (cc)	Time (Min.)	Rate (cc/hr.)	Corrected Rate (cc/hr.)
15	35,000	80	90	60	90	.068	82	.050	12.27	50	14.7	14.7
44		80	37	14	160	.036	130	.016	.0027	10	.016	-
55		350	97	24	243	.015	56	.016	.0027	23	.007	-
45	36,000	80	60	26	185	.036	130	.016	.0055	23	.014	-
16		200	112	55	122	.068	82	.050	.890	128	.417	.412
56		350	45	14	192	.015	56	.016	.0027	15	.011	-
46	37,000	80	67	34	118	.036	130	.016	.025	34	.044	.028
17		350	120	95	76	.068	82	.050	.370	90	.247	.197
57		350	52	14	244	.015	56	.016	.0014	17	.005	-
47	38,000	80	67	25	162	.014	50	.017	.014	32	.026	.009
58		350	60	15	240	.015	56	.016	.0041	17	.014	-
18		395	112	30	224	.068	82	.050	.185	50	.222	.172
48	39,000	80	67	16	250	.014	50	.017	.014	20	.042	.025
59		350	105	30	210	.015	56	.016	.011	29	.023	.007
49	40,000	80	67	22	182	.014	50	.017	.0068	20	.020	.003
60		350	30	15	120	.015	56	.016	.014	16	.054	.038

TABLE 9

SUMMARY OF CENTRIFUGAL HYDROGEN SEPARATOR TESTING WITH COLUMBIUM WINDOW

PUMP CONDITIONS; INLET PRESSURE 5.5 PSIA; OUTLET PRESSURE, 350 PSIA

	Pump		Injection			Vacuum System Check			Hydrogen Removal			
Test No.	Speed (RPM)	Temp. (°F)	Volume (cc)	Time (Min.)	Rate cc/hr.	Volume (cc)	Time (Min.)	Leak Rate (cc/hr.)	Volume (cc)	Time (Min.)	Rate (cc/hr.)	Corrected Rate (cc/hr.)
20	35,000	80	127	80	95	.068	82	.050	.096	75	.077	.027
50		80	175	60	175	.014	59	.014	.026	62	.025	.011
26		350	30	20	90	.040	75	.032	.110	22	.300	.268
61		350	37	9	250	.019	65	.017	.007	8	.052	.035
21	36,000	80	90	70	77	.068	82	.050	.096	82	.070	.020
51		80	180	60	180	.032	56	.034	.007	60	.007	-
27		340	75	60	75	.040	75	.032	.137	30	.274	.242
62		350	67	13	310	.019	65	.017	.003	13	.013	-
22	37,000	80	90	60	90	.068	82	.050	.075	60	.075	.025
52		80	67	20	201	.032	56	.034	.004	21	.011	-
29		340	90	70	77	.040	75	.032	.008	40	.012	-
28		350	45	40	90	.040	75	.032	.026	60	.026	-
63		350	67	25	160	.025	72	.021	.004	24	.010	-
23	38,000	80	75	60	75	.068	82	.050	.322	56	.345	.340
52		80	30	10	180	.032	56	.034	.003	10	.018	-
30		350	60	50	72	.089	70	.076	.055	45	.073	-
24	39,000	80	30	15	120	.068	82	.050	.068	12	.340	.335
53		80	90	20	270	.032	56	.034	.004	20	.012	-
31		350	15	15	60	.089	70	.076	.021	15	.084	.008

TABLE 10

SUMMARY OF CENTRIFUGAL HYDROGEN SEPARATOR TESTING WITH IRON* WINDOW

PUMP CONDITIONS; INLET PRESSURE 8.5 PSIA; OUTLET PRESSURE 350 PSIA

Test No.	Pump		Injection			Vacuum System Check			Hydrogen Removal			
	Speed (RPM)	Temp. (°F)	Volume (cc)	Time (Min.)	Rate (cc/hr.)	Volume (cc)	Time (Min.)	Blank Rate (cc/hr.)	Volume (cc)	Time (Min.)	Rate (cc/hr.)	Corrected Rate (cc/hr.)
65	38,000	350	22	10	132	.018	71	.015	.016	10	.096	.081
66	38,000	350	138	30	276	.018	71	.015	.027	31	.052	.037
67	38,000	350	101	30	202	.068	57	.072	.068	30	.136	.064
68	38,000	350	142	91	94	.092	86	.064	.110	92	.072	.008

*1010 Steel Tube - 3/16" Dia. O.D.
Tube was removed, sanded and polished with rubbing compound after each attempt.

VI EVALUATION AND RESULTS

A. Mercury

After termination of the loop tests, the power to the loop was shut off and the loop was allowed to cool. Once cool, the mercury was removed from both the bottom of the boiler and the diaphragm pump outlet. Draining was accomplished through lines connecting both points to the sump. However, instead of allowing the mercury to flow into the sump, an external tap was used so that the mercury could be collected in a glass flask (approximately 16-pound capacity). The flask was connected to a vacuum pump so that the mercury could be drained under vacuum. A total of three flasks (48 pounds) were removed from the boiler.

The first flask appeared to be clean. However, the second and third flasks had a layer of scum on the surface. The amount of scum found in the second flask was quite light compared to that found in the third flask. A fourth flask (15 pounds) of mercury was removed from the diaphragm pump outlet under vacuum. The mercury removed appeared to be clean. All four flasks of mercury were then exposed to air to see if any more scum would be formed. However, the condition of the mercury after exposure to air appeared to be the same as while it was under vacuum.

A six-pound representative sample of the mercury from each flask was removed for chemical analysis. After the samples were taken, the scum from the second and third flask was collected. The scum from each of the two flasks was added to the respective sample. The samples were then submitted to chemistry for analysis.

The results of the analysis of the mercury and scum removed from the loop are shown in Table 11.

TABLE 11

ANALYSIS OF MERCURY FROM WORK-HORSE LOOP*

	Co	Cr	Ni	Fe	W	Ash**	Total
Weight of element (gm)	1.5980	.2400	.1470	.0800	.0990	.1190	2.2830
Percent of total	70.0	10.5	6.5	3.5	4.5	5.0	100
Amount in Hg (ppm)	56.0	8.5	5.0	3.0	3.5	4.0	80.0

*The compositions listed are based on the total 63 pounds of mercury removed from the loop.

**Residual ash formed after ignition of perchloric acid precipitate. The ash consisted of Ta and W with minor or trace amounts of Co, Cr, Fe, Si, Ni, and Mg.

The results shown in Table 11 are based on wet analyses conducted on the total 24 pounds of mercury submitted. Although the initial analyses were based on the 24 pounds of mercury, the results listed are calculated for the full 63 pounds of mercury removed from the loop. As shown, a total of 2.238 grams of metallic elements were found in the mercury. Of this, 70 percent was found to be cobalt. A small amount of ash (5 percent) remained unidentified. This ash was formed during the last step of the analysis which was the determination of the tungsten content. Spectrographic analysis of the ash showed strong lines for tantalum and tungsten. Minor or trace amounts of Co, Cr, Fe, Si, Ni, and Mg were also found. Also shown in Table 11 are the fractional amounts of the elements found based on the total weight of mercury.

B. Loop

Once drained, the loop was split into its components (boiler, superheater, and condenser-subcooler). Each component was then cut into sections. Figure 29 shows the manner in which the loop was sectioned. Each section was then brushed out to remove any loosely adherent deposits. The deposit removed was collected and held for examination. After this, the sections were split in half lengthwise and visually examined. Notes were made on the presence, location and appearance of all deposits found.

After the condition of the I.D. surface of the tubing had been determined, metallographic specimens were cut from the sections. In general, the specimens were removed at each thermocouple location. Also specimens were removed at all points where the tubing was joined by welding. The locations of the metallographic specimens are shown in Figure 29.

Once the metallographic specimens were removed, the remaining pieces of the sections were scraped to remove all of the adhering deposit. The deposit removed from each section was then combined with the deposit brushed from each section and submitted to chemistry for analyses. The deposits from each section were kept separate so that the variation in deposit composition from section to section could be determined.

1. Metallographic Examination

The specimens removed from the loop were mounted and polished. Evaluation of the extent and type of attack incurred in each specimen was made in both the unetched and etched conditions. In general, the corrosive attack by mercury can be classified into the following categories:

(1) Layer - a depleted or leached zone.

The leached zone may be intergranular or uniform in progression. Intergranular cusps or slight advance of layer in grain boundaries over bulk grains may be seen in some layers.

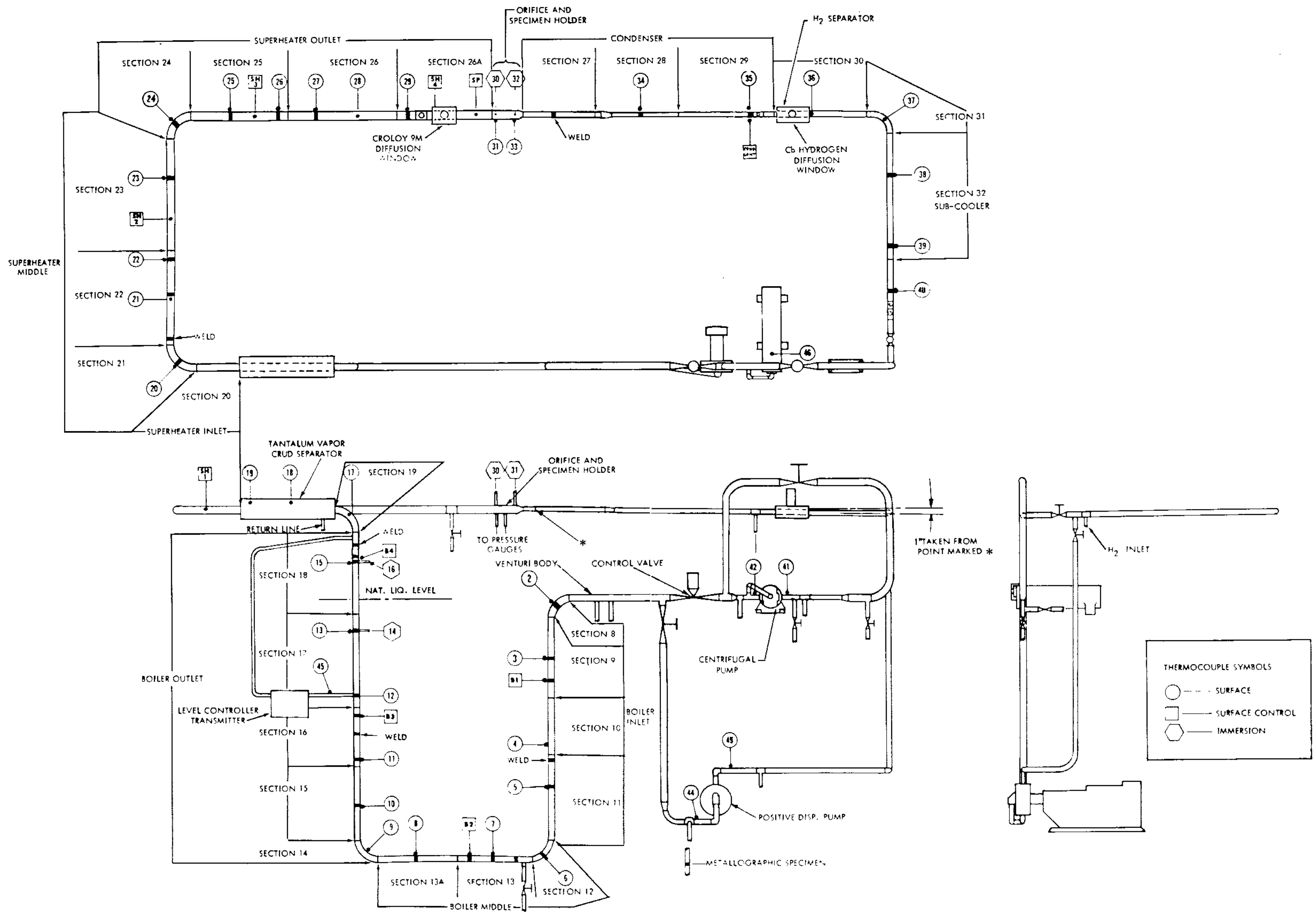

FIGURE 29 SCHEMATIC DRAWING SHOWING THE MANNER IN WHICH THE LOOP WAS SECTIONED AND THE LOCATION OF THE VARIOUS METALLOGRAPHIC SPECIMENS REMOVED

(2) Intergranular penetration -

The grain boundaries are selectively attacked and penetrated. However, the bulk of the grain is relatively unaffected. Some leaching of constituents from the bulk of the grain may take place.

(3) Crevice -

Crevice attack is the removal of metal resulting in irregularly-shaped fissures. The crevice may be intergranular or may run parallel to and just under the surface.

(4) Pitting -

Pitting is the removal of metal resulting in semicircular depressions.

(5) Wedge -

Wedge attack is the removal of metal resulting in a wedge-shaped fissure.

a. Boiler

The results of the examination of the specimens removed from the boiler are shown in Table 12. Along with the results from metallographic examination, the weighted average temperature for Runs 13 and 15 are shown. However, in interpreting the corrosion results, these temperatures must be used with judicious care. The temperatures given reflect only 3026 hours of the 5262 hours total operating life. Also, as shown in Figures 12 and 13, which give the temperature profile for the two runs, the temperatures, recorded for the two runs vary quite widely. In general, the attack incurred throughout the boiler was in the form on leaching along with a wedge type of attack of the grain boundaries. However, in several instances the attack differed. In the upper region of the boiler inlet, the attack was in the form of pitting and crevice formation to a depth of 0.001 in. This type of attack is illustrated in Figure 30 (section No. 8, thermocouple No. 2).

The heaviest concentration of attack was found in the specimen removed from a weld area in the lower region of the boiler inlet (section 11). As shown in Figure 31, the attack incurred was in the form of leaching and intergranular penetration to a maximum depth of 0.005 in. The weld in this area resulted when the new section of tubing was installed in the boiler inlet. This new section replaced the piece of tubing removed because of the tube failure which occurred after 3876 hours of operation. The appearance of the weld and weld-affected area revealed very little (.001 in.) corrosion. The weld, which was made with material exposed to mercury for 3876 hours fused to new unaffected tubing, looked very sound as shown in Figure 32. Also, there was no evidence of any deposit adhering to the surface of the newer section of tubing.

TABLE 12

RESULTS OF METALLOGRAPHIC EXAMINATION OF SPECIMENS REMOVED FROM THE BOILER

Boiler Region	Section Number	Location	Temp.[(1)] °F	Type of Attack	Maximum Depth of Attack (in.)
Inlet	8	TC No. 2	414	Moderate Pitting and Crevice Formation	.001
	9	TC No. 3	706	Same	<.001
		TC No. B1	NR[(2)]	Same	.001
	11	Weld	NR	Leached Layer With Heavy Intergranular Penetration	.005
Middle	12	TC No. 6	991	Leached Layer With Intergranular Penetration	.004
	13	Weld	NR	Same	.004
		TC No. 7	1106	Same	.004
		TC No. B2	NR	Same	.001
	13A	TC No. 8	1124	Same	.003
Outlet	14	TC No. 9	1066	Same	.003
	15	TC No. 10	1129	Same	.003
	16	TC No. 11	1113	Same	.005
		TC No. B3	NR	Same	.003
		Weld	NR	Same	.002
	17	Weld	NR	Same	.001
		TC No. 13	1162	Same	.002
	18	TC No. 15	1128[(3)]	Same	.003
		TC No. B4	NR	Leached Layer	.001
		Weld	NR	Same	.002

(1) Temperature listed is the weighted average temperature recorded during Run Nos. 13 and 15. The average temperature during each Run is given in Figures 12 and 13.

(2) Temperature was not recorded.

(3) Average temperature for Run No. 13.

Etchant: None 250X

Figure 30. I.D. Surface of Specimen Removed from the Upper Region of the Boiler Inlet (Section No. 8, Thermocouple No. 2).

Etchant: None 250X

Figure 31. Appearance of Corrosive Attack Found on the I.D. Surface of the Specimen Removed from the Weld in the Lower Part of the Boiler Inlet (Section No. 11, Weld).

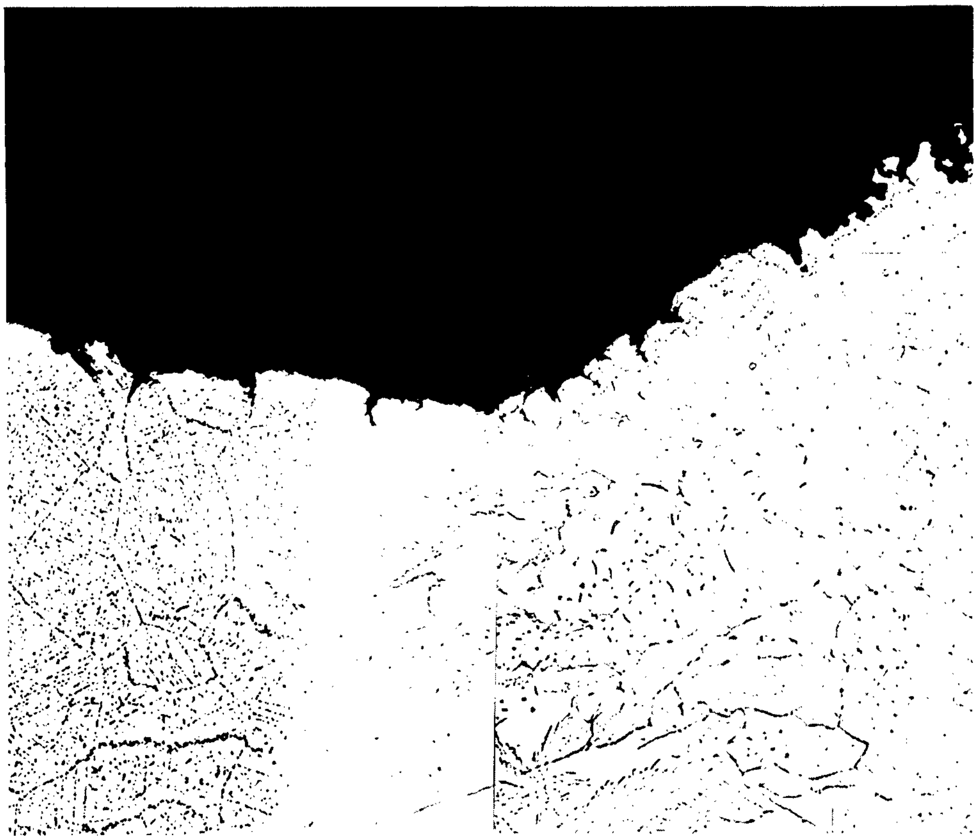

Etchant: $HF-HNO_3-H_2SO_4-H_2O$ 250X

Figure 32. Appearance of the I.D. Surface of the Weld Bead in the Specimen Removed from the Lower Part of the Boiler Inlet (Section No. 11 Weld).

Throughout the middle region of the boiler, the attack found was in the form of leaching and a wedge type of attack on the grain boundaries. The depth of attack varied from 0.001 in. to 0.004 in. Figure 33 (Section 12, thermocouple No. 6) illustrates the type and extent of attack incurred. The smallest amount of attack was found in Section 13, thermocouple No. B2. Thermocouple No. B2 was a control thermocouple which was located outside of its respective heater.

The predominant form of attack in the boiler outlet was the same as found in the boiler middle. The depth of attack varied from 0.001 to 0.005 in. Figures 34 and 35 illustrate the type and extent of attack found in the outlet region. (Specimens from Section 15, thermocouple No. 10; and Section No. 18, thermocouple B4.) The heaviest concentration of attack in the boiler outlet region was found on the specimen removed from Section 16, thermocouple No. 11. The attack incurred in this area was of the same general type and occurred to a maximum depth of 0.005 in. It is interesting to note that this specimen was removed from the unheated bend connecting the middle and outlet regions of the boiler.

b. Superheater

Compared to the boiler, the attack incurred in the superheater was light. The results of the examination of the specimens removed from the superheater are shown in Table 13. Again, the weighted average temperature for Run Nos. 13 and 15 are shown. However, as discussed before, these temperatures are shown just for informative purposes. In general, a light crevice type of attack to a depth of 0.0005 in. was found. Figure 36 (Section 21, thermocouple No. 20) shows the general appearance of the attack. The greatest amount of attack in the superheater was found in the specimens removed from the outlet region of the superheater. The attack again was in the form of a crevice type with a small amount of pitting to a maximum depth of 0.001 in. Figure 37, (Section 26A, TC No. 29) is representative of the maximum attack found.

Along with the attack, deposits of corrosion products were found along the tube wall within the superheater. These deposits were metallic in appearance and appeared to be metallurgically bonded to the inside surface of the tubing. The greatest amount was found in the superheater inlet (Section 20 and 20A). Section 20A was removed after 3833 hours so that the crud separator could be installed in the superheater. Figure 38 (Section 20, thermocouple SH 1) shows the general appearance of the deposit at 100 magnification. In this region, the deposit was rather uniform in nature as shown in Figure 39 (macrograph of a portion of Section 20). The thickness of the deposit varied from 0 to .03 in. in depth.

Etchant: $HF-HNO_3-H_2SO_4-H_2O$ 250X

Figure 33. I.D. Surface of Specimen Removed from the Middle Region of the Boiler (Section 12, Thermocouple No. 6).

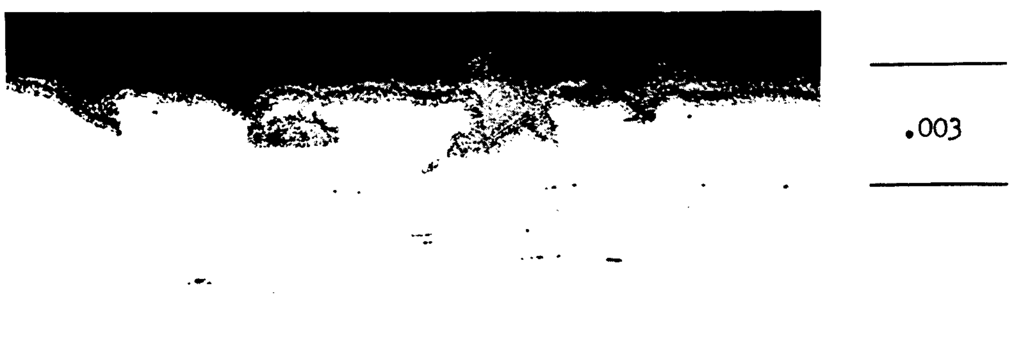

Etchant: None 250X

Figure 34. I.D. Surface of Specimen Removed from the Lower Part of the Boiler Outlet (Section No. 15, Thermocouple No. 10).

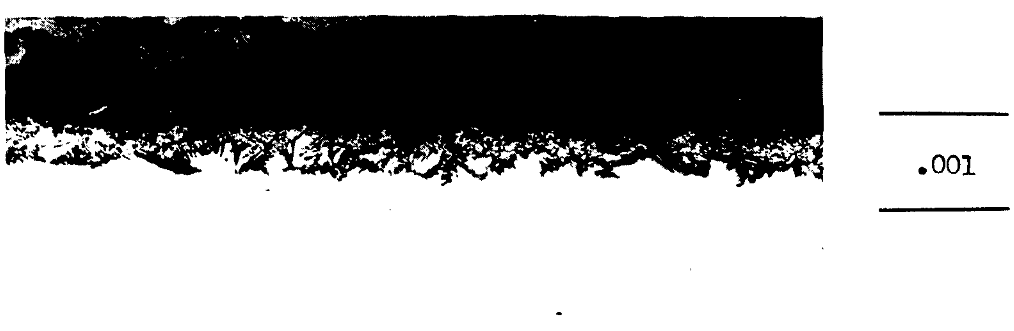

Etchant: None 250X

Figure 35. I.D. Surface of Specimen Removed from the Upper Part of the Boiler Outlet (Section No. 18, Thermocouple No. B4).

TABLE 13

RESULTS OF EXAMINATION OF SPECIMENS REMOVED FROM THE SUPERHEATER, CONDENSER, AND SUBCOOLER

Region	Section Number	Location	Temp.[1] (°F)	Type of Attack	Maximum Depth of Attack (in.)	Maximum Deposit Thickness (in.)
Super-heater	20	TC No. SH 1	NR[2]	Light Crevice Formation	.0005	.012
	21	TC No. 20	1080	Light Crevice Formation	.0005	.000
	22	Weld	NR	Light Crevice Formation	.0005	.004
		TC No. 21	1302	Light Crevice Formation	.0005	.010
		TC No. 22	1367	Light Crevice Formation	.0005	.005
	23	TC No. 23	1443	Light Crevice Formation	.0005	.003
	24	TC No. 24	1230	Light Crevice Formation	.0005	.002
	25	TC No. 25	1446	Light Crevice Formation, Slight Depletion	.001	-
		TC No. 26	1267	Light Crevice Formation	.0005	.014
	26	TC No. 27	1215	Light Crevice Formation	.001	-
	26A	TC No. 29	1320	Light Pitting and Crevice Formation	.001	-
Condenser	27	Weld	NR	Light Pitting	.0005	-
	28	TC No. 34	503	Light Pitting	.0005	-
	29	TC No. 35	570	Light Pitting	.0005	-
Subcooler	32	TC No. 38	559	Negligible	-	-
		TC No. 39	422	Negligible	-	.001

(1) Temperature listed is the weighted average temperature recorded during Run Nos. 13 and 15. The average temperature during each Run is given in Figures 12 and 13.

(2) Temperature was not recorded.

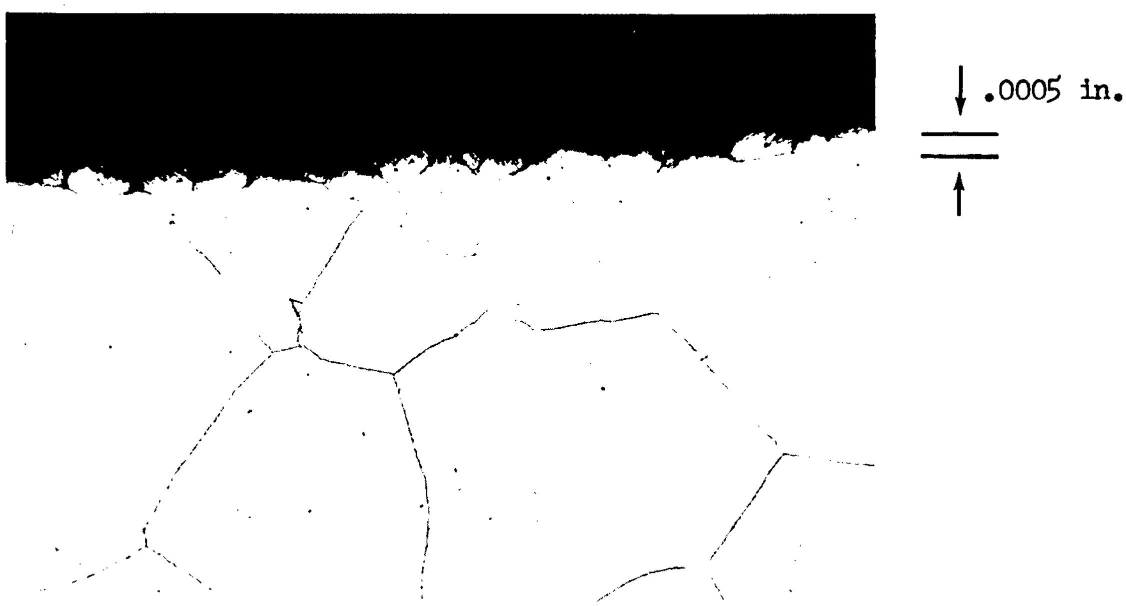

Etchant: $HF-HNO_3-H_2SO_4-H_2O$ 250X

Figure 36. I.D. Surface of Specimen Removed from Superheater Inlet (Section No. 21, Thermocouple No. 20).

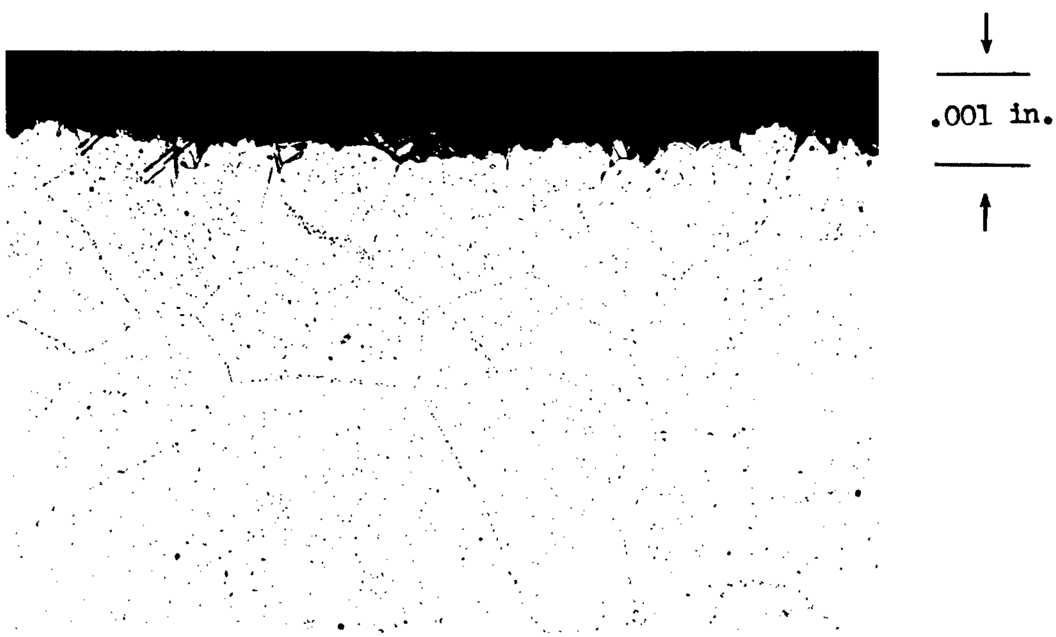

Etchant: $HF-HNO_3-H_2SO_4-H_2O$ 250X

Figure 37. I.D. Surface of Specimen Removed from the Outlet Region of the Superheater (Section No. 26A, Thermocouple No. 24).

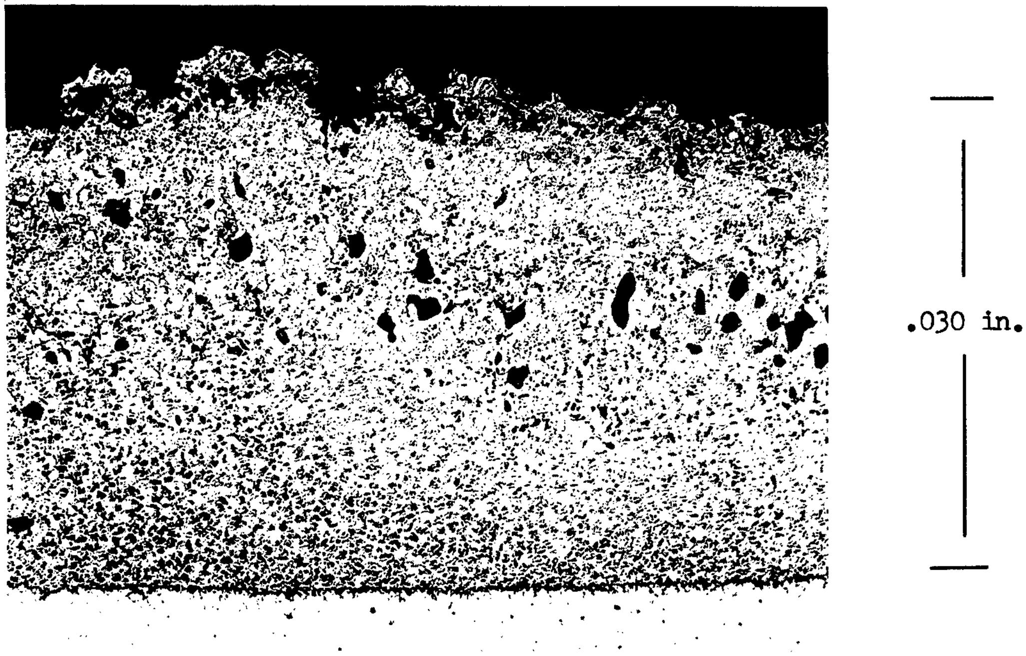

Etchant: None 100X

Figure 38. Appearance of Deposit Found on the I.D. Surface of the Specimen Removed from the Superheater Inlet (Section 20, Thermocouple No. SH 1).

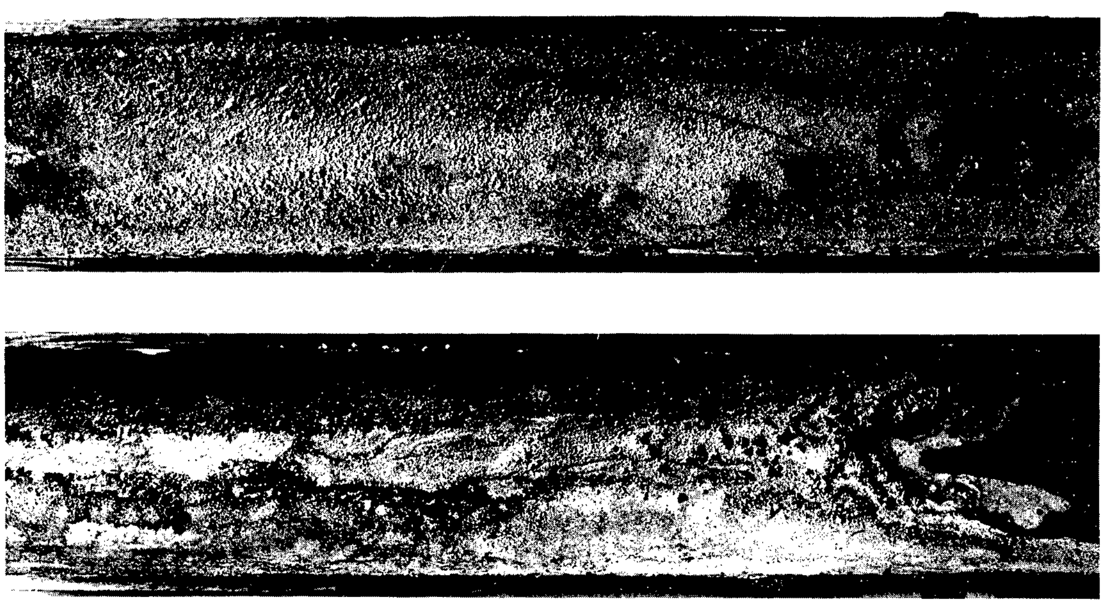

Flow 1.3X

Figure 39. Macrograph of Deposit Found Along the I.D. Surface of the Superheater Inlet (Section No. 20).

The middle of the superheater (Section 22 and 23) also contained a deposit similar in nature, although, the concentration of the deposit was not as heavy. In general, the deposit appeared to follow the contour of the swirl wire. Figure 40, (macrograph of sections 22 and 23) shows the overall appearance of the I.D. surface of the tubes. Figure 41 (Section 22, thermocouple No. 21) shows a general appearance of the deposit. In the middle of the superheater the deposit reached a maximum thickness of 0.010 in. in thickness. Scattered areas of deposit were also found in the outlet region of the superheater. The thickest deposit in this region was found near a weld area (Section No. 25, weld). As shown in Figure 42 (Section No. 25, weld) the deposit was crescent shape and .014 inch thick.

Within the superheater region, two sections of tubing were replaced during the operation of the loop. The first section was replaced after 3833 hours in order that the location of the vacuum hydrogen separator could be changed. Although new tubing was fused to tubing which had been exposed to mercury for either 262 or 3833 hours, no unusual effects were found. Both the weld beads and the heat affected areas appeared sound.

c. Condenser

The results of the examination of the specimens removed from the condenser region are shown in Table 13. As shown, the attack found was limited to a light pitting to a maximum depth of 0.0005 in. Figure 43 (Section No. 29, thermocouple No. 35) shows the general appearance of the type of attack found. A weld area in the condenser was also examined for any possible attack. The area examined was in Section No. 27 where the condenser tubing was reduced in size from 5/8" O.D. to 1/2" O.D. tubing. As was the case with the rest of the welds examined, the weld appeared sound.

d. Subcooler

Examination of the sections removed from the subcooler region revealed negligible attack, as shown in Table 13. One small area of deposit was found. Figure 44 (Section No. 32, thermocouple No. 39) shows the general appearance of the deposit.

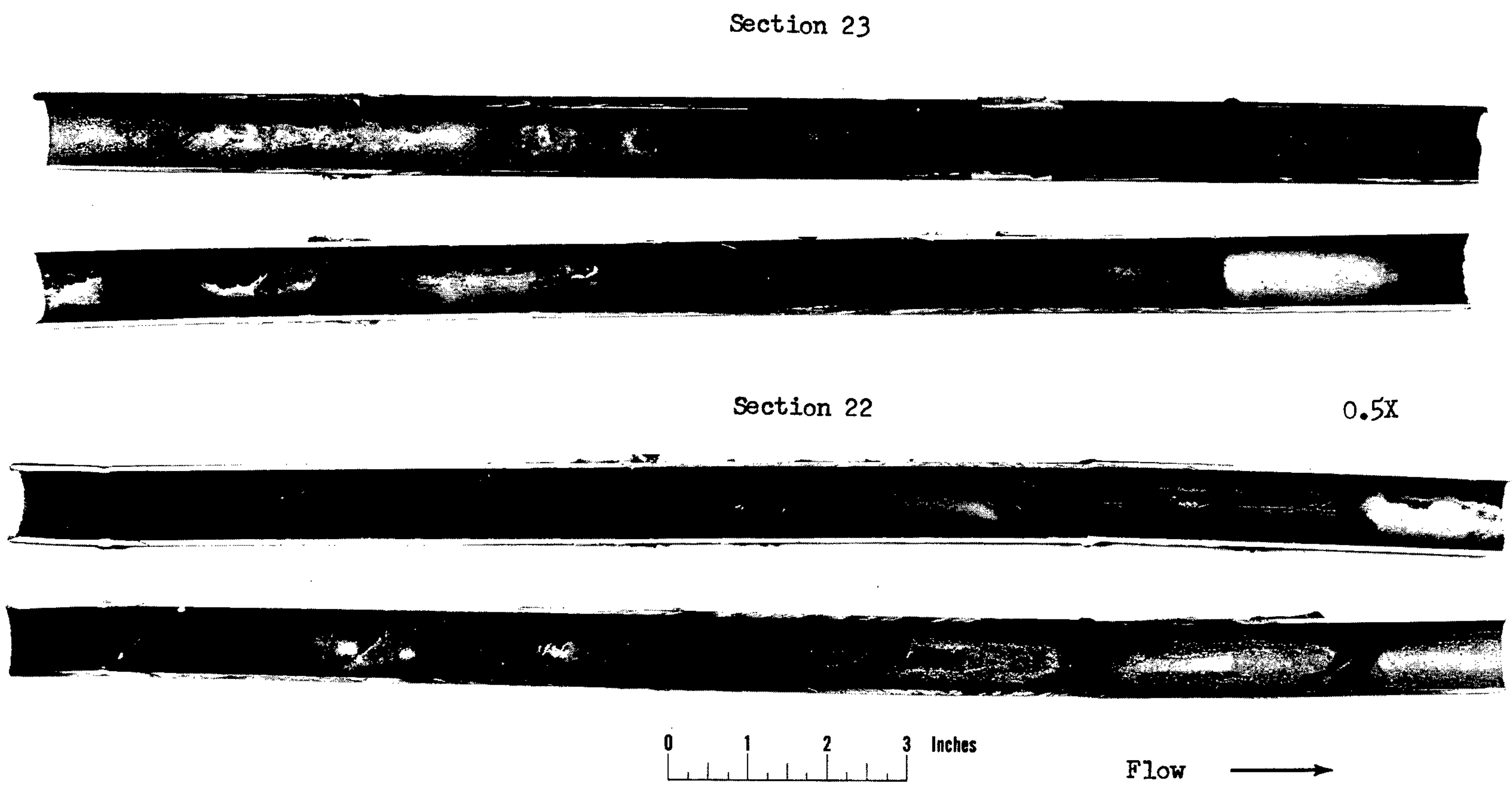

Figure 40. Macrograph of the I.D. Surfaces of the Sections Removed from the Middle Region of the Superheater (Section Nos. 22 and 23).

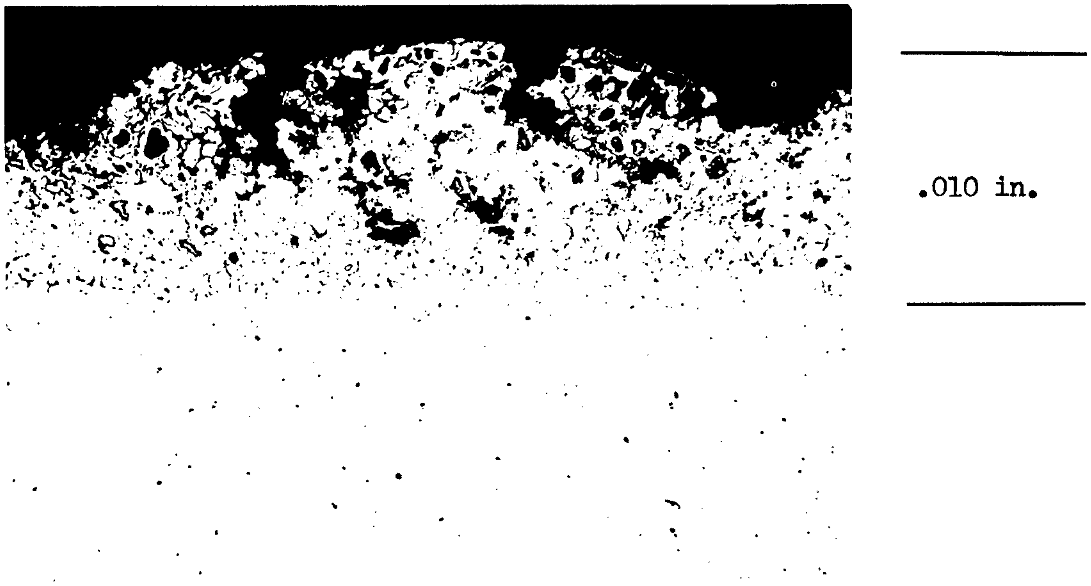

Etchant: None 250X

Figure 41. Appearance of Deposit Found Along the I.D. Surface of the Specimen Removed from the Middle Region of the Superheater (Section No. 22, Thermocouple No. 22).

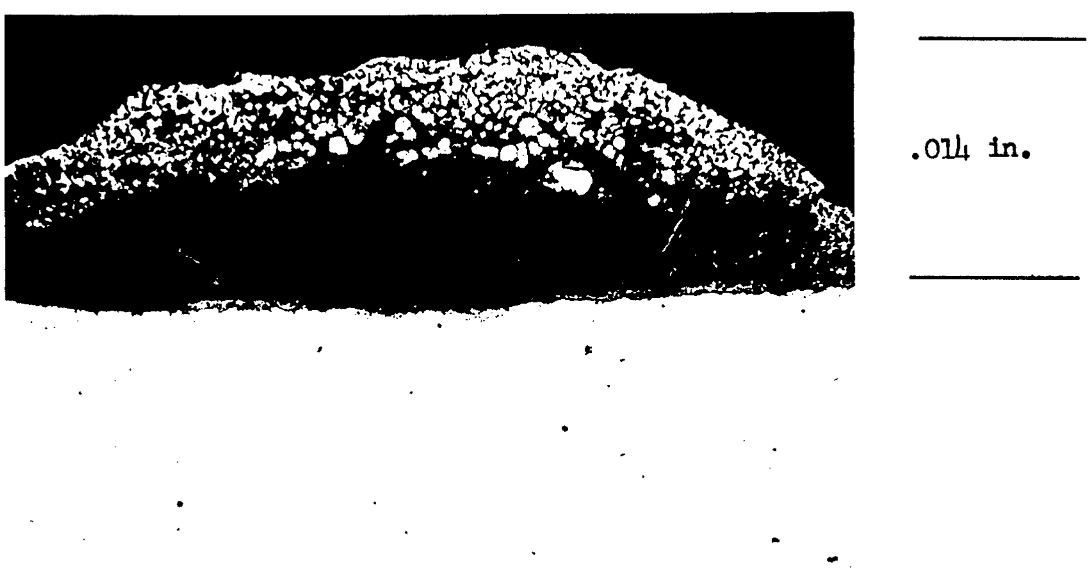

Etchant: None 100X

Figure 42. Appearance of Deposit Found on the I.D. Surface Near the Weld Area of the Specimen Removed from the Outlet Region of the Superheater (Section No. 25, Weld).

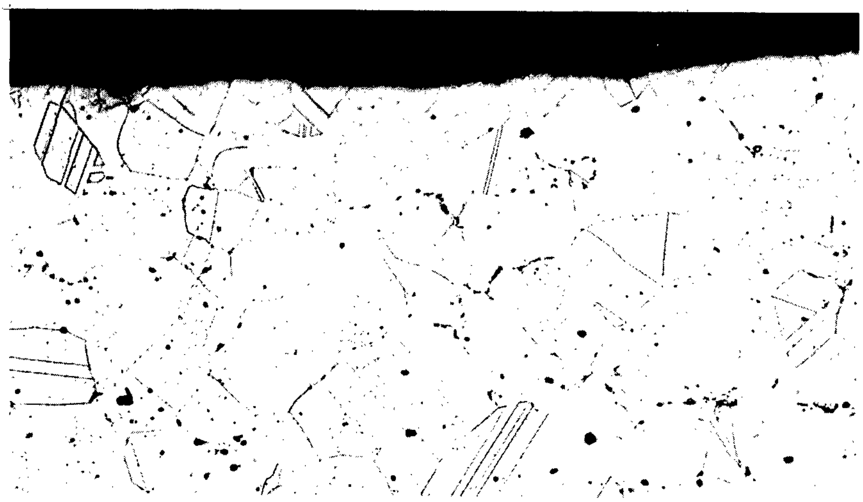

Etchant: $HF-HNO_3-H_2SO_4-H_2O$ 250X

Figure 43. Appearance of the I.D. Surface of the Specimen Removed From the Condenser (Section No. 29, Thermocouple No. 35).

Etchant: None 250X

Figure 44. Appearance of the I.D. Surface of the Specimen Removed from the Subcooler (Section No. 32, Thermocouple No. 39).

2. Analysis of Deposits and Corrosion Layers

Visual examination of the sections of tubing from the boiler revealed a deposit and corrosion layer adhering to the inside tube wall. This layer was found throughout except for the unheated bend connecting the inlet and middle regions of the boiler, and the section of tubing in the boiler inlet region that was replaced after 3876 hours. Physically, the layer varied from very thin and tenacious to rather heavy and loosely adherent. The layer had a grayish-black non-metallic appearance. The areas of the boiler where the layers were found were also wetted.

A heavy deposit was found along the bottom of the entrance section of the superheater. The deposit was crystalline and metallic in nature. Also, it was quite hard and adherent as if metallurgically bonded. The appearance of this deposit is shown in Figure 39.

Throughout the rest of the superheater various areas were found that had a gray-black surface, whereas others were silvery in nature. In several places, a metallic-like build-up along the tube wall was found which followed the contour of the swirl wire where the swirl wire came into contact with the tube wall. The general appearance of the inside tube walls described are shown in Figure 40.

The first 29 inches of the condenser appeared to be wetted by mercury. Also, in the first half of this region, a loose scale was found along the tube wall. The balance of the condenser (approximately 30 inches) was not wetted, nor was there any deposit.

The walls in the section removed from the subcooler were slightly discolored. Only a slight amount of wetted surface was found. No evidence of scales or other deposits were found.

All the sections were scraped and every attempt was made to remove as much of the deposits as was physically possible. The results of the chemical analysis have been separated according to the loop region, and are listed in Tables 14 through 16.

Table 14 gives the results on the analysis of the corrosion layer removed from the boiler. As shown, a total of 11.4 grams of material were removed from the boiler. Of this, approximately 48 w/o was removed from the inlet region. Approximately 22 w/o and 30 w/o of the material were removed from the middle and exit regions of the boiler, respectively. Analysis of the material revealed that the major components were cobalt and tungsten. Small amounts of nickel, chromium and iron were also detected. In the same manner as the mercury analysis, a residual ash was obtained. However, as compared to the mercury, the ash in this instance was present in more significant amounts (14-19 w/o). Spectrographic analysis of the ash again revealed the major constituents of the ash to be tantalum and tungsten.

TABLE 14

CHEMICAL ANALYSIS OF THE DEPOSIT AND CORROSION LAYER REMOVED FROM THE BOILER

Boiler Region	Total Metallic Weight (gm)	Co	Cr	Ni	Fe	W	Ash*	w/o of Deposit Found in Each Region
Inlet	5.4420	45.5	3.0	0.8	1.7	34.7	14.4	47.7
Middle	2.4960	43.8	5.5	0.3	1.7	31.0	17.7	21.9
Outlet	3.4750	46.6	6.0	0.9	2.3	25.1	19.0	30.4
Boiler Total	11.4130	45.4	4.5	0.7	1.9	31.0	16.5	

*Residual ash formed after ignition of perchloric acid precipitate. The ash consisted of Ta and W with minor amounts of Co, Cr, Fe, Si, Ni, and Mg.

TABLE 15

CHEMICAL ANALYSIS OF DEPOSITS REMOVED FROM THE SUPERHEATER

Superheater Region	Total Metallic Weight (gm)	Co	Cr	Ni	Fe	W	w/o of Deposit Found in Each Region
Inlet(1)	3.6540	58.9	19.8	18.5	2.8	T	72.3
Inlet	.8560	45.1	29.1	22.6	2.7	0.5	17.0
Middle	.3630	56.0	22.9	13.7	4.0	3.4	7.2
Outlet	.1740	42.0	15.1	11.5	2.4	29.0	3.5
Superheater Total	5.0470	56.0	21.5	18.5	2.8	1.2	

(1)This section of tubing was removed from the superheater after 3833 hours of operation so that the tantalum crud separator could be installed.

A total of approximately 5.05 grams of metallic corrosion products were removed from the superheater regions. The amounts and composition of the products removed are shown in Table 15. As shown, the greatest amount of this (89 percent) came from the inlet region to the superheater. Approximately seven percent and four percent of the deposit were removed from the middle and exit regions of the superheater, respectively. Analysis of the deposits revealed that the major component was cobalt which was present in quantities varying from 42 to 59 percent in the various regions. Chromium and nickel were present in significant amounts and for the most part present in equal quantities. The average amount of each was 20 percent. Small quantities of iron and tungsten were also found. In general, except for the small amount of deposit removed from the outlet region, their presence was less than five percent. The tungsten content of the small amount of deposit removed from the exit region was 29 percent.

Only 0.04 gram of solid matter was removed from the condenser-subcooler region of the loop. As shown in Table 16, this deposit was composed of primarily tungsten and cobalt. Minor amounts (less than five percent) of chromium and nickel were found. Iron was present only in a trace quantity.

TABLE 16

CHEMICAL ANALYSIS OF DEPOSITS REMOVED FROM THE CONDENSER AND SUBCOOLER

Total Metallic Weight, gm	Composition, w/o				
	Co	Cr	Ni	Fe	W
.0440	40.9	4.8	1.8	T	52.5

C. Tantalum Crud Separator

The separator was cut open for examination. From visual examination, the tantalum appeared to be only slightly wetted by the mercury. No great amounts of corrosion products were found entrained by the wool. The complete charge of wool from the separator was submitted to chemistry for analyses. Included in the analysis were the total weight of metallic corrosion products entrained and the composition.

The results of the analysis are shown in Table 17.

TABLE 17

RESULTS OF CHEMICAL ANALYSIS OF THE TANTALUM WOOL FROM THE CRUD SEPARATOR

Total Weight of Material Removed, gm	Composition, percent					
	Co	Cr	Ni	Fe	W	Ash*
1.3290	14.1	23.5	15.6	24.5	17.7	4.6

*Residual ash formed after ignition of perchloric acid precipitate. The ash consisted of primarily tantalum and tungsten with minor or trace amounts of cobalt, chromium, iron, silicon, nickel, and magnesium.

As shown, a total of approximately 1.3 grams of corrosion products were removed by the tantalum wool. Analysis of the wool showed no single element to be present in a predominant amount. Both chromium and iron were found in the greatest amount (23.5 and 24.5 percents, respectively). Cobalt, nickel and tungsten were found in approximately equal amounts. However, their presence was in the range between 14 and 18 percent. Again a residual ash was found after the final separation for the tungsten content. Spectrographic analysis of the ash revealed results similar to the ash found during the analysis of the boiler deposits, that is, the ash was predominantly tungsten and tantalum.

D. Electron Beam Microprobe Analysis

As a further study of the amount of corrosion incurred by the loop, electron beam microprobe analyses were conducted on four of the metallographic specimens. The analytical work was conducted by Advanced Metal Research Corp. Two of the specimens (Section No. 16, thermocouple No. 11; and Section No. 17, thermocouple No. 13) were from the boiler outlet region. The other two (Section 20A, thermocouple No. 18 and Section No. 22, thermocouple No. 21) were from the inlet and middle regions of the superheater, respectively. Two separate areas on the specimen Section No. 20A, thermocouple No. 18 were analyzed. Figure 45 shows the approximate location and scan paths made on the specimens.

Scan analyses were conducted on all five areas of interest. The elements analyzed for were: cobalt, chromium, nickel, iron, and tungsten. Also, each area was surveyed for the presence of mercury. Photomicrographs of the areas analyzed and the traverse path of the electron beam are shown in Figures 46 through 49. The results of the analyses have been averaged out and are shown in Table 18. In all four specimens, no composition gradients were found in the electron beam traverses made across the base metal. However, once the beam crossed the interface between the base metal and the various deposits, significant changes in composition were found.

The analyses conducted on the two specimens from the boiler outlet region support the results obtained on wet chemical analysis of the deposits removed from the inside tube wall. However, three different compositional areas were found in the deposit along the surface of specimen Section No. 17, thermocouple No. 13, The grayish appearing phase is similar in composition to the corrosion layer found along the surface of the specimen Section No. 16, thermocouple No. 11 (Figure 46). As shown in Table 18, this phase is high in cobalt and tungsten with only small amounts of chromium and nickel. The white areas (marked C in Figure 47) within the deposit were found to be essentially the base metal depleted of chromium, whereas the edge of the deposit (marked B in Figure 47) was found to be essentially base material depleted in tungsten and nickel.

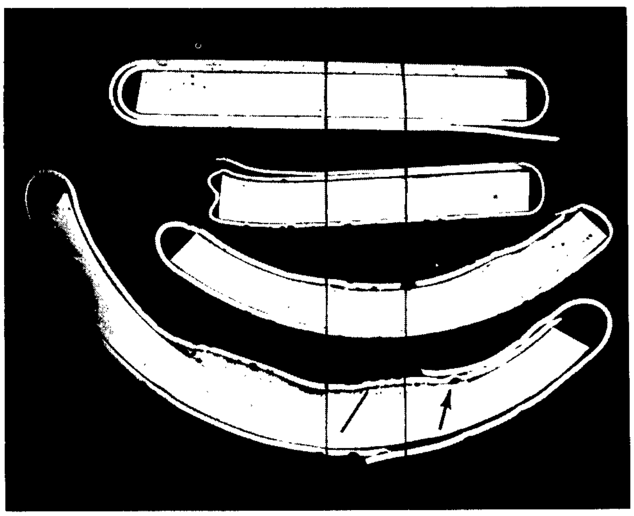

- Section 16, Thermocouple 11
- Section 17, Thermocouple 16
- Section 22, Thermocouple 21
- Section 20A, Thermocouple 18

4X

Figure 45. Macrograph of Mount Showing the Location of the Microprobe Scan Analyses. Except for the one area marked by the arrow, the rest of the analyses were conducted within the area bounded by the two scratch marks. The line on the bottom specimen indicates the orientation of the scan trace.

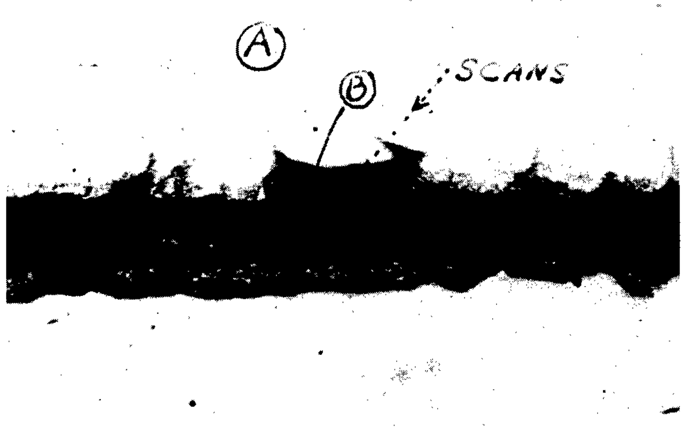

Etchant: None 250X

Figure 46. I.D. Surface of Specimen Removed from Section No. 16, Thermocouple No. 11, Showing the Microprobe Scan Path and Areas Analyzed.

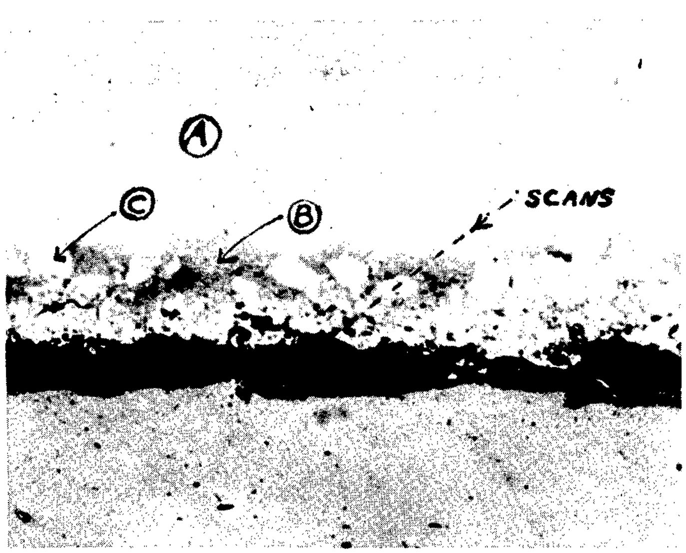

Etchant: None 540X

Figure 47. I.D. Surface of Specimen Removed from Section No. 17, Thermocouple No. 13, Showing the Microprobe Scan Path and Areas Analyzed.

Etchant: None. 120X

Figure 48. I.D. Surface of Specimen Removed from Section No. 20A, Thermocouple No. 18, Showing the Microprobe Scan Path.

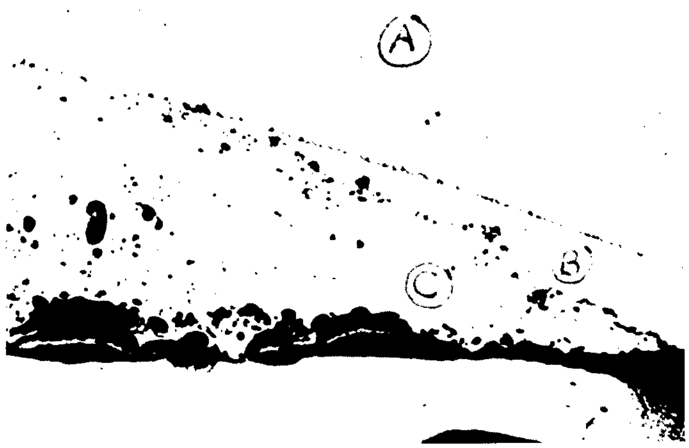

Etchant: None 120X

Figure 49. I.D. Surface of the Specimen Removed from Section No. 20A, Thermocouple No. 18, Showing the Areas Analyzed. This area is the area marked by the arrow in Figure 45.

TABLE 18

RESULTS OF MICROPROBE ANALYSIS OF WORKHORSE LOOP SAMPLES

Sample	Composition w/o				
	Co	Cr	W	Ni	Fe
Haynes Alloy No. 25 Matrix*	49-51	19-21	14-16	9-11	1.7
Section 16, Thermocouple No. 11**					
B Reaction Zone	47-49	6- 8	35-37	1- 2	1.5
Section 17, Thermocouple No. 13					
B Gray Phase	54-56	5- 7	30-32	~1	1.5
C White Phase	58-60	12-14	16-18	10-12	2
Edge Layer	67-69	22-24	2- 4	1- 2	3
Section 20, Thermocouple No. 18					
Average Reaction Zone	0.1	21-23	<0.05	76-78	< 0.05
B Interlayer	0.6	98-99	<0.05	0.6	< 0.05
C Zone	0.2	25-27	<0.05	73-75	< 0.05
Section 22, Thermocouple No. 21					
B Interlayer	.6	92-94	< 0.05	4- 6	<0.05
C Zone	.1	21-23	<0.05	75-77	<0.05

*Also 1 Si, 1-2 Mn, 0.1 C

**Possible 5-10 w/o Si

From these results it appears that the surface of the specimen Section No. 17, thermocouple No. 13 suffered a leaching type of attack. And, a deposit of corrosion products filled the void areas left by the leaching of base material.

Two areas of different composition were found within the deposit on the specimen Section No. 20A, thermocouple No. 18. As shown in Table 18, the bulk of the deposit (Figure 48 and marked C in Figure 49) was predominantly nickel with about 25 to 27 percent chromium. Only minor amounts of tungsten, iron and cobalt were found. However, another phase, (marked B in Figure 29) was found that was almost pure chromium (98-99 percent). Cobalt, tungsten, iron and nickel were found only in small or trace amounts. The results of the analysis of the specimen Section No. 22, thermocouple No. 21 were approximately the same. However, the chromium-rich phase was present in a greater quantity within the deposit. Also, there was not the same amount of distinction between the phases as was found in the specimen Section No. 20A, thermocouple No. 18.

E. Orifice and Erosion Specimen Holder

The orifice and erosion specimen holder was cut open for examination of the orifice plate and the three erosion specimens. The general appearance of the assembly after test is illustrated in Figure 50. Except for the orifice plate, visual inspection of the parts did not reveal any significant changes except for the pickup of a slight oxide scale. However, the orifice plate was somewhat distorted. As shown in Figure 51, the 0.032 inch thick plate became dish-shaped. The depth of the dish was measured and found to be 0.071 inch.

The diameter of the orifice hole was measured by use of a visual comparator. After test the hole was found to have become slightly eliptical in shape. The major diameter was 0.058 inch. The minor diameter was 0.046 in. Except for the distortion, examination of the hole under a 20-power microscope revealed no evidence of erosion of the hole.

Weight and hardness measurements were made on the erosion specimens. The results are compared with the measurements made before test in Table 19.

As shown, the weight changes experienced by the erosion specimens during the operation of the loop were extremely small. What weight changes that did occur were all weight gains. The greatest change was for the PH15-7Mo stainless steel, heat-treated to the condition RH 950, which gained a total of 2.3 mg. This was a 0.06 percent weight gain compared to the original weight of the specimen. Also, as shown, the weight gains per unit area for the specimens were between 0.1 to 0.3 mg/cm^2 in 5000 hours.

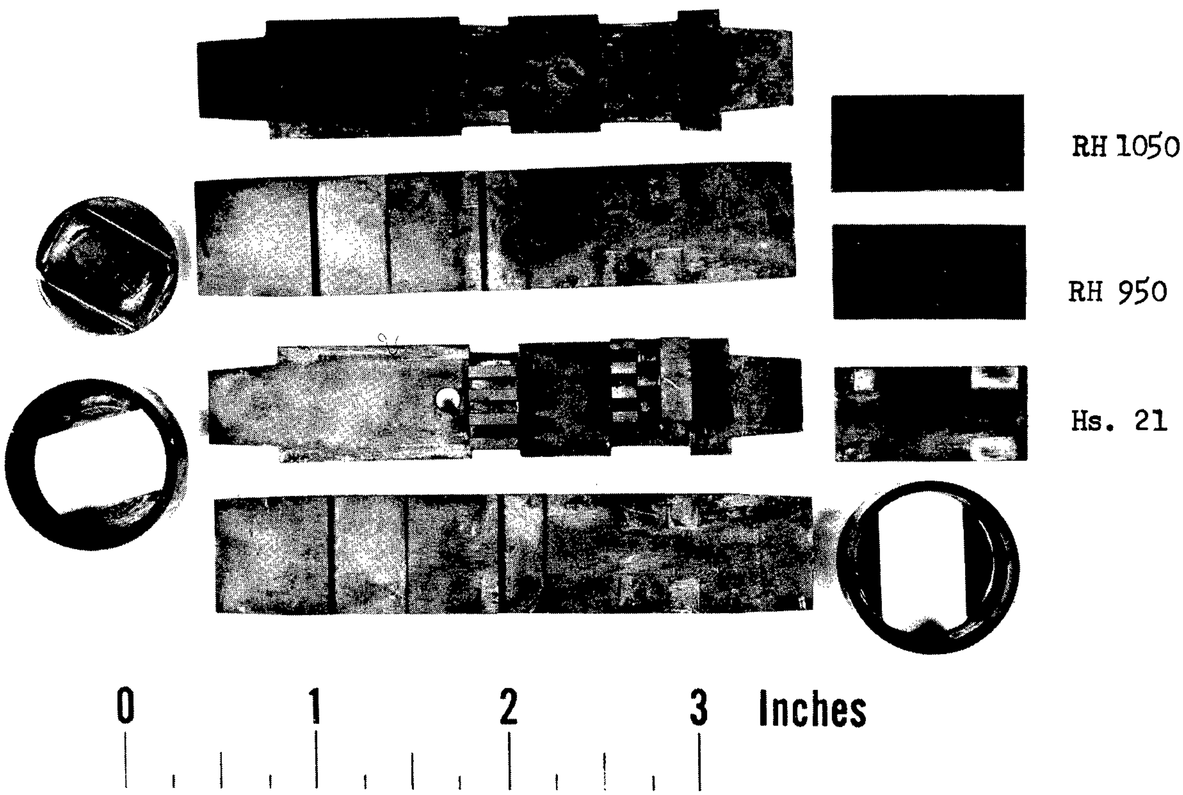

Figure 50. Appearance of Orifice and Specimen Holder Assembly After Test. Actual size.

Figure 51. Macrograph of the Orifice Plate Showing the Amount of Distortion Incurred. Mag. 2.6X

TABLE 19

COMPARISON OF HARDNESS AND WEIGHT OF THE THREE SPECIMENS

Specimen	Heat Treat Condition	Hardness (Rc)* Before Test	Hardness (Rc)* After Test	Weight (gm) Before Test	Weight (gm) After Test	Weight Change (gm)	Weight Change Per Unit Surface Area (mg/cm^2)
PH15-7Mo	TH 1050	45.0	25	3.6813	3.6822	+.0009	0.12
PH15-7Mo	RH 950	44.7	32.5	3.6579	3.6602	+.0023	0.30
Haynes Alloy No. 21		31.0	60	4.2047	4.2057	+.0010	0.13

*Rockwell C hardness numbers were converted from Kentron microhardness numbers determined with a 100-gram load.

Changes in the hardness of the erosion specimens, however, were more apparent. The PH15-7Mo stainless steel in both heat treatments (TH 1050 and RH 950) showed significant losses in hardness. As shown, the erosion specimen heat treated to TH 1050 changed from Rockwell C of 45 to Rockwell C of 25. In comparison the RH 950 heat treated erosion specimen changed from 44.7 Rc to 32.5 Rc. The before test hardness determinations were obtained by use of a Rockwell superficial hardness tester.

In contrast to the loss in hardness by the PH15-7Mo stainless steel, the Haynes alloy No. 21 erosion specimen increased in hardness. As shown in Table 19, the hardness increased from Rockwell C of 31 up to Rockwell C of 60. The before and after-test hardness determinations were made in the same manner as for the PH15-7Mo stainless steel erosion specimens.

Figure 52 shows before and after test photomicrographs of the PH15-7Mo erosion specimen heat treated to the RH 950 condition. As shown by the photomicrographs, the edge of the specimen was relatively unaffected by the exposure to high velocity mercury vapor. However, as can be seen, the microstructure of the specimen in the after test condition changed from an acicular martensitic structure to that of a tempered martensite. Also as shown, carbon diffused into the ferrite stringers.

Photomicrographs in the before and after test condition of the PH15-7Mo erosion specimen heat treated to the TH 1050 condition are shown in Figure 53. As shown, the surface of the specimen was relatively unaffected by the exposure conditions. Also, the microstructure of the specimen in the after test condition changed as compared to the structure in the before test condition. The changes which occurred are essentially the same as those discussed for the PH15-7Mo erosion specimen heat treated to the RH 950 condition.

As shown in Figure 54, the surface of the Haynes alloy No. 21 erosion specimen was only slightly affected by the test exposure. A very light depletion attack occurred to a maximum depth of 1/2 mil.

F. Centrifugal Pump

The final loop component to be examined was the centrifugal pump, which was fabricated from Type 316 stainless steel. The pump head was dismantled and examined visually for any possible damage. The pump components examined are shown in Figure 55. Evidence of cavitation damage was found only on the volute tongue. Figure 56 shows macrographs of the tongue and the extent of damage incurred. Sections were removed from the top part of the tongue (Figure 56) at the damaged area. These sections were then mounted and polished for metallographic examination.

A. Before Test. 250X

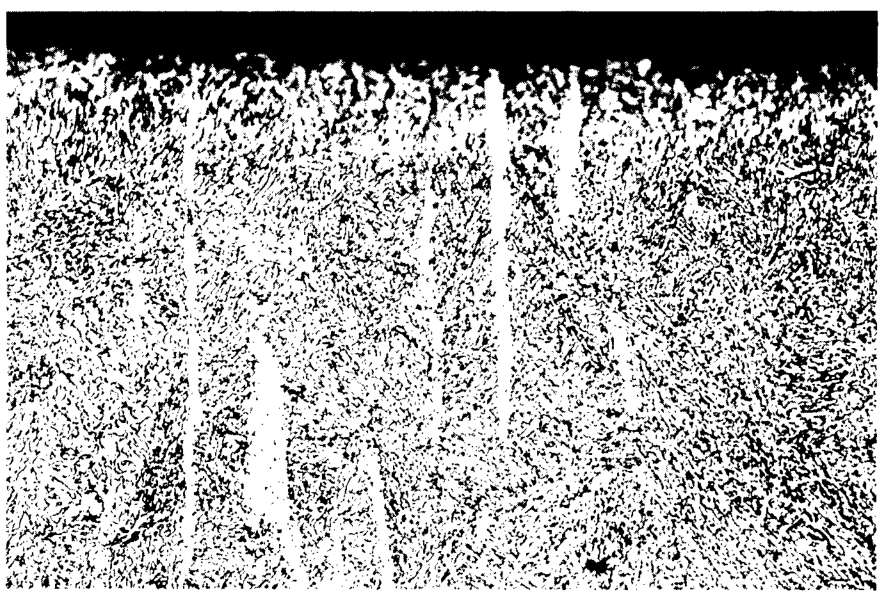

B. After Test. 250X

Figure 52. Condition of the Edge of the PH15-7Mo Erosion Specimen Heat Treated to the Condition RH 950.

Etchant: $CuSO_4 \cdot 5H_2O$-HCl-H_2O

A. Before Test. 250X

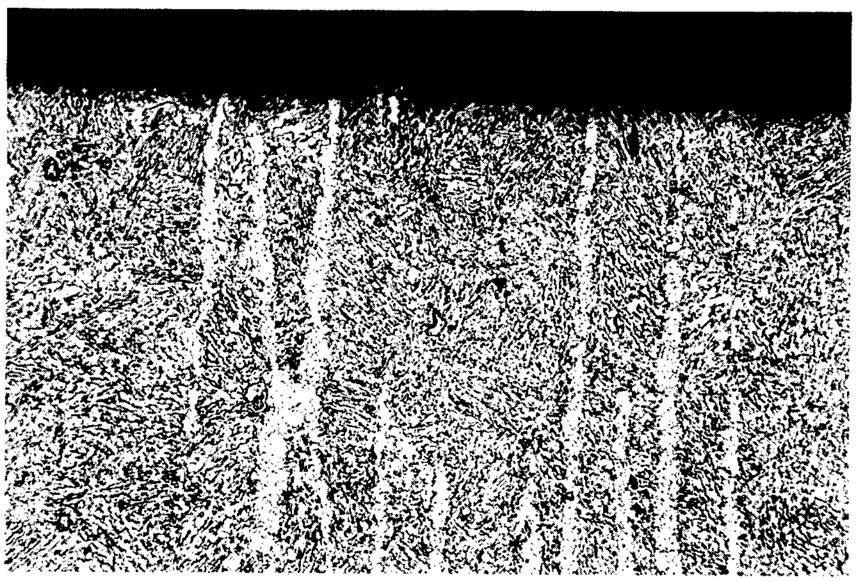

250X

Figure 53. Condition of the Edge of the PH15-7Mo Erosion Specimen Heat Treated to the Condition TH 1050.

Etchant: $CuSO_4 \cdot 5H_2O$-HCl-H_2O

A. Before Test. 250X

B. After Test. 250X

Figure 54. Appearance of the Edge of the Haynes Alloy No. 21 Erosion Specimen.

Etchant: $HF\text{-}HNO_3\text{-}H_2SO_4\text{-}H_2O$

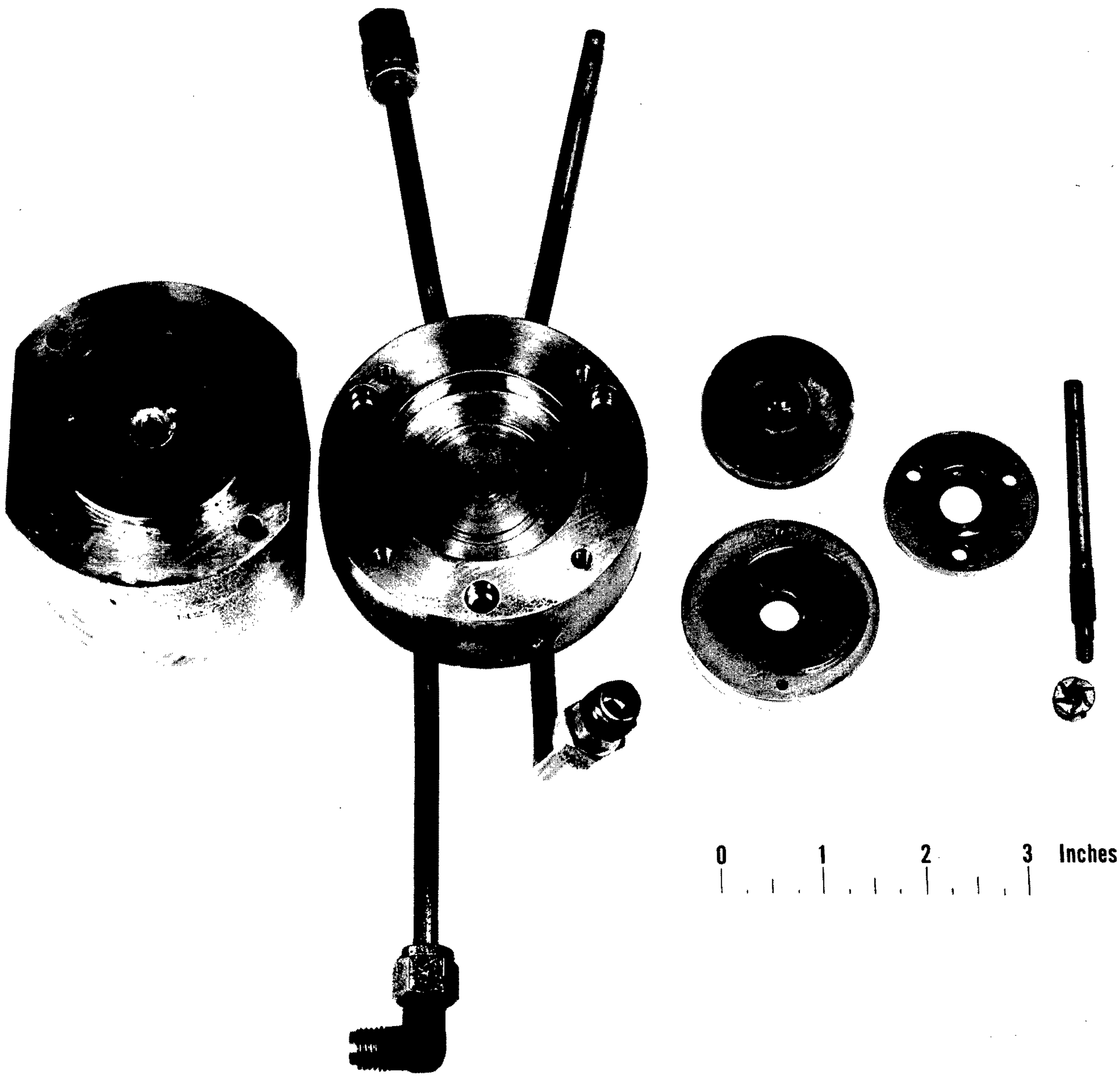

Figure 55. Condition of Centrifugal Pump Components After Test.
Size of components reduced to three-quarters original size.

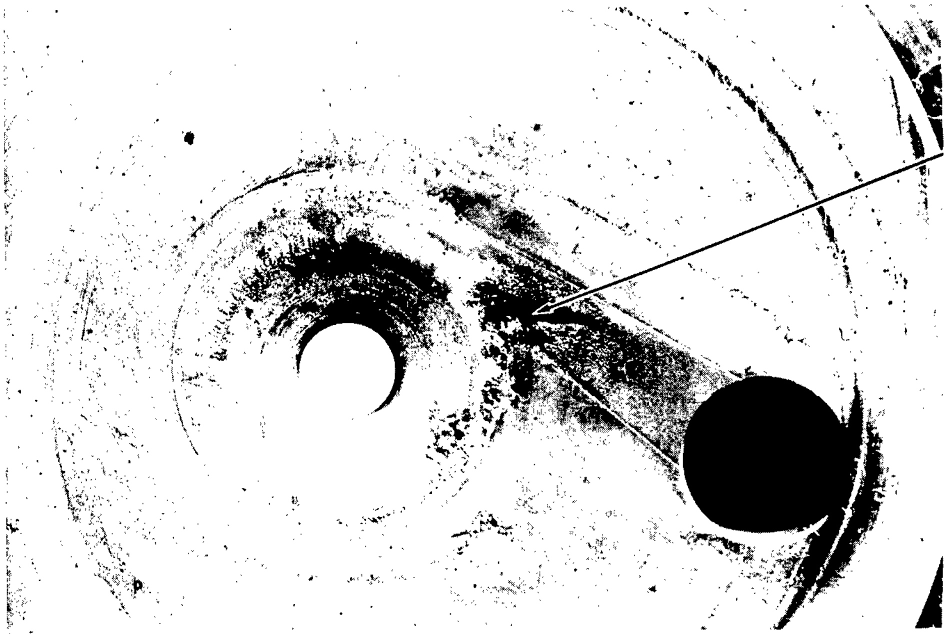

Top Half of Centrifugal Pump Body. Magnification 3X

Bottom Half of Centrifugal Pump Body. Magnification 3X

Figure 56. Macrograph of Centrifugal Pump Body Showing the Extent of Damage Incurred.

Figure 57 (50X) is a photomicrograph of the damaged area. As shown, material was literally torn away to form the cavity. The maximum depth of the damage was .085 inch.

The only other component to be affected was the Type 316 stainless steel impeller. As shown in Figure 58 the side of the impeller was abraded. From the appearance of the markings, the impeller apparently rubbed against the side of the housing during operation. The impeller blades appeared to be completely undamaged as shown in Figure 58.

G. Loop Failures

As was discussed in earlier sections, two tube wall failures were experienced during loop operation. The first failure occurred in the superheater after 262 hours of operation and was in the form of a small crack in the tube wall. The second failure occurred after 3865 hours of operation in the lower end of the boiler inlet. In this case, the tube wall appeared to have ruptured.

1. Failure After 262 Hours

Metallographic specimens were removed from the section of tubing containing the crack. The location of the two specimens removed at the crack are shown in Figure 11. Also, two specimens each were removed from either side, about 3-1/2 inches away from the crack. The specimens were examined primarily to determine the cause of failure. Along with this, however, the specimens were also examined to determine the extent of any possible corrosive attack.

Figure 59 shows the general appearance of the crack in the tube wall. As can be seen, the crack is intergranular in nature. Also, along the crack, smaller cracks were found extending into the grain boundaries from the failed surface. The mode of failure appears to be a brittle type of fracture.

Because of the configuration of the superheater, it was impossible to anneal the tubing after fabrication. Also, the temperature of this region before the failure was about 1400°F. Considering the temperature and cold-worked condition of the tubing, there is the possibility that the tubing in this region was embrittled. Previous investigations on Haynes alloy No. 25 have shown that the alloy has a tendency to embrittle rapidly if exposed to elevated temperatures in the cold-worked condition (1).

Examination of the I.D. surface near the crack revealed a crevice type of corrosive attack, as shown in Figure 60. The maximum depth of the attack was 0.001 in. A similar type of attack was found on the I.D. surface of the specimens removed on either side of the crack. The depth of penetration was also about the same.

Etchant: $HF-HNO_3-H_2SO_4-H_2O$ 50X

Figure 57. Appearance of the Damage Incurred Around the Volute Tongue. Specimen removed from the top half of the pump body which was fabricated from Type 316 Stainless Steel.

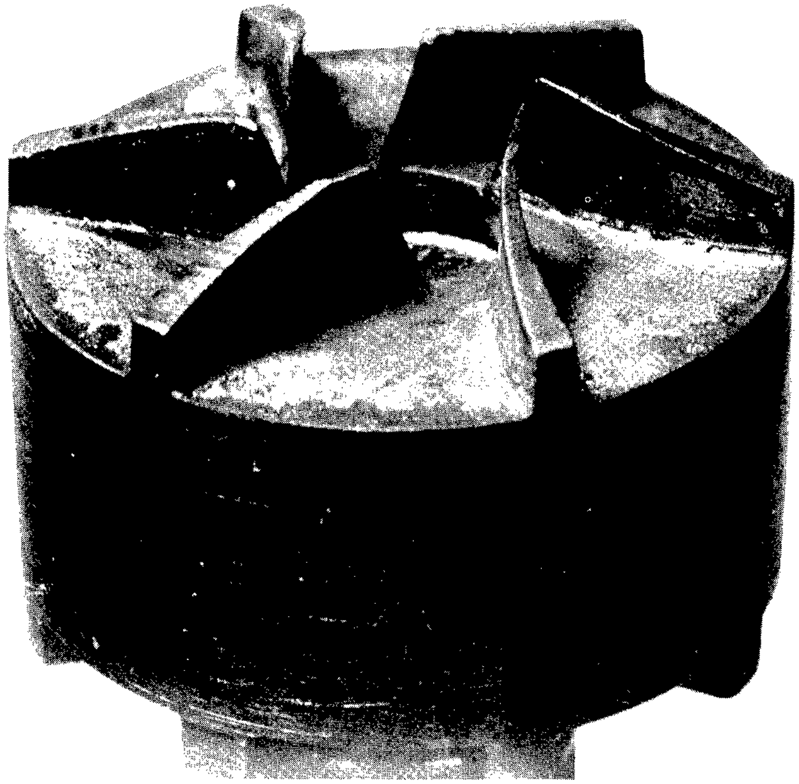

Magnification 10X

Magnification 3X

Figure 58. Macrographs of the Centrifugal Pump Impeller Showing the After Test Condition. Impeller was fabricated of Type 316 Stainless Steel.

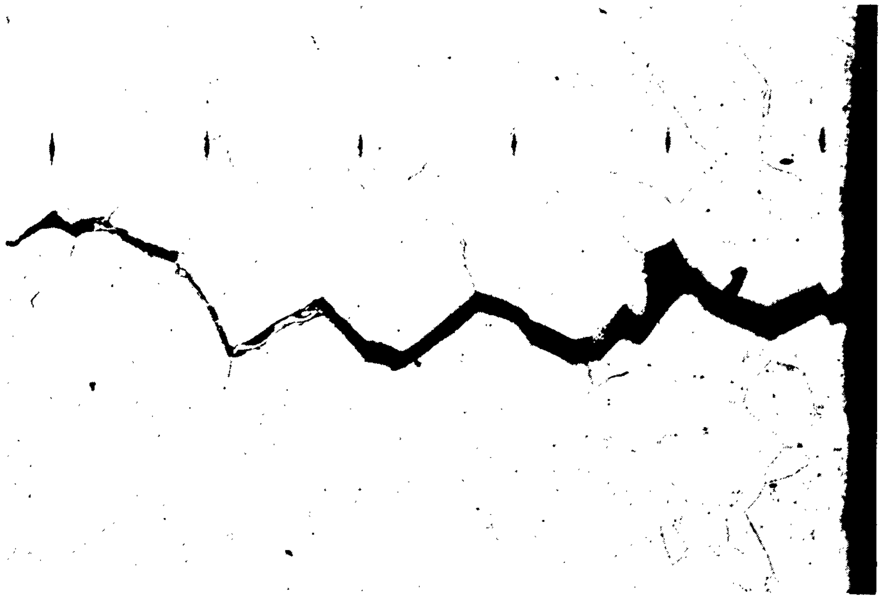

Etchant: $HF-HNO_3-H_2SO_4-H_2O$ 100X

Figure 59. Appearance of the Crack Found in the Tube Wall of the Superheater After 262 Hours of Operation.

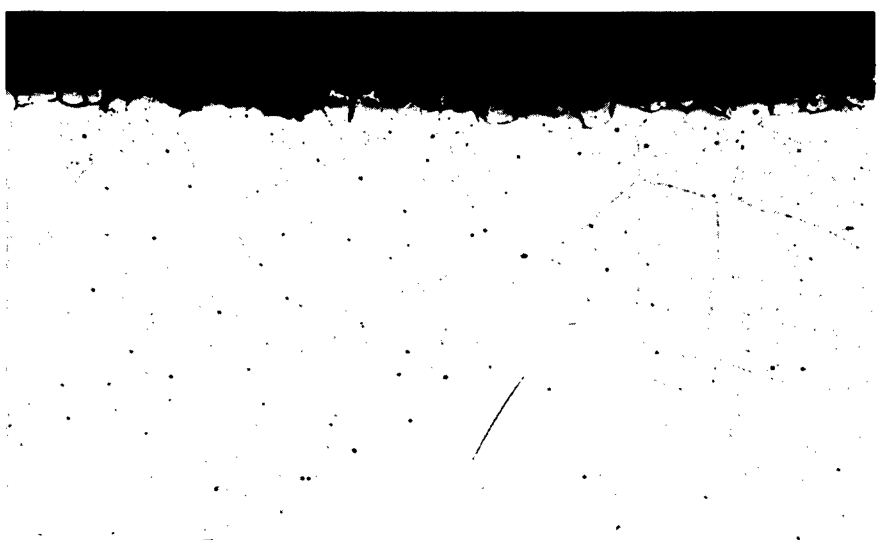

Etchant: $HF-HNO_3-H_2SO_4-H_2O$ 250X

Figure 60. Appearance of the I.D. Surface of the Specimen Removed Near the Crack which Occurred After 262 Hours.

2. Failure After 3876 Hours

Again, metallographic specimens were removed at the point of failure as well as on either side of the failure. The location of the specimens removed is shown in Figure 11. The crack was again intergranular in nature as shown in Figure 61. However, in this case, the tube wall near the crack was necked down. Also, numerous cracks were found along both the I.D. and O.D. surfaces as well as within the tube wall. The crack density was greatest within the necked down area. The appearance of the tube wall in this case points to a creep rupture type of failure. The appearance and mode of failure indicate that the tube wall was locally overheated and that the rupture may have been the result of a pressure overload at the local thermal condition.

In addition to the cause of failure, the specimens were also examined for the extent of corrosive attack found. In general, the I.D. surface on each specimen was found to have undergone a combination of layer, crevice, and depletion attack to a maximum depth of 0.003 inch. Figure 62 is typical of the corrosive attack found. Examination of the surface of the specimen removed from the inlet end of the section revealed a deposit about 0.015 in. thick. Figure 63 shows the appearance of the deposit. Unfortunately, there was not enough deposit present in the section of tubing to obtain an analyses.

Etchant: $HF-HNO_3-H_2SO_4-H_2O$ 100X

Figure 61. Appearance of the Tube Wall of the Boiler Showing the Failure which Occurred After 3876 Hours.

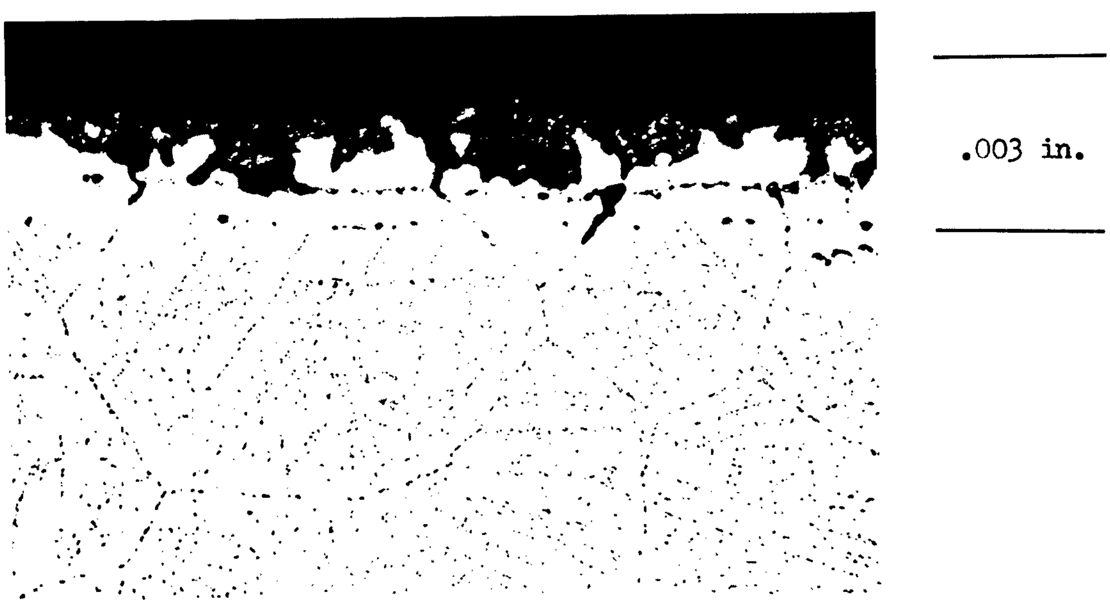

Etchant: $HF-HNO_3-H_2SO_4-H_2O$ 250X

Figure 62. Appearance of the I.D. Surface Near the Failure which Occurred in the Boiler After 3876 Hours.

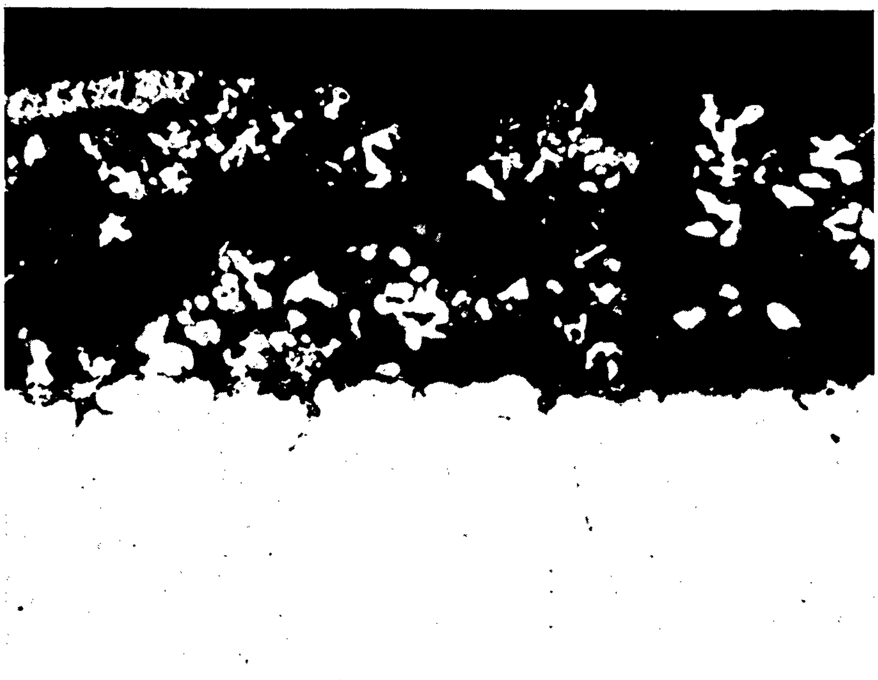

.015 in.

Etchant: None 100X

Figure 63. Appearance of the Deposit Which was Found in the Inlet Region of the Section of Tubing that was Replaced After 3876 Hours.

VII DISCUSSION

A. Hydrogen Removal

1. Hydrogen Diffusion Windows

As was stated previously, the attempts to remove hydrogen from the vapor regions of the loop met with very limited success. In no case did the removal rate come close to matching the injection rate. During one test a removal rate of 5.4 cc/hr. was obtained. However, the injection rate for this test was 450 cc/hr. Also, the loop, as discussed, was apparently overloaded with hydrogen during the test.

Several factors could have attributed to the apparent lack of success. The test parameters in an experiment in diffusion such as this must be carefully controlled. First of all, the surfaces of the medium through which the hydrogen is to diffuse should be kept clean of any films which might hinder the diffusion process. An oxidized surface, even one atom layer in thickness, is such a barrier to diffusion. Secondly, the pressure conditions on either side of the diffusion medium should be accurately known so that the efficiency of the diffusion process can be determined.

During fabrication of the Haynes alloy No. 25 and Croloy 9M test sections, there was no method available to protect the surfaces of the tubes from oxidation. Once installed, it was virtually impossible to clean the tube surfaces. During the operation of the loop, the test section in both the superheater and condenser region was protected with an argon cover gas when it was not in use. During a test run, the section in use was kept under a vacuum of 1 to 10 μ. However, when the test sections were removed, examination revealed that slight oxidation of the outer surface of each tube had occurred.

Both of the columbium tubes were vacuum annealed before they were installed in the condenser test section. Also, cotton gloves were used while handling the tubes after the anneal. As before, once the tube was installed, there was no method of insuring an oxide free surface. As with the Haynes alloy No. 25 and Croloy 9M sections, examination of the columbium test sections after testing revealed an oxidized outer surface.

After termination of the loop, examination of several of the components revealed that the inner surfaces of the loop had been exposed to an oxidizing atmosphere at one time or another. Thus it appears that both surfaces of the various test sections were oxidized at one time or another. This would undoubtedly affect the test results.

Another factor which might have influenced the diffusion of hydrogen is the presence of a mercury heat transfer surface on the inside surfaces of the test sections. This heat transfer surface is a relatively stagnant layer of mercury vapor which is quite thin and not too dense. However, its presence might have acted as a resistance towards the hydrogen reaching the tube surface.

Other factors which influenced the experiment were that neither the partial pressure of the hydrogen nor the location of the hydrogen in the loop could be determined. Since the ability of hydrogen to diffuse through a metallic medium depends on the pressure differential across the thickness of the medium, the partial pressure of hydrogen inside the loop was quite critical. If the hydrogen pressure inside the loop was low, then the driving force for diffusion could be small.

A rough analysis of one test where the loop was flooded with hydrogen was made. Assuming that both surfaces of the tube were unoxidized, the partial pressure of hydrogen was calculated using the collection rate of 5.4 cc/hr. This analysis indicated that the partial pressure of hydrogen in the loop was less than one atmosphere. As shown in Table 3, the volume of hydrogen injected into the loop in the subsequent tests was less than in this test. Thus the partial pressure of hydrogen in the loop during each of the tests was probably less than one atmosphere.

Also during the tests, examination of the loop conditions indicated that the hydrogen was collecting in discrete areas of the loop. At times it appeared to be collecting in the condenser. There appeared to be no correlation between the point of injection, subcooler or superheater, and the area where the hydrogen collected. The rate and volume of hydrogen injected appeared to influence the change in loop conditions as the result of the buildup of hydrogen. However, again no distinct correlation could be determined.

2. Centrifugal Hydrogen Separator

As with the hydrogen diffusion windows, the centrifugal separator also met with very limited success. However, much of this can be attributed to the lack of adequate data on the permeability of columbium to hydrogen. During the design of the separator, the permeability value was determined by extrapolation of high temperature data. Later, experimental results at 600°F indicated that the value used during the design was too high by a factor of approximately $4 \times 10^{+5}$. Although, again in these tests, oxidation of the columbium tube and subsequently the iron tube definitely played an important role.

Because of the manner in which the centrifugal pump shaft was sealed, it was virtually impossible to pull a vacuum lower than 50μ on the centrifugal pump bypass. Also, the lowest vacuum leak rate attainable was between 10 and 40μ /hr. Thus the inside surfaces of the bypass line could not be protected from oxidation.

In the same manner, neither the columbium tube nor the iron tube could be protected from oxidation before installation in the separator. Periodically, the tubes were removed from the separator and examined. Each time the surface of the tube was found to be slightly oxidized. Before the tube was reinstalled it was sanded and polished. However, this apparently did not have any affect.

Because of the difficulties experienced with the various columbium windows, the question arose as to whether adsorbed oxygen on the tube wall could significantly affect the hydrogen permeability at temperatures of 600°F and lower. In light of this, laboratory tests were conducted in an effort to evaluate the relative influence of small quantities of oxygen on the permeability of hydrogen through columbium.

A tube test specimen was employed in this study. The experimental apparatus and method of analysis were identical to those previously described (10). The experimental results are summarized in Figure 64 where the permeability of pure and oxygen contaminated hydrogen through columbium is presented. As the temperature increases (approaching 1200°F) the permeability of uncontaminated hydrogen approaches the high value predicted by diffusivity and solubility data. The presence of 0.5 percent (volume) oxygen in the hydrogen produced a slight decrease in the hydrogen permeability. The relatively small effect produced by the rather large degree of oxygen contamination, particularly at the lower test temperature, suggests that the small amount of oxygen adsorbed on the tube wall does not represent a significant factor controlling the low permeability at low temperature. Also, the results indicated that improved cleaning or bake-out methods to remove adsorbed oxygen would not improve the permeability of columbium at temperatures of 600°F and lower to any significant degree.

From these results, it definitely appears that the lack of success with the columbium windows was the result of inadequate data on hydrogen permeability of columbium.

B. Centrifugal Pump Testing

The results obtained from the injection of single bubbles into the centrifugal pump for the most part were inconclusive. No true correlations could be found as to the quantity of hydrogen required to cause loss of prime as a function of pump speed and pump inlet and outlet pressure. However, in retrospect it was found that as the pump inlet pressure was increased from 5.5 psia to 11.5 psia, the overall amount of hydrogen that could be accepted increased.

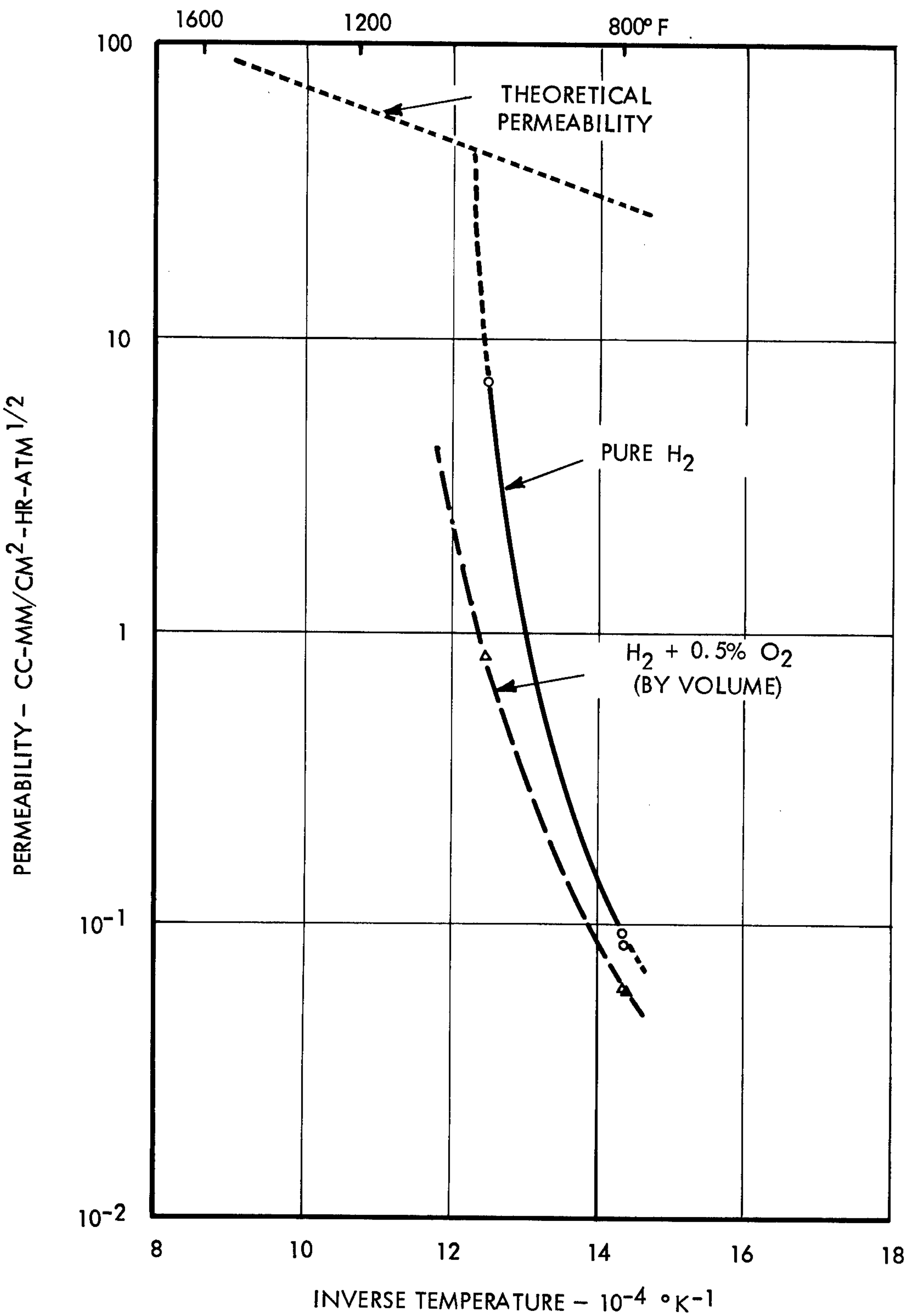

FIGURE 64 PERMEABILITY OF HYDROGEN AND OXYGEN CONTAMINATED HYDROGEN THROUGH COLUMBIUM

In general, this trend could be the result of the change in the actual bubble volume as a function of pressure. All of the bubble volumes quoted were the volume at standard conditions. However, when the bubble entered the pump inlet lines, it expanded an amount determined by the inlet pressure. As the inlet pressure increased towards 11.5 psia, the bubble size would decrease. Also, it is suspected that the larger volumes injected broke up into a series of smaller bubbles, thus making it easier for the hydrogen to pass through.

Another possibility is that part of the hydrogen leaked out around the shaft seals. If such leakage did occur, then the pump would not receive the full effect of the bubble.

As discussed with the single bubble tests, no distinct correlations could be determined with the constant rate injection tests. In general, only the expected was found. That is, as the injection rate was increased, the time required for loss of prime decreased. Increasing the pump outlet pressure tended to result in an increase in time required to cause loss of prime at a specific injection rate. Operation of the centrifugal hydrogen separator or operating the pump at room temperature or 350°F did not appear to affect the results.

The inconclusiveness of the data may have been caused by several factors. First, as discussed with the single bubble tests, part of the hydrogen probably leaked through the pump shaft seal. Another point is that it was difficult to keep the pump at steady state conditions. More refined controls over and above what were used would be needed to keep the pump operating smoothly. For example, at a given voltage setting the pump would vary as much as 1000 rpm. Also, because of the seal leakage, it was difficult to keep the inlet and outlet pressures steady. During a run, the Variac which controlled the pump speed, and the valve used to give the required pressure drop had to be continuously adjusted. Also, it appeared that the hydrogen tended to collect in the by-pass line; and that large quantities of hydrogen entered the pump, causing loss of prime. The result of this would be that, rather than reflecting on the effect of a continuous stream of hydrogen gas, the data would reflect on the effect of a large pocket of gas passing through the pump.

Throughout all the testing, the centrifugal pump was operated for approximately 1000 hours. An exact length of operation cannot be given because the pump was operated intermittently. In general, the overall performance of the pump was below that of other pumps of the same design (6). As discussed, throughout the program considerable difficulty was experienced with leakage of mercury to the atmosphere from around the pump shaft lipseal. Also, the impeller blade would intermittantly rub against the side of the impeller housing. The pump was reworked several times by re-placing the O-rings and lipseals. Also the impeller and pump shaft were realigned. However, for the most part this did not improve the performance of the pump.

Examination of the pump after completion of the test revealed only one area of damage to the pump components. This was around the entrance to the volute tongue. The pump impeller was relatively undamaged except for the abrasions around the side. Examination of the damaged area around the volute tongue indicated that the pitting resulted from an erosive action. This could have resulted from either cavitation or impacting of the mercury in the general area.

In general, these results are somewhat contrary to the usual damage found after the operation of a centrifugal pump (7). Normally, the impeller, especially the blades, suffer the worst damage. The presence of hydrogen in the mercury might explain this difference. The greatest amount of the 1000 hours of operation of the pump was accumulated during the hydrogen injection tests. There is the possibility that the hydrogen behaved as a compressible fluid within the impeller cavity. If this is true, then the hydrogen possibly acted as a cushion and prohibited any shocks from being transmitted to the impeller blades.

However, once the bubble reached the volute tongue it might have gone into solution because of the higher pressure within the region. If this occurred fast enough, a high pressure cavity within the mercury could result. This cavity essentially would implode thus causing the mercury to impact against the tongue.

C. Corrosion and Mass Transfer

In general, the depth and mode of corrosion incurred in the boiler regions compare favorably with results obtained from previous corrosion tests. As shown in Figure 65, the attack incurred has been plotted as a function of the temperature. The results as plotted fall below or near to the curve, which is the maximum expected corrosion rate plotted as a function of the temperature (3).

However, the data, as plotted, should be used only for comparative purposes. As discussed with the results on metallographic examination, the temperatures listed for the various specimens are not truly representative of the total operating life. In view of this, the results seem to confirm the previous data on the corrosion of Haynes alloy No. 25 as obtained from thermal convection loops and capsule tests (2) (4).

Overall, the attack incurred in the superheater region of the loop was quite low. Considering the temperature profile of the superheater versus the degree of attack, it appears that the vapor being passed through the superheater was relatively dry.

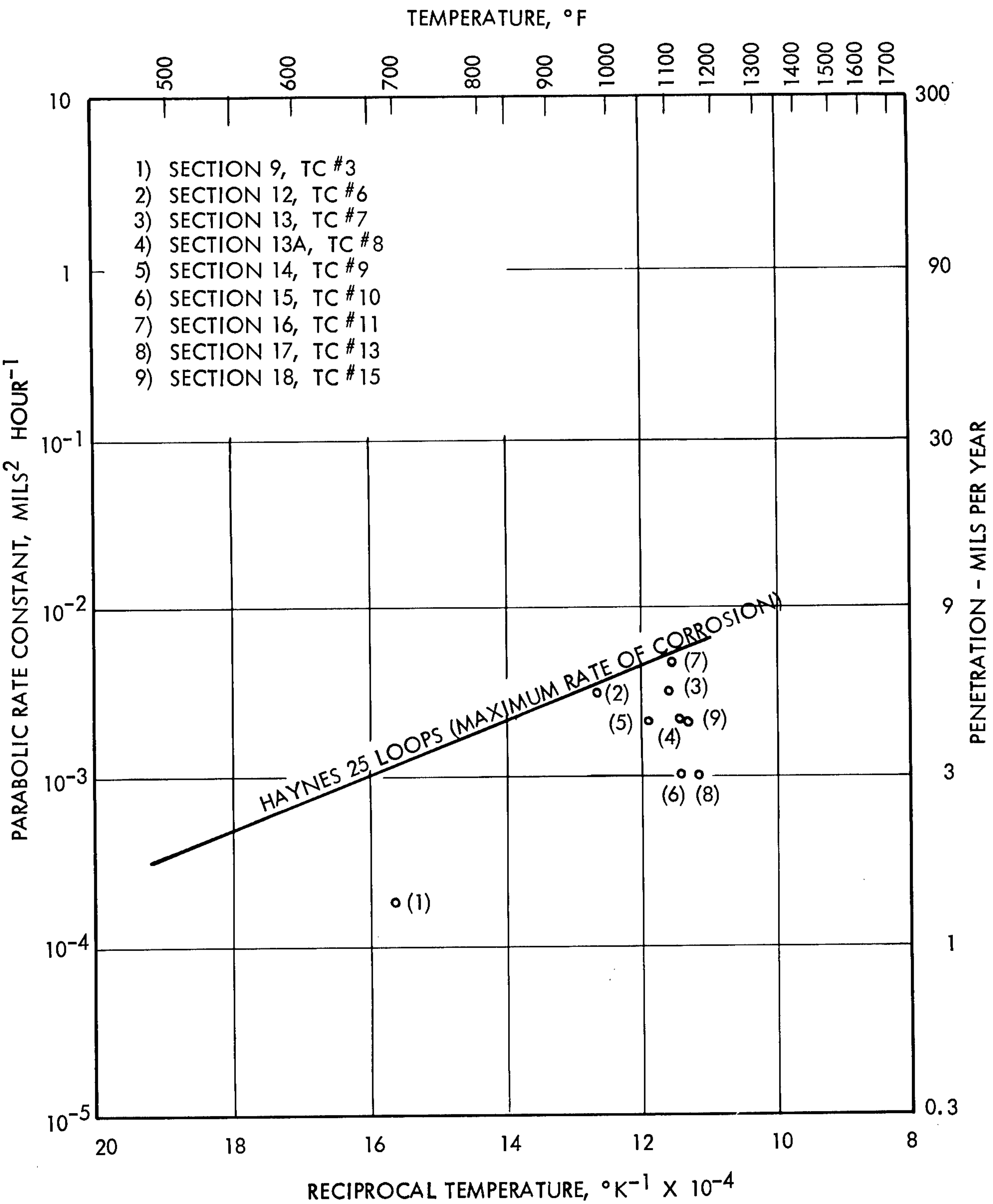

FIGURE 65 COMPARISON OF HAYNES ALLOY NO. 25 MERCURY PENETRATION FROM THE WORK HORSE LOOP WITH TWO-PHASE THERMAL CONVECTION LOOPS

In general, very little damage was experienced by both the orifice plate and the erosion specimens. Neither of the two revealed the presence of corrosive attack. Also, the surfaces of both showed no evidence of erosion. Considering the condition of the surface of both the orifice plate and the specimens and the slight weight gain experienced by the specimens, it appears that both were exposed to an oxidizing atmosphere sometime during test.

Although the PH15-7Mo specimens were not appreciably attacked or eroded, the loss in hardness and change in microstructure is quite significant. These changes resulted from the overaging of the precipitation hardened structure. This overaging results in the loss of mechanical strength with respect to the Sunflower turbine. The results somewhat preclude the use of PH15-7Mo as a structural material for components where tight tolerances need to be maintained over extended time periods. This is also reflected by the deformation experienced by the orifice plate which was tested in the RH 950 heat treat condition.

In contrast, the Haynes alloy No. 21 erosion specimen increased in hardness. This is probably the result of an age hardening reaction similar to that found in Haynes alloy No. 25 (1). Thus it appears that Haynes alloy No. 21 would be a better candidate material for the turbine than PH15-7Mo, providing other engineering considerations such as embrittlement and matching coefficients of expansion are met.

Practically no attack was found in either the condenser or subcooler regions. However, from the results obtained on the test specimens it appears that the inside surfaces of the loop, especially those of the superheater and condenser, were exposed to an oxidizing atmosphere at one time or another. Also, both regions were exposed to hydrogen. Previous studies conducted with capsules have indicated that both oxygen and hydrogen have an inhibiting effect on mercury corrosion. Thus the surfaces of both might have been inhibited from attack (2).

A total of 20.5 grams of corrosion products were removed from the loop. Of this, approximately 55 percent was removed from the boiler, 27 percent from the superheater, 6.4 percent from the crud separator, 0.2 percent from the condenser and subcooler regions, and 11.4 percent from the mercury. In general, the weight of the products removed agree with data previously obtained on the generation of corrosion products in thermal convection loops and capsule tests (2).

This agreement continues into the analysis of the corrosion layer found in the boiler regions. As discussed, the wet chemical analysis of the corrosion layer revealed that the predominant constituents were cobalt and tungsten. Results obtained through microprobe analysis confirmed this. These results indicate that chromium, nickel and iron were selectively removed leaving a porous cobalt and tungsten rich phase. In general, this is the result which has been gleaned from previous corrosion testing of Haynes alloy No. 25 (2) (4).

However, analysis of the deposits removed from the superheater does not fall into place quite as easily. Comparison of the results obtained by wet chemical analysis with those obtained by use of the electron microprobe shows complete disagreement. Wet chemical analysis indicated that the deposit in the superheater inlet contained primarily cobalt with smaller but equal amounts of chromium and nickel. Also about three percent iron was found. In contrast, the microprobe indicated that the deposit contained two phases, with the predominant phase containing 76-78 percent nickel and 21-23 percent chromium. The secondary phase was close to pure chromium. Cobalt, iron, and tungsten were present in both, but only in minor amounts.

It is believed that this deposit resulted from liquid being bumped up from the boiler. Because of the loop orientation any liquid which was carried up into the superheater inlet region tended to stay there until it evaporated. Also, during approximately the first 1250 hours of operation, vapor of very low quality was entering the superheater. Of all the corrosion products accounted for, 4.5 grams or approximately 22 percent was removed from this region.

As previously discussed, the vapor crud separator was placed in the inlet region of the superheater after 3833 hours of operation. To install the separator, 18 inches of tubing out of the 24 inches total length of the inlet section was removed to make room for the separator. Of the 4.5 grams of material removed from the inlet, 3.6 grams came from this 18-inch length.

Analysis of the deposit removed from the middle region of the superheater showed the same discrepancy as found during the analysis of the deposit in the boiler region. Essentially, the difference in composition of the deposit, as indicated by wet-chemical and microprobe methods, was the same as found in the boiler inlet. The deposit probably occurred from liquid carried over from the boiler.

Wet chemical analysis of the 3.5 grams of deposit removed from the outlet region of the superheater revealed the presence of cobalt, chromium, and nickel in the same general amounts as the rest of the superheater. However, along with this, 29 percent of tungsten was found.

It is not known which of the analyses are correct. However, the results of the microprobe analysis conducted on the two superheater sections demonstrate a better fit to the corrosion picture. In the boiler regions, chromium, nickel and iron were removed from the tube wall. Analysis of the mercury did not reveal any great quantities of these elements. Thus, the three had to deposit out somewhere within the loop. According to the microprobe the region where the chromium, nickel and iron deposited was within the superheater.

D. Tantalum Crud Separator

During the 1459 hours in which the vapor crud separator was in place, it collected around 6.5 percent of the corrosion products formed. Wet chemical analysis of the products contained within the tantalum wool indicated that the wool was able to collect approximately equal amounts of cobalt, chromium, nickel, iron and tungsten. In general, the results indicate that the separator was able to remove corrosion products from the wet vapor coming out of the boiler. However, the efficiency and total effectiveness of the separator could not be determined since the loop had already operated for 3833 hours before the separator was installed.

If the separator had been in place during the full life time, the quantity of corrosion products removed probably would have been greater. The rate at which corrosion products are generated, like the rate at which a metal is corroded by mercury, is initially high and then decreases with time. This is caused by the development of a corrosion layer which acts as a resistance to the removal of mercury soluble elements (8).

VIII CONCLUSIONS

1. Attempts to remove hydrogen from the system through Haynes alloy No. 25, Croloy 9M, and columbium diffusion windows located in both the vapor and liquid regions of the system met with very limited success. Factors which could have affected the results include oxide films on the surface of the windows, the film of mercury in contact with the tube wall, a low partial pressure of hydrogen in the system, and the tendency for the hydrogen to collect in various regions of the system.

2. Attempts to remove hydrogen from the system through a centrifugal separator employing a columbium or a 1010 steel diffusion window also met with limited success. The poor success with the columbium window can be attributed to the lack of adequate data on the permeability of columbium to hydrogen at low temperatures. The design of the windows was based on a theoretical permeability extrapolated from high temperature (>1000°F) permeability data. However, later data indicated that the permeability of hydrogen through columbium dropped off quite drastically at temperatures below approximately 1000°F. Oxide films were also observed on the surface of both the columbium and 1010 steel windows after test and could account for the low removal rates.

3. No distinct correlations could be determined concerning the ability of the centrifugal mercury pump to accept either single bubbles of hydrogen or hydrogen entering the pump inlet at a constant rate. Throughout the tests, leakage around the pump seals contributed to the problem of obtaining accurate and reproducible data.

4. After approximately 1000 hours of intermittent operation, only one area of the centrifugal pump was found to be damaged. This area was around the volute tongue where an erosive action had occurred.

5. Corrosive attack of the boiler was primarily of the leached layer and intergranular penetration types. The maximum attack of 0.005 inch occurred in the outlet region of the boiler. However, the low quality regions of the boiler were generally penetrated to a depth of 0.004 inch.

6. Light crevice attack was observed in the superheater regions of the system, and was generally less than 0.001 inch in depth.

7. The condenser and subcooler sections of the loop suffered negligible attack.

8. Very little damage (both corrosive and erosive) was experienced by the PH15-7Mo orifice plate and the PH15-7Mo and Haynes alloy No. 21 erosion specimens. However, both PH15-7Mo erosion specimens suffered significant losses in hardness from overaging indicating a significant metallurgical instability. This precludes their use as turbine materials. The increase in hardness of the Haynes alloy No. 21 erosion specimen indicates a potential use for turbine blades providing other engineering considerations such as embrittlement and matching coefficients of expansion are met.

9. Deposition was observed in the system and occurred primarily in the boiler and superheater regions. Negligible deposition was observed in the remainder of the system.

10. The corrosion layer in the boiler was rich in cobalt and tungsten, indicating that chromium, nickel, and iron had been selectively removed from this region.

11. The chromium, nickel, and iron removed from the boiler deposited throughout the length of the superheater. Approximately 72 percent of the deposit in the superheater was found at the entrance of this section where liquid carried over from the boiler tended to condense.

12. The crud separator located at the superheater entrance collected approximately 6.5 percent of the corrosion products found in the system. However, the separator was utilized for only the last 1459 hours of loop operation and thus did not have the opportunity to remove the corrosion products formed during the initial 3833 hours of operation.

coB

Oxidation [illegible] end

APPENDIX I

COMPOSITION OF MATERIALS TESTED IN CONJUNCTION WITH THE WORKHORSE LOOP

	Composition (w/o)											
	Fe	Co	Ni	Cr	Mo	W	C	Si	Mn	Al	Cb	Ta
1010 Steel	Bal						.10		.35			
Croloy 9M	Bal			8.8	.97		.11	.46	.49			
316 Stainless Steel	Bal		13.1	17.5	2.40		.05	.42	1.71			
PH15-7Mo	Bal		7.2	15.5	2.5		.09	.80	.90	1.3		
Haynes Alloy No. 21	1.7	Bal	2.7	28.7	5.70		.27	.90	.85			
Haynes Alloy No. 25	2.0	Bal	9.8	20.0		15.0	.08	.60	1.5			
Columbium							.02				Bal	
Tantalum	.03						.03					Bal

APPENDIX II

STANDARD HEAT TREATMENTS FOR PH15-7Mo

Mill Annealed 1950 ±25°F
Condition A

Fabricate

Heat to 1400°F ±25°F Hold for 90 Min.	Heat to 1750°F ± 15°F Hold for 10 Min. Air Cool to Room Temp. Results in Condition A 1750
Cool to 60°F $^{+0}_{-10}$°F Within 1 Hour Hold for 1/2 Hour Results in Condition T	Cool to -100°F ±10°F Hold for 8 Hours Results in Condition R-100
Heat to 1050°F ±10°F Hold for 90 Min. Air Cool to Room Temp. Results in Condition TH 1050	Heat to 950°F ±10°F Hold for 60 Min. Air Cool to Room Temp. Results in Condition RH 950

REFERENCES

1. Evans, E. B., Vargo, E. J., and Pearson, J. B. Jr., "Embrittlement of Haynes Alloy No. 25 (L-605) During High Temperature Exposure," TM 3488-67, TRW Inc., August, 1962.

2. Nejedlik, J. F., "The SNAP II Power Conversion System Topical Report No. 14, Mercury Materials Evaluation and Selection," ER 4461, TRW Inc., April 1961.

3. Nejedlik, J. F., "The Analysis of Sunflower CSUI-3 Turbine Inlet Housing Corrosion and Deposits," TM 3613-67, TRW Inc., January, 1963.

4. Nejedlik, J. F., and Vargo, E. J., "Kinetics of Corrosion in a Two-Phase Mercury System," ER 5694, TRW Inc., January 1964.

5. Owens, J. J., Nejedlik, J. F., and Vogt, J. W., "The SNAP II Power Conversion System Topical Report No. 7," ER 4103, TRW Inc., June, 1960.

6. Private communication between D. B. Cooper and C. W. Grennan of TRW Inc., July, 1962.

7. Private communication between R. C. Schulze and C. W. Grennan of TRW Inc., April 1964.

8. Private communication between R. C. Schulze and J. F. Nejedlik of TRW Inc., April 1964.

9. Steigerwald, E. A., "The Permeation of Hydrogen Through Constructional Materials," ER 4776, TRW Inc., November, 1961.

10. Steigerwald, E. A., "The Permeation of Hydrogen Through Materials for the Sunflower System," ER 5623, TRW Inc., November, 1963.

11. Cooper, D. B., "Operation of a Forced Circulation, Haynes Alloy No. 25, Mercury Loop to Study Corrosion Product Separation Techniques," ER 5985, TRW Inc., May 1, 1964.

NASA-Langley, 1965 E-2914

"The aeronautical and space activities of the United States shall be conducted so as to contribute . . . to the expansion of human knowledge of phenomena in the atmosphere and space. The Administration shall provide for the widest practicable and appropriate dissemination of information concerning its activities and the results thereof."

—NATIONAL AERONAUTICS AND SPACE ACT OF 1958

NASA SCIENTIFIC AND TECHNICAL PUBLICATIONS

TECHNICAL REPORTS: Scientific and technical information considered important, complete, and a lasting contribution to existing knowledge.

TECHNICAL NOTES: Information less broad in scope but nevertheless of importance as a contribution to existing knowledge.

TECHNICAL MEMORANDUMS: Information receiving limited distribution because of preliminary data, security classification, or other reasons.

CONTRACTOR REPORTS: Technical information generated in connection with a NASA contract or grant and released under NASA auspices.

TECHNICAL TRANSLATIONS: Information published in a foreign language considered to merit NASA distribution in English.

TECHNICAL REPRINTS: Information derived from NASA activities and initially published in the form of journal articles.

SPECIAL PUBLICATIONS: Information derived from or of value to NASA activities but not necessarily reporting the results of individual NASA-programmed scientific efforts. Publications include conference proceedings, monographs, data compilations, handbooks, sourcebooks, and special bibliographies.

Details on the availability of these publications may be obtained from:

SCIENTIFIC AND TECHNICAL INFORMATION DIVISION

NATIONAL AERONAUTICS AND SPACE ADMINISTRATION

Washington, D.C. 20546